



Universidade de
Aveiro
2015

Departamento de Química

**Pedro Duarte de
Oliveira Esteves**

**Extração e Purificação de Teobromina
usando Líquidos Iónicos**

**Extraction and Purification of
Theobromine using Ionic Liquids**



Universidade de
Aveiro
2015

Departamento de Química

**Pedro Duarte de
Oliveira Esteves**

**Extração e Purificação de Teobromina
usando Líquidos Iónicos**

**Extraction and Purification of
Theobromine using Ionic Liquids**

Dissertação apresentada à Universidade de Aveiro para cumprimento dos requisitos necessários à obtenção do grau de Mestre em Bioquímica, ramo de Bioquímica Clínica, realizada sob a orientação científica da Doutora Mara Guadalupe Freire Martins, Investigadora Coordenadora do Departamento de Química, CICECO, da Universidade de Aveiro, e da Doutora Isabel Maria Delgado Jana Marrucho Ferreira, Investigadora Coordenadora do Instituto de Tecnologia Química e Biológica António Xavier, da Universidade Nova de Lisboa.

Aos pilares que seguram o meu templo...

O júri

Presidente

Professor Doutor Pedro Miguel Dimas Neves Domingues
Professor Auxiliar com Agregação do Departamento de Química da Universidade de Aveiro

Doutora Mara Guadalupe Freire Martins
Investigadora Coordenadora do Departamento de Química da Universidade de Aveiro

Doutora Liliana Sofia Carvalho Tomé
Estagiária de Pós-Doutoramento do Instituto de Tecnologia Química e Biológica António Xavier da Universidade Nova de Lisboa

Agradecimentos

Em toda esta dissertação, esta página talvez seja a mais difícil de escrever: por um lado devido ao misto de emoções que sinto neste momento, uma vez que estou a terminar de subir mais um lanço de escadas nesta longa escadaria que é a vida, por outro lado o receio de me esquecer de alguém.

Foram 15 meses de pura diversão, adrenalina, stress, discussão, alegria, e muito mais...Mas também, foram 15 meses de descobrimento, investigação e conhecimento. Não foi fácil, mas também se o fosse não tinha piada nenhuma.

Quero agradecer à professora Mara por todo o apoio prestado e mais algum, pelos conselhos dados e por todo o tempo perdido comigo.

À professora Isabel, apesar de termos estado poucas vezes juntos fisicamente, virtualmente estive sempre presente e pronta a ajudar. Por isso e por tudo mais, o meu grande agradecimento.

Ao Hugo, sem ele muitas coisas não eram possíveis; ele é teimoso, mas teve azar, porque eu sou muito mais. Muito obrigado por todo o tempo perdido comigo.

À Ana Filipa, nem sei o que dizer, nesta fase final seria complicado sem a ajuda dela, muito obrigado por tudo.

Um grande obrigado a todos os membros do Path e Mini-Path pelo apoio prestado.

Por fim, e porque os últimos são sempre os primeiros, “aos pilares que seguram o meu templo”, os meus pais, irmão e avó muito obrigado por tudo, não só de agora, mas de sempre. Sempre presentes e a dar o maior apoio do mundo, o apoio emocional, o resto eles já sabem...estou a ficar sem espaço...

Estou prestes a tornar-me num cientista cantor, por isso vou pensar em escrever um musical “O Fantasma da Ciência!”.

♪ The Phantom of the Science is here, inside my mind ♪

Palavras-chave

Biomassa, Cacau, Alcaloides, Teobromina, Sistemas Aquosos Bifásicos (SAB), Líquidos Iônicos (LIs)

Resumo

A teobromina é um alcaloide utilizado no tratamento de aterosclerose, hipertensão, angina, entre outros. Dada a sua importância medicinal, o principal objetivo deste trabalho consistiu no desenvolvimento de uma técnica eficiente e sustentável para extrair teobromina das sementes de cacau.

Visando o desenvolvimento de uma técnica de purificação para o extrato obtido a partir do cacau, primeiramente estudaram-se sistemas aquosos bifásicos (SABs) constituídos por líquidos iônicos (LIs) para inferir sobre os sistemas mais promissores. Foram utilizados LIs à base do catião colínio, catião não tóxico e biocompatível, em conjunto com 2 polímeros (PPG 400 e PEG 400) e um sal inorgânico (K_3PO_4) para a formação de SABs. Determinaram-se os diagramas de fase, à temperatura de 298 K e à pressão atmosférica, assim como as eficiências de extração destes sistemas para a teobromina. Os resultados obtidos indicam que o K_3PO_4 apresenta uma maior capacidade de induzir a formação de SABs do que o PPG 400 e o PEG 400. Os SABs constituídos por K_3PO_4 também demonstraram ter um grande potencial para a extração da teobromina, com eficiências de extração entre 96,4 e 99,9 %.

Tendo por base os LIs mais promissores para a etapa de purificação, estes foram posteriormente utilizados em solução aquosa para a extração de teobromina a partir das sementes de cacau, tendo sido obtidos valores de extração de teobromina entre 4,5 e 6,5 (m/m) %. Por fim, procedeu-se à utilização de SABs como método de purificação a partir da solução aquosa contendo o extrato, e obtiveram-se valores de eficiências de extração entre 96,7 e 99,0 %.

Keywords

Biomass, Cocoa, Alkaloids, Theobromine, Aqueous Biphasic Systems (ABS), Ionic Liquids (ILs)

Abstract

Theobromine is an alkaloid present in cocoa and it is used in the treatment of atherosclerosis, hypertension, angina, among others. Due to its importance, the aim of this work consists on the development of an efficient and sustainable technology for the extraction of theobromine from cocoa beans.

For the development of a purification technique for theobromine extracted from cocoa, aqueous biphasic systems (ABS) composed of ionic liquids (ILs) were initially studied to infer on the most promising systems. Cholinium-based ILs, based on a non-toxic and biocompatible cation, were used combined with two polymers (PPG 400 and PEG 400) and an inorganic salt (K_3PO_4). The respective phase diagrams at 298 K and atmospheric pressure were determined, as well as their extraction efficiencies for theobromine. The results obtained indicate that K_3PO_4 has a greater ability to induce the formation of ABS compared to PEG 400 and PPG 400. ABS consisting of K_3PO_4 also have a high potential for the extraction of theobromine, with extraction efficiencies ranging between 96.4 and 99.9 %.

Based on the most promising ILs for the purification step, they were further used in aqueous solution to extract theobromine from cocoa beans, with extraction yields ranging between 4.5% and 6.5 wt%.

Finally, ABS were applied to the aqueous solutions containing theobromine from the cocoa extract, with extraction efficiencies ranging between 96.7 and 99.0%.

Contents

Contents.....	XIII
List of Tables.....	XV
List of Figures.....	XVII
List of Symbols.....	XXI
List of Abbreviations.....	XXIII
1. General Introduction.....	1
1.1. Scope and Objectives	3
1.2. Alkaloids.....	4
1.2.1. Biological Chemistry	4
1.2.2. Pharmacologic Effects	6
1.2.3. Alkaloids in Biomass	7
1.2.4. Extraction of Alkaloids from Biomass.....	9
1.3. Aqueous Biphasic Systems (ABS).....	9
1.4. Ionic Liquids (ILs).....	11
2. Phase diagrams for ABS containing Cholinium-based ILs.....	17
2.1. Introduction	19
2.2. Experimental Section.....	20
2.2.1. Materials.....	20
2.2.2. Experimental Procedure	23
2.3. Results and Discussion	25
3. Extraction of Theobromine using IL-based ABS	31
3.1. Introduction	33
3.2. Experimental Section.....	34
3.2.1 Materials.....	34
3.2.2. Experimental Procedure	35
3.3. Results and Discussion	36
4. Extraction and Purification of Theobromine from Biomass	39
4.1. Introduction	41
4.2. Experimental Section.....	41
4.2.1 Materials.....	41
4.2.2. Experimental Procedure	42

4.3. Results and Discussion	45
5. Final Remarks.....	55
5.1. Conclusions and Future Work.....	57
6. References	59
Appendix A - Experimental binodal data	73
A.1. Experimental binodal data for systems composed of IL + PPG 400 + H ₂ O	75
A.2. Experimental binodal data for systems composed of IL + K ₃ PO ₄ + H ₂ O.....	79
A.3. Correlation parameters	81
Appendix B – Additional experimental data	83
B.1. Ternary phase diagrams in molality.....	85
B.2. Examples of TLs obtained	86
B.3. Calibration curves	88
B.4. GC-MS spectrum	90
Appendix C – Weight fraction percentage (wt %) of ABS	91
C.1. Weight fraction percentage (wt %) of ABS composed of IL + salting-out species + H ₂ O.....	93
Appendix D – Theobromine extraction	95

List of Tables

Table 3.1. Thermophysical properties of theobromine [102,103].	33
Table A.1.1. Experimental weight fraction data for the system composed of [Ch][Adi _{1:1}] (1) + PPG 400 (2) + H ₂ O (3) at 298 K and at atmospheric pressure.	75
Table A.1.2. Experimental weight fraction data for the system composed of [Ch][Adi _{1:2}] (1) + PPG 400 (2) + H ₂ O (3) at 298 K and at atmospheric pressure.	76
Table A.1.3. Experimental weight fraction data for the system composed of [Ch][Ac] (1) + PPG 400 (2) + H ₂ O (3) at 298 K and at atmospheric pressure.	77
Table A.1.4. Experimental weight fraction data for the system composed of IL (1) + PPG 400 (2) + H ₂ O (3) at 298 K and at atmospheric pressure.	78
Table A.2.1. Experimental weight fraction data for the system composed of [Ch][Ac] (1) + K ₃ PO ₄ (2) + H ₂ O (3) at 298 K and at atmospheric pressure.	79
Table A.2.2. Experimental weight fraction data for the system composed of [Ch][Adi _{1:2}] (1) + K ₃ PO ₄ (2) + H ₂ O (3) at 298 K and at atmospheric pressure.	79
Table A.2.3. Experimental weight fraction data for the system composed of IL (1) + K ₃ PO ₄ (2) + H ₂ O (3) at 298 K and at atmospheric pressure.	80
Table A.3.1. Correlation parameters for the fitting using equation 2.1.[93].	81
Table C.1.1 Weight fraction percentage (wt %) of each compound at the coexisting phases of the ABS investigated and respective TLL.	93
Table D.1. % EE _{TB} for the IL-rich phase, and respective standard deviation (σ), for commercial theobromine, using the ABS composed of IL + PPG 400/PEG 400/K ₃ PO ₄ + H ₂ O at 298 K.	97
Table D.2. % TB, and respective standard deviation (σ), from cocoa peels and cocoa core, using different solutions of ILs (1.5 M), in a solid-liquid extraction, at 343 K.	97
Table D.3. % TB from cocoa beans, over time, using ethanol as solvent in a Soxhlet extraction.	97
Table D.4. % TB from cocoa beans, over time, using dichloromethane as solvent in a Soxhlet extraction.	98
Table D.5. % TB, and respective standard deviation (σ), from cocoa beans using different solvents at 343 K: ILs + H ₂ O (1.2 M to [Ch][Bic] and 1.5 M for the remaining ILs), H ₂ O and ethanol.	98

Table D.6. % TB, and respective standard deviation (σ), from treated and untreated biomass, using different solutions of ILs (1.5 M) at 343 K..... 99

Table D.7. Mixture points..... 99

Table D.8. Theobromine extraction efficiencies and respective standard deviation (σ) with commercial theobromine and with theobromine extracted from biomass. 99

List of Figures

Figure 1.1. Flowchart for the extraction and purification of theobromine from cocoa beans.	4
Figure 1.2. Chemistry reactions to form methylxanthines. E1: IMP dehydrogenase, E2: 5'-nucleotidase, E3: xanthosine 7-N-methyltransferase, E4: 7-methylxanthosine nucleosidase, E5: theobromine synthase, E6: caffeine synthase, SAM: S-Adenosyl methionine [6].	6
Figure 1.3. Cocoa beans used in this work.	8
Figure 1.4. IL-based ABS (a dye was added for a better perception of the two phases in equilibrium).	10
Figure 1.5. Orthogonal representation of a phase diagram (ABS). Adapted from Freire <i>et al.</i> [45].	11
Figure 1.6. Number of published articles, <i>per year</i> , comprising ILs [55].	12
Figure 1.7. Chemical structure of IL cations: (i) pyrrolidinium, (ii) imidazolium, (iii) piperidinium, (iv) pyridinium, (v) ammonium and (vi) phosphonium.	13
Figure 1.8. Chemical structure of IL anions: (i) acetate, (ii) tosylate, (iii) dicyanamide, (iv) thiocyanate, (v) methylsulfate, (vi) triflate, (vii) tetrafluoroborate, (viii) hexafluorophosphate and (ix) bis(trifluoromethylsulfonyl)imide.	13
Figure 1.9. Number of published manuscripts <i>per year</i> on ABS with ILs [55].	15
Figure 2.1. Chemical structures of the ions of the ILs investigated: (i.) [Ch] ⁺ , (ii.) [Pro] ⁻ , (iii.) [But] ⁻ , (iv.) [Pent] ⁻ , (v.) [Hex] ⁻ , (vi.) [Hept] ⁻ , (vii.) [Oct] ⁻ , (viii.) [Non] ⁻ , (ix.) [Adi] ⁻ , (x.) [Aze] ⁻ , (xi.) [PFHept] ⁻ , (xii.) [PFOct] ⁻ , (xiii.) [PFBut] ⁻ , (xiv.) [TFAc] ⁻ , (xv.) [Ac] ⁻ , (xvi.) [DHph] ⁻ , (xvii.) Cl ⁻ , (xviii.) [Bit] ⁻ , (xix.) [Bic] ⁻ and (xx.) [DHcit] ⁻	21
Figure 2.2. Chemical structures of the salting-out species investigated: (i.) Dextran, (ii.) Maltodextrin, (iii.) PVP; (iv.) PPG, (v.) PEG and (vi.) K ₃ PO ₄	22
Figure 2.3. Schematic representation of the cloud point titration method.	24
Figure 2.4. Ternary phase diagrams for systems composed of IL + PPG 400 + water, at 298 K and atmospheric pressure: (■) [Ch][DHph] [90], (◆) [Ch][Ac], (▲) [Ch]Cl [90], (■) [Ch][Bit] [90], (●) [Ch][Bic], (◆) [Ch][DHcit] [90], (▲) [Ch][Adi _{1:1}], (●) [Ch][Adi _{1:2}], (■) [Ch][Aze], and (◆) [Ch][TFAc].	27
Figure 2.5. Ternary phase diagrams for systems composed of IL + PEG 400 + water, at 298 K and atmospheric pressure: (■) [Ch][DHph] [84], (◆) [Ch][Bic] [84], (▲) [Ch][Ac] [84], (●) [Ch][Bit] [84], (■) [Ch]Cl [84], and (◆) [Ch][DHcit] [84].	27

Figure 2.6. Ternary phase diagrams for systems composed of IL + K ₃ PO ₄ + water, at 298 K and atmospheric pressure: (◆) [Ch][Adi _{1,2}], (▲) [Ch]Cl [91], (■) [Ch][Ac], (●) [Ch][Pro], (▲) [Ch][But], (●) [Ch][Pent], (■) [Ch][Hex] and (◆) [Ch][Non].	29
Figure 3.1. Chemical structure of theobromine.	34
Figure 3.2. Extraction efficiencies for theobromine of the ABS composed of cholinium-based ILs + PPG 400/PEG 400/K ₃ PO ₄ + H ₂ O at 298 K.	36
Figure 4.1. A – untreated grinded cocoa beans and B – treated grinded cocoa beans.	43
Figure 4.2. ABS formed with the IL aqueous solution containing the cocoa extract and K ₃ PO ₄ .	44
Figure 4.3. Weight percentage of theobromine extracted from cocoa peel □ and cocoa core □ using IL aqueous solutions (1.5 M) at 343 K.	45
Figure 4.4. Weight percentage of theobromine extracted from cocoa beans, over time, using ethanol as solvent in a Soxhlet extraction.	46
Figure 4.5. Weight percentage of theobromine extracted from cocoa beans, over time, using dichloromethane as solvent in a Soxhlet extraction.	46
Figure 4.6. Weight percentage of theobromine extracted from cocoa core beans using different solvents: H ₂ O, ethanol and ILs aqueous solutions (1.2 M for [Ch][Bic] and 1.5 M for the remaining ILs) at 343 K.	47
Figure 4.7. Mass percentage of theobromine extracted from treated □ and untreated □ cocoa core beans, using different solutions of ILs (1.5 M) at 343 K.	48
Figure 4.8. Extraction efficiencies for theobromine of the ABS composed of cholinium-based ILs + K ₃ PO ₄ + H ₂ O at 298 K using commercial □ and the aqueous solution containing the cocoa core extract □.	50
Figure 4.9. Spectra of the diluted aqueous solutions of commercial theobromine (—), [Ch][Ac] with commercial theobromine (—), [Ch][Ac] with treated cocoa core beans after extraction (—) and IL (—) and K ₃ PO ₄ phases (—) after an extraction with [Ch][Ac].	51
Figure 4.10. SEM images of the cocoa core samples: untreated (A) and treated (B) with petroleum ether.	52
Figure 4.11. SEM images of the cocoa core samples, untreated (C) and treated with petroleum ether (D) after extraction with an aqueous solution of [Ch][Ac].	52
Figure B.1.1. Ternary phase diagrams for systems composed of IL + PPG 400 + water, at 298 K and atmospheric pressure: (■) [Ch][DHph], (◆) [Ch][Ac], (▲) [Ch]Cl, (■)	

[Ch][Bit], (●) [Ch][Bic], (◆) [Ch][DHcit], (▲) [Ch][Adi](1:1), (●)[Ch][Adi](1:1), (■) [Ch][Aze], (◆) [Ch][TFAc].	85
Figure B.1.2. Ternary phase diagrams for systems composed of IL + PEG 400 + water, at 298 K and atmospheric pressure: (■) [Ch][DHph], (◆) [Ch][Bic], (▲) [Ch][Ac], (●) [Ch][Bit], (■) [Ch]Cl, (◆) [Ch][DHcit].	85
Figure B.1.3. Ternary phase diagrams for systems composed of IL + K ₃ PO ₄ + water, at 298 K and atmospheric pressure: (◆) [Ch][Adi _{1:2}], (▲) [Ch]Cl, (■) [Ch][Ac], (●) [Ch][Pro], (▲) [Ch][But], (●) [Ch][Pent], (■) [Ch][Hex] and (◆) [Ch][Non].	86
Figure B.2.1. Phase diagram for [Ch][Adi _{1:1}] + PPG 400 + H ₂ O. Binodal equilibrium data (◆); TL data (■); correlation using equation 2.1. (—).	86
Figure B.2.2. Phase diagram for [Ch][Aze] + PPG 400 + H ₂ O. Binodal equilibrium data (▲); TL data (■); correlation using equation 2.1. (—).	87
Figure B.2.3. Phase diagram for [Ch][But] + K ₃ PO ₄ + H ₂ O. Binodal equilibrium data (●); TL data (■); correlation using equation 2.1. (—).	87
Figure B.3.1. Theobromine calibration curve with water as solvent using the UV-microplate reader, with maximum of absorbance at a wavelength of 273 nm.	88
Figure B.3.2. Theobromine calibration curve with water as solvent using the UV-Spectrometer, with maximum of absorbance at a wavelength of 273 nm.	88
Figure B.3.3. Theobromine calibration curve with ethanol as solvent using the UV-Spectrometer, with maximum of absorbance at a wavelength of 273 nm.	89
Figure B.3.4. Theobromine calibration curve with dichloromethane as solvent using the UV-Spectrometer, with maximum of absorbance at a wavelength of 273 nm.	89
Figure B.4.1. GC-MS spectrum of treated cocoa after extraction with [Ch][Ac].	90

List of Symbols

wt %	weight fraction percentage (%)
λ	wavelength (nm)
Σ	standard deviation
Abs	absorbance (dimensionless)
M_w	molecular weight ($\text{g}\cdot\text{mol}^{-1}$)
R^2	correlation coefficient (dimensionless)
α	ratio between the top weight and the total weight of the mixture (dimensionless)
% EE _{TB}	extraction efficiency of theobromine
[IL]	concentration of ionic liquid (wt % or $\text{g}\cdot\text{L}^{-1}$)
[IL] _{IL}	concentration of ionic liquid in the ionic-liquid rich phase (wt %)
[IL] _{SO}	concentration of ionic liquid in the salting-out-rich phase (wt %)
[IL] _M	concentration of ionic liquid in the initial mixture (wt %)
[SO]	concentration of salting-out species (wt % or $\text{g}\cdot\text{L}^{-1}$)
[SO] _{IL}	concentration of salting-out species in the ionic-liquid-rich phase (wt %)
[SO] _{SO}	concentration of salting-out species in the salting-out-rich phase (wt %)
[SO] _M	concentration of salting-out species in the initial mixture (wt %)
Conc _{TB} ^{IL}	concentration of theobromine in the ionic-liquid-rich aqueous phase ($\text{g}\cdot\text{L}^{-1}$)
Conc _{TB} ^{SO}	concentration of theobromine in the salting-out-rich aqueous phase ($\text{g}\cdot\text{L}^{-1}$)
[TB]	concentration of theobromine ($\text{g}\cdot\text{L}^{-1}$)
V _{solvent}	volume of solvent (L)
w _{cocoa}	weight of cocoa ground beans (g)
% TB	weight percentage of theobromine extracted
[PPG 400]	concentration of PPG 400 (wt % or $\text{g}\cdot\text{L}^{-1}$)
[PEG 400]	concentration of PEG 400 (wt % or $\text{g}\cdot\text{L}^{-1}$)
[K ₃ PO ₄]	concentration of K ₃ PO ₄ (wt % or $\text{g}\cdot\text{L}^{-1}$)

List of Abbreviations

ABS	aqueous biphasic systems
AMP	adenosine 5-monophosphate
GC-MS	gas chromatography–mass spectrometry
GMP	guanosine 5-monophosphate
IMP	inosine 5-monophosphate
PPG	polypropylene glycol
PEG	polyethylene glycol
PPG 400	polypropylene glycol with a molecular weight of 400 g·mol ⁻¹
PEG 400	polyethylene glycol with a molecular weight of 400 g·mol ⁻¹
SAM	S-adenosyl methionine
SEM	scanning electron microscopy
TB	Theobromine
TL	tie-line
TLL	tie-line length
UV	Ultraviolet
VOC	volatile organic compound
XMP	xanthosine 5-monophosphate
[Ch][Pro]	(2-hydroxyethyl)trimethylammonium propanoate
[Ch][But]	(2-hydroxyethyl)trimethylammonium butanoate
[Ch][Pent]	(2-hydroxyethyl)trimethylammonium pentanoate
[Ch][Hex]	(2-hydroxyethyl)trimethylammonium hexanoate
[Ch][Non]	(2-hydroxyethyl)trimethylammonium nonanoate
[Ch][Adi _{1:1}]	(2-hydroxyethyl)trimethylammonium adipate (1:1)
[Ch][Adi _{1:2}]	(2-hydroxyethyl)trimethylammonium adipate (1:2)
[Ch][Aze]	(2-hydroxyethyl)trimethylammonium azelate
[Ch][PFHept]	(2-hydroxyethyl)trimethylammonium perfluoroheptanoate
[Ch][PFOct]	(2-hydroxyethyl)trimethylammonium perfluorooctanoate
[Ch][PFBut]	(2-hydroxyethyl)trimethylammonium perfluorobutanoate

[Ch][TFAc]	(2-hydroxyethyl)trimethylammonium trifluoroacetate
[Ch][Ac]	(2-hydroxyethyl)trimethylammonium acetate
[Ch][DHph]	(2-hydroxyethyl)trimethylammonium dihydrogen phosphate
[Ch]Cl	(2-hydroxyethyl)trimethylammonium chloride
[Ch][Bit]	(2-hydroxyethyl)trimethylammonium bitartrate
[Ch][Bic]	(2-hydroxyethyl)trimethylammonium bicarbonate
[Ch][DHcit]	(2-hydroxyethyl)trimethylammonium dihydrogen citrate.

1. General Introduction

1.1. Scope and Objectives

This work addresses the extraction of theobromine from cocoa beans and further purification using ionic-liquid-based processes. Traditional extraction techniques of small added-value molecules, such as alkaloids from plant matrices, still depend on the use of non-environmentally friendly solvents [1]. Environmental and human health concerns associated with the use of volatile solvents, like dichloromethane, hexane, petroleum ether and ethyl acetate, which tend to be toxic and non-biodegradable, and that depending on the process conditions may leave traces behind, have been pushing forward the development of “greener” techniques, by the use of more effective extraction schemes and less toxic solvents [2–5].

The aim of this work is to develop efficient and sustainable technologies for the extraction of theobromine from cocoa beans. For that purpose, the initial part of this study addresses the extraction of commercial theobromine from aqueous solutions using aqueous biphasic systems (ABS) formed by cholinium-based ionic liquids (ILs) to infer on their potential as purification strategies. To this end, several ternary systems composed of cholinium-based ILs, water and a number of salting-out agents were evaluated. Further, aqueous solutions of promising ILs identified in the previous study (those that allow high extraction efficiencies) were applied in the extraction of theobromine from cocoa beans. The effect of the biomass pre-treatment was also addressed.

The main idea behind this thesis is presented in the flowchart shown in Figure 1.1. Although several aspects were not explored in this work due to its limited timeframe, fundamental steps were here carried out ensuring the success of the envisaged extraction scheme for theobromine from cocoa beans.

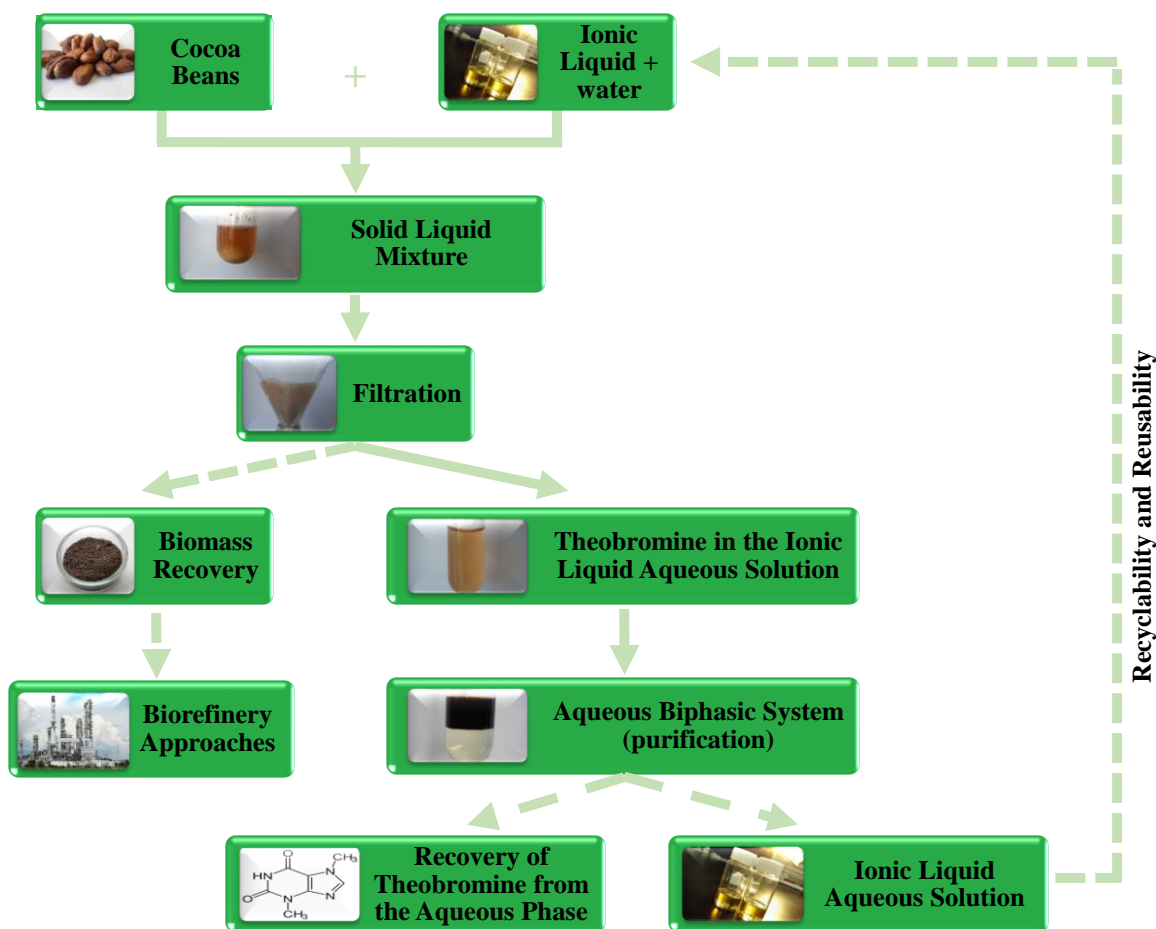


Figure 1.1. Flowchart for the extraction and purification of theobromine from cocoa beans.

1.2. Alkaloids

Alkaloids are substances that have a low molecular weight and are constituted by nitrogen, oxygen, hydrogen and carbon. They contain one or more nitrogen atoms as primary, secondary or tertiary amines, which are responsible for the basicity of alkaloids, and their name derives from the word “alkaline”. However, this basicity may vary depending on the chemical structure of the molecule and presence of other functional groups [6]. There are more than 27,000 different alkaloid structures, where about 78% are found in plants and the remaining 22% in animals and microorganisms [6].

1.2.1. Biological Chemistry

Amino acids are usually involved in the biological synthetic path of alkaloids. Although the carbon skeleton of these amino acids is kept in the alkaloid structure, the carboxylic acid carbon is lost during decarboxylation [6]. Ornithine, lysine, tyrosine,

tryptophan and histidine are amino acids that are usually involved in the formation of alkaloids. The nitrogen atoms in a large number of alkaloids are obtained via transamination reactions, only incorporating one nitrogen from amino acid, while the rest of the molecule may be derived from acetate or shikimate [6]. Other alkaloids are generated from terpenoids or steroids, being designated as pseudoalkaloids [6].

Theobromine, caffeine and theophylline are purine alkaloids or pseudoalkaloids, secondary metabolites derived from xanthine (purine nucleotide) by methylation and they may co-occur in a given plant [7]. The position and the number of methyl substitutions on the xanthine ring determine differences between the main food methylxanthines: theobromine (3,7-dimethylxanthine) and theophylline (1,3-dimethylxanthine), both dimethylxanthines; and caffeine (1,3,7-trimethylxanthine), a trimethylxanthine [7]. These pseudoalkaloids are based on a purine ring that undergoes various reactions and gathering small components of primary metabolism. Initially, a glycine is incorporated, and the remaining carbon atoms are obtained by addition of formate and bicarbonate. Two nitrogen atoms are obtained by glutamine and a third by aspartic acid. Thereafter, the synthesis of adenosine 5-monophosphate (AMP) and guanosine 5-monophosphate (GMP) by inosine 5-monophosphate (IMP) and xanthosine 5-monophosphate (XMP) occurs. Then, 7-methylxanthosine is synthesized by methylation and loss of phosphate occurs. Through methylation reactions, the nitrogen atom forms theobromine and then caffeine. Theophylline is formed by a different sequence of methylation reactions, but may also be obtained by demethylation of caffeine [6]. These reactions occur in the metabolism of plants, such as coffee, cocoa and tea, and are represented in Figure 1.2. These methylxanthines have important pharmacological properties being currently used as therapeutic agents. They have stimulating effects on central nervous, respiratory, and cardiovascular systems, among others [8].

disclosed that infants treated with caffeine showed no impairment in neurological development, compared with other children treated with placebo, reducing the risk of apnea. Treatment with caffeine and theophylline also reduce incidence of cerebral palsy and altered adenosinergic neuromodulation of the respiratory system [12].

Theophylline is the methylxanthine that has the major diuretic and bronchodilator effects [12]. However, an excessive intake may cause tachycardia, convulsions and gastrointestinal distress [13].

Theobromine has similar effects to caffeine but does not cause hypertension [14], and has relaxing effects [8]. Theobromine has many therapeutic applications, namely in the central nervous, gastrointestinal, respiratory and renal systems [15], acting as a diuretic [16], muscle relaxant, coronary stimulant and vasodilator [17]. Moreover, it has been used in the treatment of arteriosclerosis [17], angina and hypertension [17]. Recently, several studies have demonstrated the benefits of cocoa consumption in the prevention of gestational hypertension [18,19]. However, theobromine has also been showed to be toxic to some mammals, including pets, like dogs [17], indicating that its action mechanisms in humans may differ from those observed in other mammals. These controversial facts led to the development of several clinical studies that showed that theobromine is not toxic to humans [20,21]. In addition, Berends *et al.* [22] demonstrated that there are beneficial cardio-metabolic effects after cocoa consumption, due to the presence of theobromine, by improving arterial pressure, lipoprotein and insulin resistance and biomarkers levels.

1.2.3. Alkaloids in Biomass

Caffeine, a methylxanthine found in various drinks such as coffee, cola and guaraná, is largely consumed worldwide due to its benefits to the central nervous system, causing wellness sensations [23]. Although caffeine is mostly present in coffee beans, cocoa also contains this methylxanthine, but in small quantities that are not significant to activate neural mechanisms. Cocoa also contains another methylxanthine, theobromine, a bitter tasting substance that contributes to the characteristic cocoa flavour and has beneficial effects on human health [23].

Cocoa (*Theobroma cacao* L.) belongs to the Malvaceae family, present in tropical forests of South and Central America [24]. Originated more than 3,000 years ago, it was used for nutritional and medicinal purposes by Mayan and Aztec civilizations [25]. For

Mayans, the cocoa bean symbolized fertility and life and, according to legend, was the “food of gods”; for Aztecs, it was used for the treatment of at least 150 diseases [26]. In Europe, during the 17th and 18th centuries, cocoa was used to treat colds, digestive problems, infertility, mental illness, and was also used as an antidepressant [25,27].

Cocoa has a high nutritional value, as it mainly consists of lipids (*circa* 50%), carbohydrates and proteins [24]. Proteins, such as arginine, glutamine, leucine, albumin and globulin represent 10-15% of the cocoa seeds weight. It also contains a large number of biologically active compounds essential for various activities of the human body, namely enzymes, vitamins, oils, sterols, phospholipids, dietary fibers, methylxanthines (caffeine and theobromine), polyphenolic compounds, including flavonoids [28], and minerals, such as potassium, magnesium, copper, iron and phosphorus [26]. Nevertheless, it should be pointed out that although cocoa contains a lot of beneficial components, during grain processing (roasting, fermentation and drying), the content of these bioactive components may change [29].

Figure 1.3. depicts the macroscopic aspect of cocoa beans.



Figure 1.3. Cocoa beans used in this work.

Many studies have shown that, due to the large amount of flavonoids in cocoa, this biomass displays a high antioxidant capacity when compared to other phytochemical-rich natural sources [30–33]. Accordingly, more recently, cocoa has been used in the prevention of cardiovascular diseases [34], reduction of inflammatory processes and oxidative stress [32,35], insulin resistance thus reducing the risk of diabetes [36,37], and obesity [38]. In addition, caffeine and theobromine present in the cocoa stimulate the central nervous system and display diuretic activity [24].

1.2.4. Extraction of Alkaloids from Biomass

Due to the high value of alkaloids as natural bioactive compounds, the search on novel nontoxic solvents, as well as on new technologies for the efficient extraction of these compounds from plant matrices and biomass, is crucial for their market availability and quality. Conventional techniques used in the extraction of these valuable compounds are solid-liquid extraction followed by liquid-liquid extraction for purification purposes [39–41]. In both cases, the most used solvents are chloroform, petroleum ether, hexane and ethyl acetate [2–5], that are volatile and toxic, and may leave traces behind, hindering therefore the benefits of having a natural compound for human consumption. Since it is highly relevant to reduce the toxicity of solvents commonly used in the extraction of natural compounds, alternative solvents have been intensively researched, where water comes at the top of the list [42]. In fact, the development of novel extraction techniques using water as the main solvent followed by liquid-liquid extraction for purification approaches has been object of particular attention [43]. In the same line, the use of ionic liquids and their aqueous solutions for the extraction of value-added compounds from biomass, followed by the formation of aqueous biphasic systems for their recovery and purification, has been investigated in the past few years [43].

1.3. Aqueous Biphasic Systems (ABS)

In 1958, Albertsson [44] reported novel liquid-liquid two-phase systems, consisting of two aqueous phases enriched in different solutes, as an alternative to conventional extraction and purification techniques carried out with volatile organic compounds. It is well known that the use of these solvents presents several disadvantages, such as their high volatility and toxicity, carcinogenic properties and high flammability [1]. These new systems, the so-called aqueous biphasic systems (ABS), are composed of water and two water soluble solutes, which at certain concentrations form two immiscible phases. Typically, ABS are formed by mixtures of polymer-polymer, polymer-salt or salt-salt [45]. These systems present significant advantages, such as simplicity and technological low cost combined with the ability to provide high yields and purification factors, and allow a good selectivity [1,46]. ABS are also a mild environment for biologically active compounds due to their aqueous-rich environment [1,47]. Through their constituent's choice, it is possible to obtain the solute of interest in one phase and the contaminants in

the opposite one, allowing the purification of targeted species, as demonstrated by Martínez-Aragón *et al.* [1] using cytochrome c, myoglobin, human serum albumin and immunoglobulin G; Pérez *et al.* [48] using trypsin; and Ribeiro *et al.* [49] using saponins and polyphenols. The easiness in scale-up is one of the main advantages of these systems; in fact, ABS are used for proteins purification at an industrial scale [47].

In ABS, two components are dissolved in water and, above given concentrations, the system separates into two coexisting phases, as seen in Figure 1.4., where one phase is rich in one of the components and the other phase is rich in the second component. The solute of interest migrates throughout the two coexisting phases according to their affinity and properties of the system until the equilibrium is reached [50].

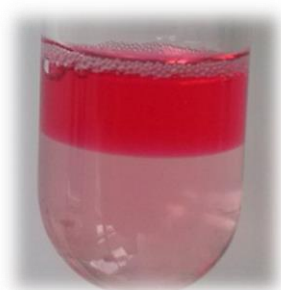


Figure 1.4. IL-based ABS (a dye was added for a better perception of the two phases in equilibrium).

ABS for extraction purposes can only be used after the knowledge of their phase equilibria data, *i.e.*, the minimum amount of phase-forming components required to form two-phase systems. The characterization of ABS includes the determination of their phase diagrams, namely, the binodal curve and the respective tie-lines (TLs), at a given temperature. Care with other experimental variables should also be taken into account since, for example, the use of certain inorganic salts may lead to specific pH conditions [51]. As shown in Figure 1.5., the binodal curve separates the monophasic region from the biphasic region, where all points with composition below the phase curve (*ABCD*) are in the monophasic region, while those above the line are in the biphasic region. A starting mixture composition (*M*) undergoes phase separation forming two coexisting phases, whose composition is given by the points *B* and *D*, the end points (nodes) of a tie-line [45]. The phase diagram of a ternary mixture can be represented in an orthogonal graphical representation, in which the vertical axis represents the less dense compound, in higher

quantity in the top phase, while the horizontal axis represents the densest compound that is mostly enriched in the lower phase [45]. The tie-line length (TLL) is often used to express the effect of the coexisting phases composition on the partitioned compound [45].

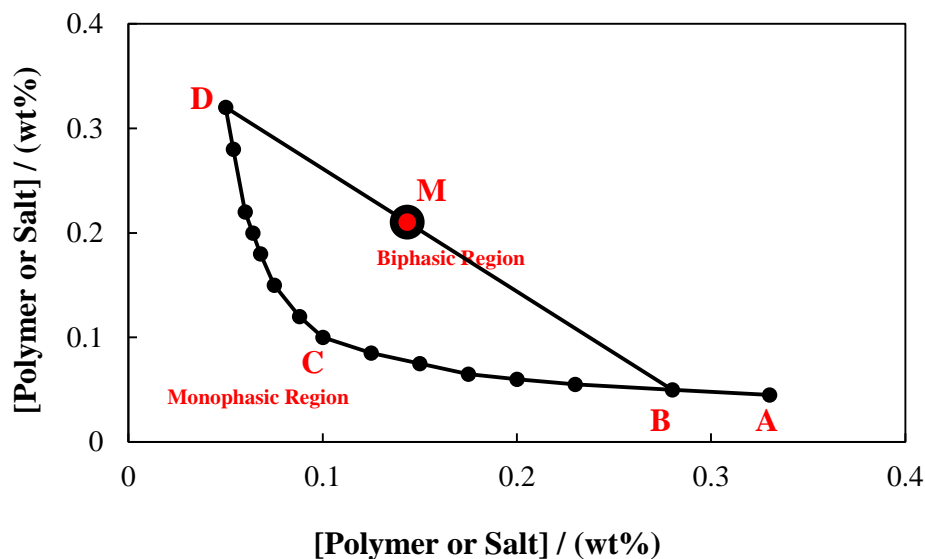


Figure 1.5. Orthogonal representation of a phase diagram (ABS). Adapted from Freire *et al.* [45].

1.4. Ionic Liquids (ILs)

Ionic liquids (ILs) were found occasionally in 1914, during the First World War, by Paul Walden, when he was testing new explosives [52]. Ethylammonium nitrate was the first synthesized ionic liquid, with a melting point of 285 K [53]. Some years later, in 1948, after the Second World War, mixtures of aluminium chloride and 1-ethylpyridinium bromide were developed for the electrodeposition of aluminium [54], which can be considered the first application of ILs. However, only in the past 30 years, research on applications and properties of ionic liquids has been more intensive, as shown in Figure 1.6. [55].

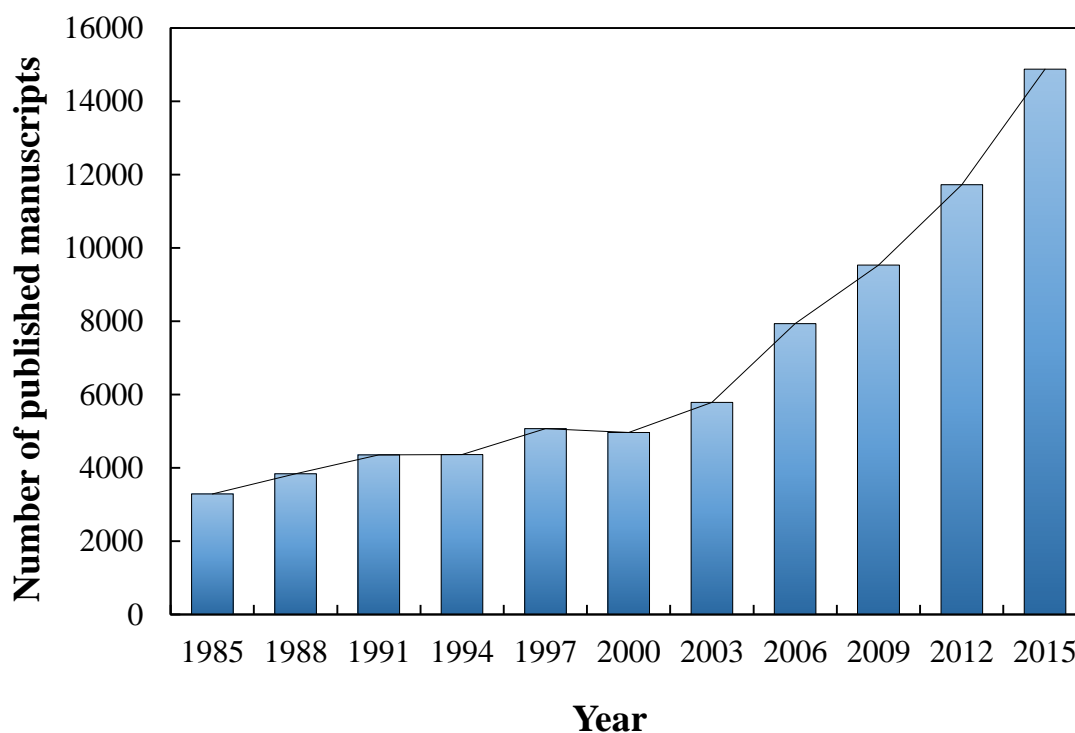


Figure 1.6. Number of published articles, *per* year, comprising ILs [55].

The ionic nature of ILs is responsible for some of the interesting and characteristic properties of ILs, including a high thermal stability and ionic conductivity, negligible vapour pressure, non-flammability and high solvation capacity for various compounds, such as organic, inorganic and organometallic compounds [56]. Indeed, some of these properties have determined their high potential to be exploited as "green solvents" and, consequently, ILs became good candidates to replace volatile organic compounds (VOCs). However, properties such as biodegradability and toxicity need also to be evaluated so that ILs can be classified as "green solvents". In other words, the fact of having negligible vapour pressure and consequently reducing the risk of air pollution, is not sufficient to ensure that these compounds are indeed "green" [57].

ILs usually consist of a large organic cation and a somewhat smaller organic or inorganic anion, which enables their liquid state at room temperature or at temperatures below 373 K [58]. Since there is a smaller number of cations than of anions, ILs are usually grouped according to the family of the cation, being the most important the pyrrolidinium, imidazolium, piperidinium, pyridinium, phosphonium and ammonium cations (Figure 1.7.).

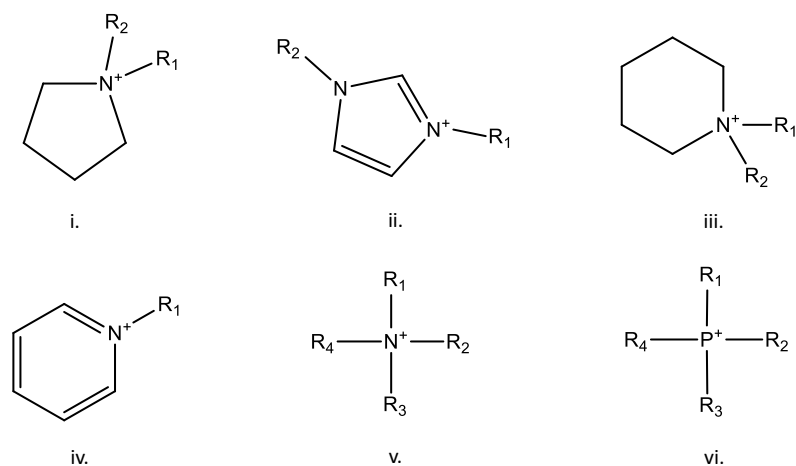


Figure 1.7. Chemical structure of IL cations: (i) pyrrolidinium, (ii) imidazolium, (iii) piperidinium, (iv) pyridinium, (v) ammonium and (vi) phosphonium.

Examples of anions of ILs are acetate, tosylate, dicyanamide, thiocyanate, methylsulfate, triflate, chloride, tetrafluoroborate, hexafluorophosphate, bis(trifluoromethylsulfonyl)imide, among others (Figure 1.8.).

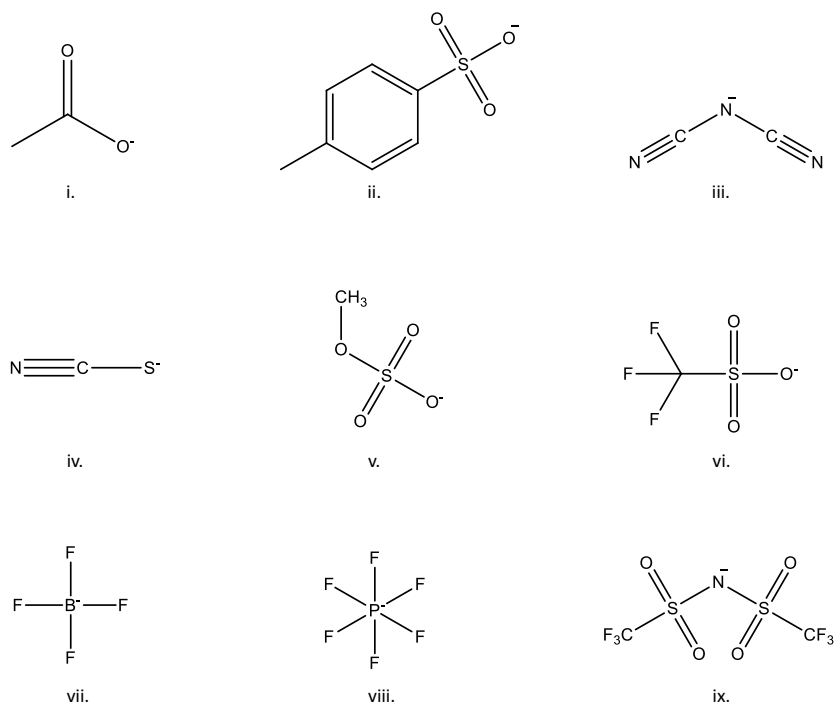


Figure 1.8. Chemical structure of IL anions: (i) acetate, (ii) tosylate, (iii) dicyanamide, (iv) thiocyanate, (v) methylsulfate, (vi) triflate, (vii) tetrafluoroborate, (viii) hexafluorophosphate and (ix) bis(trifluoromethylsulfonyl)imide.

In general, non-aromatic ILs, such as those based on pyrrolidinium- and piperidinium, are more benign than compounds based on aromatic (imidazolium and pyridinium) cations [58]. Both anion and cation influence ILs' properties, such as water and organic solvents miscibility, thermal stability, viscosity, surface tension and density [59]. This is one of the reasons why these solvents are called tuneable solvents, since there is the possibility of fine tuning their properties by the judicious choice and combination of one specific cation with one specific anion. Due to their versatility, ILs have been studied for the most diverse applications, such as in inorganic synthesis [60], catalysis [61], polymerization [62], chemical or enzymatic reactions [63,64], biofuels [65], extraction of metal ions [66], in the extraction of (bio)molecules [67,68], in chromatographic separations [69], among others.

Rogers and co-workers [70] pioneered the use of ILs in the implementation of ABS, by mixing ILs with aqueous solutions of inorganic salts. The use of ABS containing ILs is more advantageous than the use of ABS containing conventional polymer, due to their low viscosity, which affords a fast and clear phase separation, and due to their higher extraction performance [71]. The successful application of IL-based ABS in the extraction of a large variety of solutes, such as proteins [72], heavy metal ions [66], small organic molecules [73], antibiotics [74] and antioxidants [75] has already been demonstrated. One of the main advantages of using ILs in the formation of ABS consists on the ability to manipulate the ABS phases polarities and affinities [45] through the use of the built knowledge on how the ILs structure is linked to their properties, thus allowing high extraction efficiencies and purities to be attained. In general, it is important to previously know the physicochemical and biological properties of ILs so that the efficiency and benign nature of ABS can be evaluated [76].

The interest in ABS formed by ILs has significantly increased in the past few years, as seen in Figure 1.9. [55]. In particular, IL-based ABS have been used in the extraction/purification of compounds found in natural sources, *e.g.*, vanillin [77], gallic, vanillic and syringic acids [75], and nicotine, theobromine, theophylline and caffeine [78]. More recently, Keremedchieva *et al.* [79] extracted glaucine from *Glaucium flavum* Cr. and applied ABS for purification purposes.

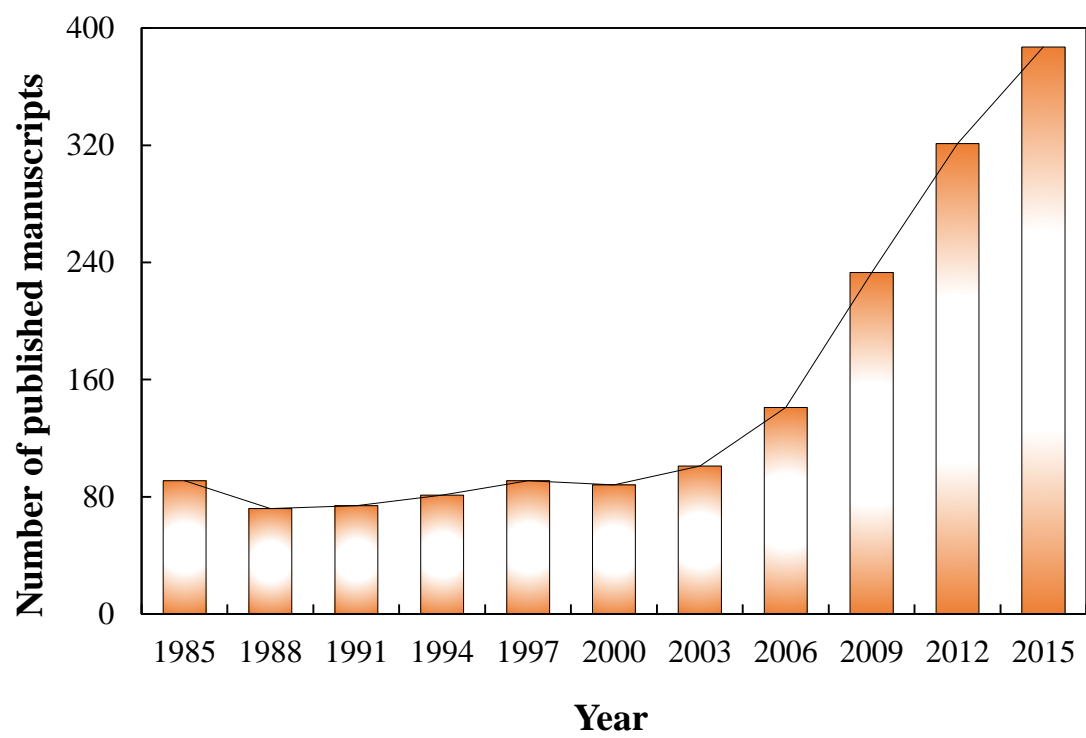


Figure 1.9. Number of published manuscripts *per* year on ABS with ILs [55].

2. Phase diagrams for ABS containing Cholinium-based ILs

2.1. Introduction

In recent years, there have been major innovations in IL-based ABS through the use of either novel ILs or new phase splitting promoters [45]. Great improvements in the development of sustainable and biocompatible ILs have been pushing the field to the so-called bio-ionic liquids which are fully composed of natural compounds, such as vitamins, amino acids and naturally occurring acids, among others [80,81]. A new sub-family of ammonium ILs has been developing at a fast pace through the use of ILs based on the cholinium cation. Cholinium chloride ([Ch]Cl), usually called choline, is used as an essential nutrient and it is known to be biodegradable, non-toxic and easy to produce [81]. Cholinium-based ILs have shown low toxicity and good biodegradability [50]. Therefore, the combination of the cholinium cation with anions derived from natural nontoxic compounds provides a suitable environmental-friendly and non-toxic pathway to develop new extraction schemes.

Although a large number of IL-based ABS have been reported in the literature, most of these studies refer to imidazolium-based ILs combined with inorganic salts [45]. Aiming at finding more benign alternatives to the salting-out agents, amino acids [82], carbohydrates [76,83] and polymers [84–88] have been considered as phase-forming components of IL-based ABS. Due to their biodegradable and non-toxic nature, the use of these compounds is highly advantageous. Although polymers, such as polyethylene glycol (PEG) or polypropylene glycol (PPG), have been used to form cholinium-based ABS [84–88], amino acids and carbohydrates have never been used due to their weak salting-out ability. Indeed, recently, it was demonstrated that cholinium-based ILs do not undergo phase splitting in presence of aqueous solutions of carbohydrates [83]. On the other hand, it has been shown that the combined use of cholinium-based ILs with PEG to create ABS yields unconventional phase splitting mechanisms that can be used to tune the extraction efficiencies of a given solute [87,89].

In this work, the ability of cholinium-based ILs to form ABS combined with dextran, maltodextrin, polyvinylpyrrolidone, PPG 400, PEG 400 and K_3PO_4 was evaluated followed by the assessment of their ability to extract theobromine from aqueous solutions.

2.2. Experimental Section

2.2.1. Materials

The ILs studied in this work were (2-hydroxyethyl)trimethylammonium propanoate, [Ch][Pro]; (2-hydroxyethyl)trimethylammonium butanoate [Ch][But]; (2-hydroxyethyl)trimethylammonium pentanoate, [Ch][Pent]; (2-hydroxyethyl)trimethylammonium hexanoate, [Ch][Hex]; (2-hydroxyethyl)trimethylammonium nonanoate, [Ch][Non]; (2-hydroxyethyl)trimethylammonium adipate (1:1), [Ch][Adi_{1:1}]; (2-hydroxyethyl)trimethylammonium adipate (1:2), [Ch][Adi_{1:2}]; (2-hydroxyethyl)trimethylammonium azelate, [Ch][Aze]; (2-hydroxyethyl)trimethylammonium perfluoroheptanoate, [Ch][PFHept]; (2-hydroxyethyl)trimethylammonium perfluorooctanoate, [Ch][PFOct]; (2-hydroxyethyl)trimethylammonium perfluorobutanoate, [Ch][PFBut]; and (2-hydroxyethyl)trimethylammonium trifluoroacetate, [Ch][TFAc]. These ILs were synthesized and kindly provided by ITQB, *Instituto de Tecnologia Química e Biológica António Xavier*, New University of Lisbon. In addition to these ILs, the following were also used, namely, (2-hydroxyethyl)trimethylammonium acetate, [Ch][Ac] (purity > 98 wt %) and (2-hydroxyethyl)trimethylammonium dihydrogen phosphate, [Ch][DHph] (purity > 98 wt %), both purchased from Iolitec. The ILs (2-hydroxyethyl)trimethylammonium chloride, [Ch]Cl (purity > 99 wt %); (2-hydroxyethyl)trimethylammonium bitartrate, [Ch][Bit] (purity of 100 wt %); (2-hydroxyethyl)trimethylammonium bicarbonate, [Ch][Bic] (purity ~ 80 wt %); and (2-hydroxyethyl)trimethylammonium dihydrogen citrate, [Ch][DHcit] (purity ≥ 98 wt %), were also used and all were acquired from Sigma–Aldrich. The chemical structures of the investigated ILs are depicted in Figure 2.1. It should be pointed out that all ILs comprise the common (2-hydroxyethyl)trimethylammonium cation. The purity of all ILs was checked by ¹H and ¹³C NMR. Furthermore and to know the amount of water before the determination of the ternary systems, the water content of each IL was determined by Karl Fischer titration using a Metrohm 831 Karl Fischer coulometer. The water contents ranged between 0.2 and 20 wt%. The reagent employed was Hydranal® - Coulomat AG from Riedel-de Haën.

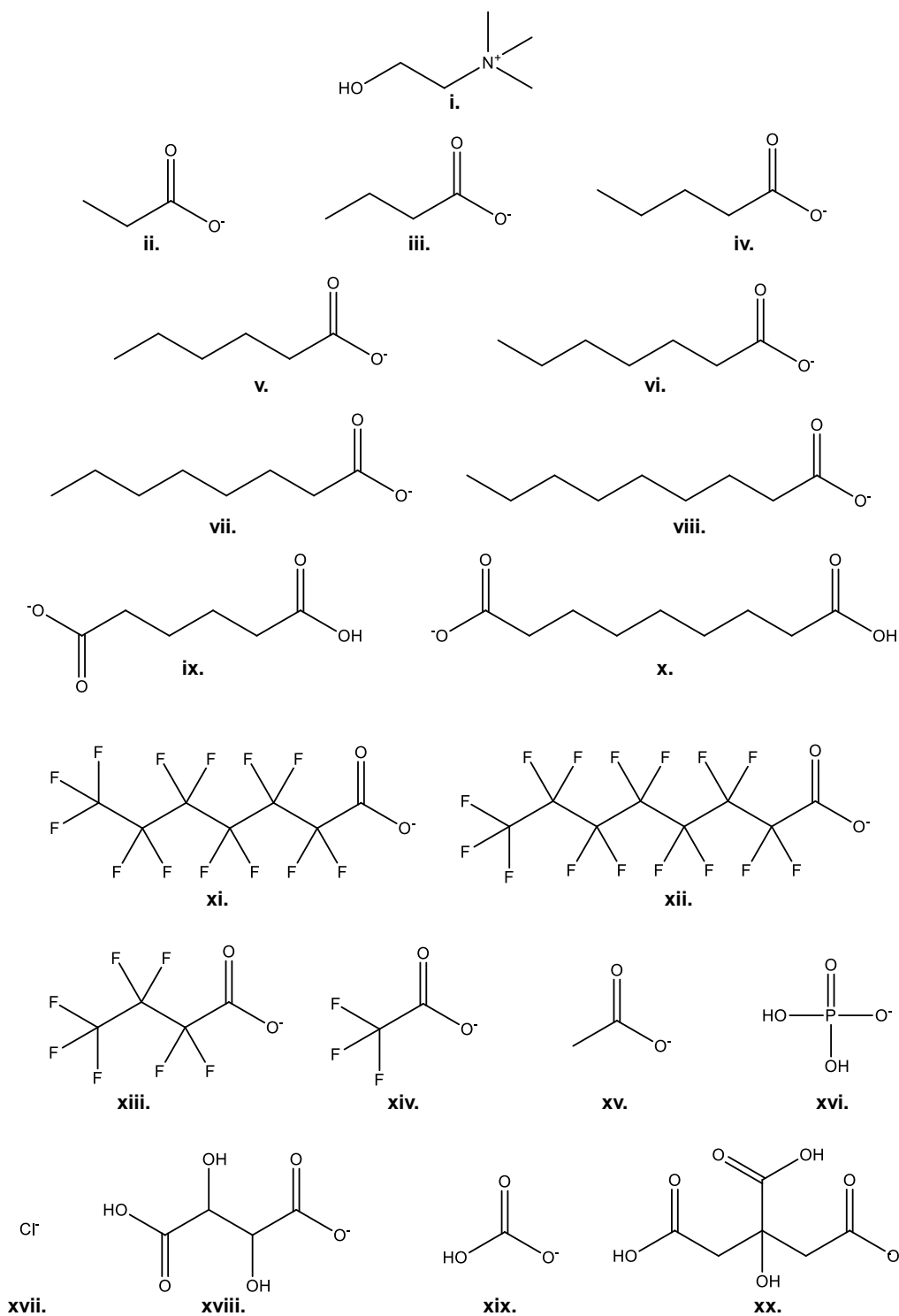


Figure 2.1. Chemical structures of the ions of the ILs investigated: (i.) [Ch]⁺, (ii.) [Pro]⁻, (iii.) [But]⁻, (iv.) [Pent]⁻, (v.) [Hex]⁻, (vi.) [Hept]⁻, (vii.) [Oct]⁻, (viii.) [Non]⁻, (ix.) [Adi]⁻, (x.) [Aze]⁻, (xi.) [PFHept]⁻, (xii.) [PFOct]⁻, (xiii.) [PFBut]⁻, (xiv.) [TFAc]⁻, (xv.) [Ac]⁻, (xvi.) [DHph]⁻, (xvii.) Cl⁻, (xviii.) [Bit]⁻, (xix.) [Bic]⁻ and (xx.) [DHcit]⁻.

The salting-out species investigated were two dextrans ($C_6H_{10}O_5$)_n of different average molecular weights, 40,000 g.mol⁻¹ (40 kDa) and 100,000 g.mol⁻¹ (100 kDa); two maltodextrins of different dextrose equivalents, namely 13.0-17.0 and 16.5-19.5; polyvinylpyrrolidone (PVP) with molecular weights 29,000 g.mol⁻¹ (29 kDa) and 40,000 g.mol⁻¹ (40 kDa); polypropylene glycol 400 g.mol⁻¹ (PPG 400); and inorganic salt potassium phosphate tribasic, K₃PO₄ (purity ≥ 98.0 wt %), all acquired from Sigma–Aldrich. Polyethylene glycol 400 g.mol⁻¹ (PEG 400), from Fluka, was also used. The chemical structure of the salting-out species are presented in Figure 2.2.

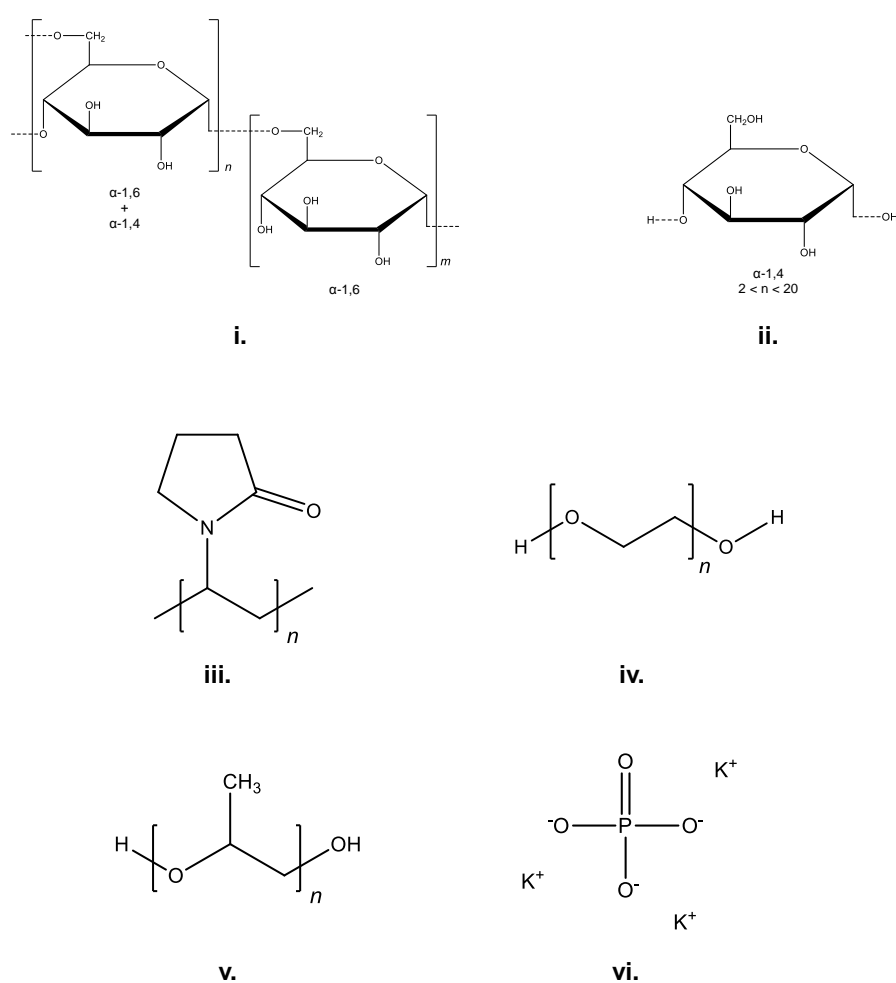


Figure 2.2. Chemical structures of the salting-out species investigated: (i.) Dextran, (ii.) Maltodextrin, (iii.) PVP; (iv.) PPG, (v.) PEG and (vi.) K₃PO₄.

Ultra-pure water, double distilled, passed by a reverse osmosis system and further treated with a Milli-Q plus 185 water purification equipment was used.

2.2.2. Experimental Procedure

The capacity of aqueous solutions of cholinium-based ILs to undergo phase splitting with several salting-out species was initially tested. The following ABS were tested using polysaccharides and PVP: Dextran 40 kDa with [Ch][PFOct]; Dextran 100 kDa with [Ch][Non], [Ch][Adi_{1:1}], [Ch][Adi_{1:2}], [Ch][Aze], [Ch][PFHept], [Ch][PFOct], [Ch][PFBut] and [Ch][TFAc]; Maltodextrin (13.0-17.0) with [Ch][Adi_{1:1}], [Ch][Adi_{1:2}] and [Ch][Aze]; Maltodextrin (16.5-19.5) with [Ch][Non] and [Ch][Adi_{1:1}]; PVP 29 kDa with [Ch][Adi_{1:1}], [Ch][Adi_{1:2}] and [Ch][Aze]; and PVP 40 kDa with [Ch][Non]. However, no ABS formation could be observed in these systems.

Consequently, other salting-out compounds were selected, namely PPG 400, PEG 400 and K₃PO₄ and the following ABS were considered: PPG 400 with [Ch][Aze], [Ch][Adi_{1:1}], [Ch][Adi_{1:2}], [Ch][PFBut], [Ch][PFHept], [Ch][PFOct], [Ch][TFAc], [Ch][DHcit], [Ch][DHph], [Ch]Cl, [Ch][Bit], [Ch][Bic], [Ch][Ac] and [Ch][Non]; PEG 400 with [Ch][Aze], [Ch][Adi_{1:1}], [Ch][Adi_{1:2}], [Ch][PFOct], [Ch][DHcit], [Ch][DHph], [Ch]Cl, [Ch][Bit], [Ch][Bic], [Ch][Ac] and [Ch][Non]; and K₃PO₄ with [Ch][Adi_{1:1}], [Ch][Adi_{1:2}], [Ch][DHcit], [Ch][DHph], [Ch]Cl, [Ch][Bit], [Ch][Bic], [Ch][Ac], [Ch][Pro], [Ch][But], [Ch][Pent], [Ch][Hex] and [Ch][Non]. No ABS formation could be observed in the systems consisting of PPG 400 with [Ch][PFBut], [Ch][PFHept], [Ch][PFOct] and [Ch][Non]; PEG 400 with [Ch][Aze], [Ch][Adi_{1:1}], [Ch][Adi_{1:2}], [Ch][PFOct] and [Ch][Non]; and K₃PO₄ with [Ch][Adi_{1:1}], [Ch][DHcit], [Ch][DHph], [Ch][Bit] and [Ch][Bic]. The phase diagrams of some of the proposed systems, namely PPG 400 with [Ch]Cl, [Ch][DHcit], [Ch][DHph] and [Ch][Bit]; PEG 400 with [Ch][Ac], [Ch][DHcit], [Ch][DHph], [Ch]Cl, [Ch][Bit] and [Ch][Bic]; and K₃PO₄ with [Ch]Cl, are already published in the open literature [84,90,91].

The binodal curves were determined at 298 K and atmospheric pressure through the cloud point titration method [92]. The cloud point titration method consists on the drop wise addition of the IL aqueous solutions to the salting-out species aqueous solution, or *vice-versa*, under constant stirring until the cloud point (biphasic region) is observed, followed by the addition of water, drop wise, until a clear solution (monophasic region) is obtained, as shown in Figure 2.3.

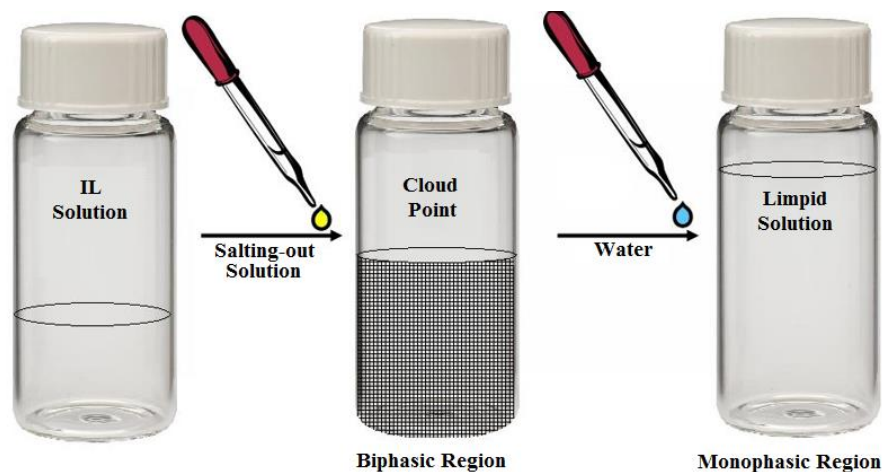


Figure 2.3. Schematic representation of the cloud point titration method.

ILs aqueous solutions were prepared with concentrations ranging from 50 wt% for [Ch][Non] to 80 wt% for [Ch][Bic]. As to salting-out species, PEG 400 and PPG 400 were used in their pure form, whereas solutions of K_3PO_4 with concentrations ranging from 40 wt% and 55 wt% were used.

All the solutions were prepared using an analytical balance, Mettler Toledo Excellence XS205 DualRange ($\pm 10^{-4}$ g), while the solutions were homogenized using a vortex VWRTM International, VV3.

The experimental data expressed in percentage weight fraction were fitted using the correlation originally proposed by Merchuk *et al.* [93], described according to equation 2.1.,

$$[\text{IL}] = A \exp[(B[\text{SO}]^{0.5}) - (C[\text{SO}]^3)] \quad (\text{eq 2.1.})$$

where [IL] and [SO] are the weight fraction percentages of ionic liquid and salting-out species, respectively, and the coefficients A , B and C are the parameters obtained through regression of the experimental data.

Tie-lines (TLs) were obtained by determining the amount of each component in each coexisting phase. For the determination of TLs, the following system of 4 equations (equation 2.2. to 2.5.) was used, and the values of the top and bottom phase concentrations ($[\text{IL}]_{\text{IL}}$, $[\text{SO}]_{\text{IL}}$, $[\text{IL}]_{\text{SO}}$, $[\text{SO}]_{\text{SO}}$) [93] estimated according to:

$$[\text{IL}]_{\text{IL}} = A \exp[(B[\text{SO}]_{\text{IL}}^{0.5}) - (C[\text{SO}]_{\text{IL}}^3)] \quad (\text{eq 2.2.})$$

$$[\text{IL}]_{\text{SO}} = A \exp[(B[\text{SO}]_{\text{SO}}^{0.5}) - (C[\text{SO}]_{\text{SO}}^3)] \quad (\text{eq 2.3.})$$

$$[\text{IL}]_{\text{IL}} = \frac{[\text{IL}]_{\text{M}}}{\alpha} - \left(\frac{1-\alpha}{\alpha}\right) [\text{IL}]_{\text{SO}} \quad (\text{eq 2.4.})$$

$$[\text{SO}]_{\text{IL}} = \frac{[\text{SO}]_{\text{M}}}{\alpha} - \left(\frac{1-\alpha}{\alpha}\right) [\text{SO}]_{\text{SO}} \quad (\text{eq 2.5.})$$

where $[\text{IL}]_{\text{IL}}$ and $[\text{IL}]_{\text{SO}}$ are the IL weight fraction in the IL-rich phase and salting-out species-rich phase, respectively, $[\text{SO}]_{\text{IL}}$ and $[\text{SO}]_{\text{SO}}$ are the salting-out species weight fraction in the IL-rich phase and salting-out-species-rich phase, respectively, and α is the ratio between the weight of the top phase and the total weight of both phases. The solution of this system provides the mass fraction percentages of IL and salting-out species in top and bottom salt-rich phases, allowing the representation of TLs.

The Tie-Line Length (TLL) is usually calculated using equation 2.6.,

$$\text{TLL} = \sqrt{([\text{SO}]_{\text{IL}} - [\text{SO}]_{\text{SO}})^2 + ([\text{IL}]_{\text{IL}} - [\text{IL}]_{\text{SO}})^2} \quad (\text{eq 2.6.})$$

This parameter is usually linked to separation efficiencies since the largest the TLL the greatest the difference between the compositions of the two phases in equilibrium, and thus, the easy it is to separate a given solute between the two phases.

2.3. Results and Discussion

The ability to form ABS with three salting-out agents, namely PPG 400, PEG 400 and K_3PO_4 , and cholinium-based ILs, namely $[\text{Ch}][\text{Ac}]$, $[\text{Ch}][\text{Pro}]$, $[\text{Ch}][\text{But}]$, $[\text{Ch}][\text{Pent}]$, $[\text{Ch}][\text{Hex}]$, $[\text{Ch}][\text{Non}]$, $[\text{Ch}][\text{Adi}_{1:1}]$, $[\text{Ch}][\text{Adi}_{1:2}]$, $[\text{Ch}][\text{Aze}]$, $[\text{Ch}][\text{PFBut}]$, $[\text{Ch}][\text{PFHept}]$, $[\text{Ch}][\text{PFOct}]$, $[\text{Ch}][\text{TFAc}]$, $[\text{Ch}][\text{DHcit}]$, $[\text{Ch}][\text{DHph}]$, $[\text{Ch}]\text{Cl}$, $[\text{Ch}][\text{Bit}]$ and $[\text{Ch}][\text{Bic}]$, was here evaluated. TLs and binodal curves were determined at 298 K and atmospheric pressure. New phase diagrams are here presented for PPG 400 with $[\text{Ch}][\text{Adi}_{1:1}]$, $[\text{Ch}][\text{Adi}_{1:2}]$, $[\text{Ch}][\text{Aze}]$, $[\text{Ch}][\text{Ac}]$ and $[\text{Ch}][\text{TFAc}]$; and K_3PO_4 with $[\text{Ch}][\text{Adi}_{1:2}]$,

[Ch][Ac], [Ch][Pro], [Ch][But], [Ch][Pent], [Ch][Hex] and [Ch][Non], while the phase diagrams corresponding to PPG 400 with [Ch][DHph], [Ch]Cl, [Ch][Bit] and [Ch][DHcit]; PEG 400 with [Ch][DHph], [Ch][Bic], [Ch][Ac], [Ch][Bit], [Ch]Cl and [Ch][DHcit]; and K_3PO_4 with [Ch]Cl were taken from the literature [84,90,91].

Initially, the formation of ABS consisting on PPG 400 or PEG 400 combined with cholinium-based ILs that have perfluorinated anions, namely [Ch][TFAc], [Ch][PFBut], [Ch][PFHept] and [Ch][PFOct], was addressed. However, no turbidity was observed for any of the systems, with the exception of [Ch][TFAc] + PPG 400. This may be related to the nature of the IL and/or their relative affinity for water and possible interactions between the IL and PEG/PPG. Usually in PEG and PPG containing systems, the ILs can be the salting-out agents since they have higher affinity for water than PEG or PPG [86,88]. In this case, and despite the more hydrophilic nature of the cholinium family of ILs, the long alkyl perfluoroalkyl chains of the anion probably contribute to a somewhat less hydrophilic IL and thus to their non-ability to create ABS with both polymers.

The next step in this work, and since the previous systems did not form ABS, consisted on the evaluation of the phase forming ability of systems composed of PPG 400 or PEG 400 and [Ch][Ac], [Ch][Non], [Ch][Adi_{1:1}], [Ch][Adi_{1:2}], [Ch][Aze], [Ch][DHcit], [Ch][DHph], [Ch]Cl, [Ch][Bit], [Ch][Bic]. Since ABS data for PPG 400 with [Ch][DHph], [Ch][DHcit], [Ch]Cl and [Ch][Bit]; and PEG 400 with [Ch][Ac], [Ch][DHcit], [Ch][DHph], [Ch]Cl, [Ch][Bit], [Ch][Bic] are available in the literature [84,90], the phase diagrams for these systems were not determined in this work. The formation of two phases was not observed in the case of PEG 400 with [Ch][Aze], [Ch][Adi_{1:1}], [Ch][Adi_{1:2}] and [Ch][Non]; and PPG 400 with [Ch][Non].

The phase diagrams measured in this work with PPG 400 and PEG 400 are shown in Figures 2.4. and 2.5., respectively. The ternary phase diagrams that were previously reported with PPG 400 and PEG 400 and cholinium-based ILs [84,90] are also included for comparison purposes. The experimental data of the systems composition in weight fraction are available in Appendix A (Tables A.1.1 to A.2.3) and in molality in Appendix B (Figures B.1.1. to B.1.3.).

In all studied ABS, the upper phase corresponds to the PPG 400/PEG 400-rich aqueous phase, while the lower phase corresponds to the IL-rich aqueous phase.

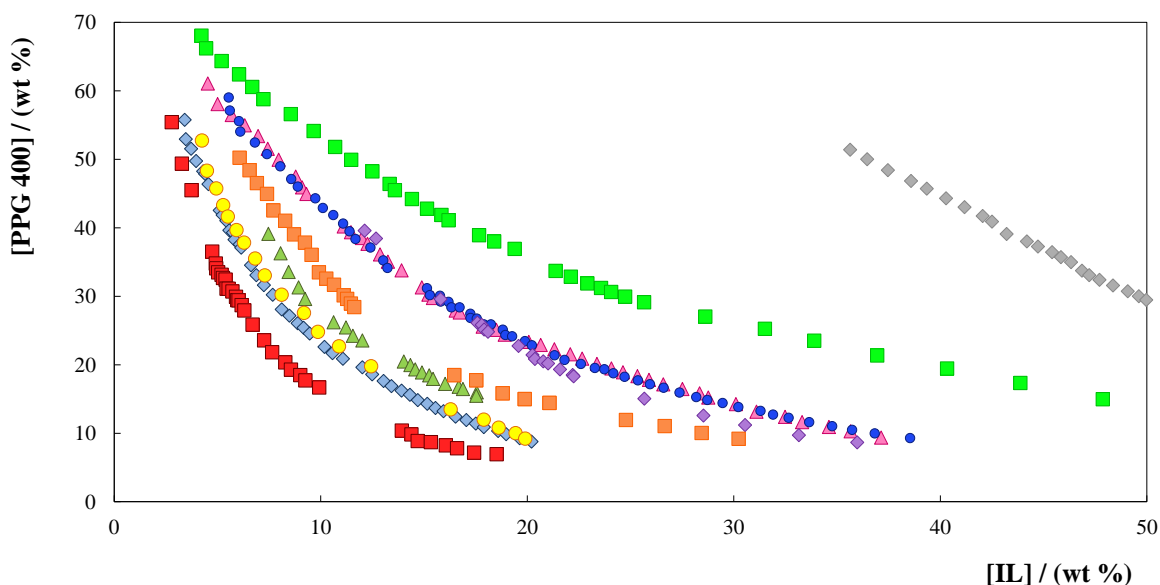


Figure 2.4. Ternary phase diagrams for systems composed of IL + PPG 400 + water, at 298 K and atmospheric pressure: (■) [Ch][DHph] [90], (◆) [Ch][Ac], (▲) [Ch]Cl [90], (□) [Ch][Bit] [90], (●) [Ch][Bic], (◇) [Ch][DHcit] [90], (△) [Ch][Adi_{1:1}], (●) [Ch][Adi_{1:2}], (■) [Ch][Aze], and (◇) [Ch][TFAc].

For the phase diagrams with PEG 400, although all the results were taken from the literature, they are shown in Figure 2.5. since the knowledge of these phase diagrams is important for the following sections.

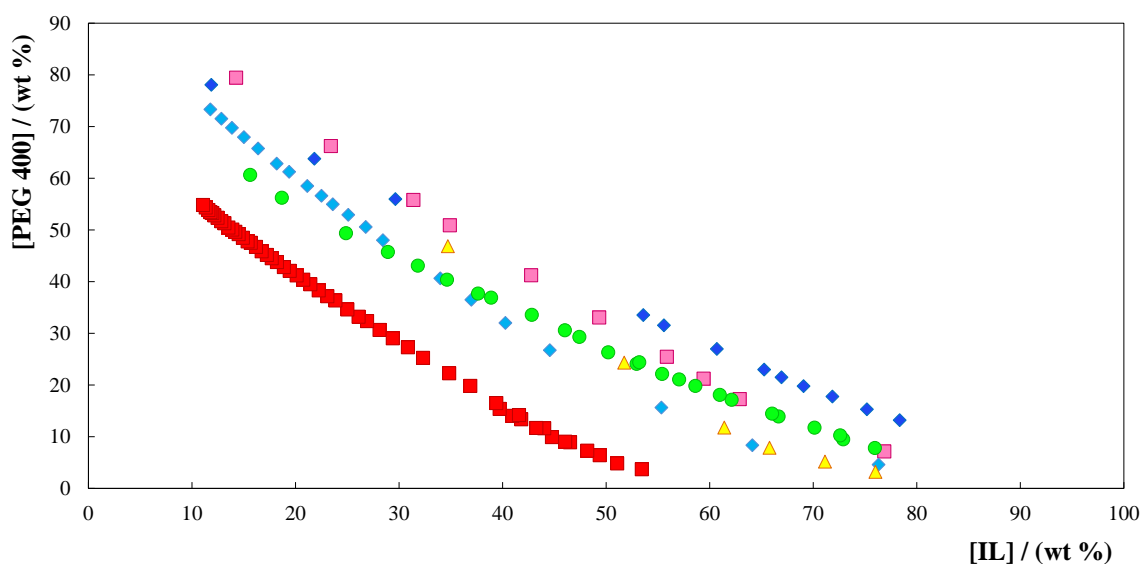


Figure 2.5. Ternary phase diagrams for systems composed of IL + PEG 400 + water, at 298 K and atmospheric pressure: (■) [Ch][DHph] [84], (◆) [Ch][Bic] [84], (▲) [Ch][Ac] [84], (●) [Ch][Bit] [84], (□) [Ch]Cl [84], and (◇) [Ch][DHcit] [84].

Since the cholinium cation is common to all ILs used in this work, the obtained results reflect the effect of the IL anion in the formation of ABS with PPG 400 and PEG 400. Ternary phase diagrams presenting larger monophasic regions indicate that a larger amount of IL and/or PPG 400 and PEG 400 needs to be added to form an ABS and are thus not very useful for extraction purposes due to the large amount of IL and salting-out agent required.

According to the binodal curves determined in this study and depicted in Figure 2.4., and for a common IL composition of 10 wt%, the ability of the studied ionic liquids to form ABS with PPG 400 is the following: [Ch][DHph] > [Ch][Ac] > [Ch][Bic] > [Ch]Cl > [Ch][Bit] > [Ch][DHcit] \approx [Ch][Adi_{1:1}] \approx [Ch][Adi_{1:2}] > [Ch][Aze] > [Ch][TFAc]. For ABS containing PEG 400, depicted in Figure 2.5., considering the IL at 50 wt%, the order of ABS-forming ability is: [Ch][DHph] > [Ch][Bic] > [Ch][Ac] \approx [Ch][Bit] > [Ch]Cl > [Ch][DHcit]. With both polymers, it can be observed that ILs with anions derived from carboxylic acids with shorter alkyl side chains have higher affinity for water and have more facility to induce the formation of a second liquid phase. In general, [Ch][DHph] is the IL that has a higher capacity to promote ABS, being in accordance with the large polar surface of the anion [45]. As observed previously with ABS formed by PEG 400 [84], also with PPG 400, [Ch][DHcit] has a low ability to create ABS. One explanation for this fact may be the self-aggregation of the citrate anion as a result of the intermolecular hydrogen-bonding between the hydroxyl hydrogen atoms and one of the oxygens of the central carboxylic group [94].

Finally, the ability of cholinium-based ILs, namely [Ch][Adi_{1:1}], [Ch][Adi_{1:2}], [Ch][DHcit], [Ch][DHph], [Ch][Bit], [Ch][Bic], [Ch][Ac], [Ch][Pro], [Ch][But], [Ch][Pent], [Ch][Hex] and [Ch][Non] to form ABS with K₃PO₄ salt (a strong salting-out agent [95–97]) was evaluated. However, the formation of cholinium-based ABS with K₃PO₄ was not observed for the systems containing [Ch][Adi_{1:1}], [Ch][DHph], [Ch][DHcit], [Ch][Bit] and [Ch][Bic]. In Figure 2.6., the phase diagrams of the remaining cholinium-based ILs able to form ABS with K₃PO₄ are represented.

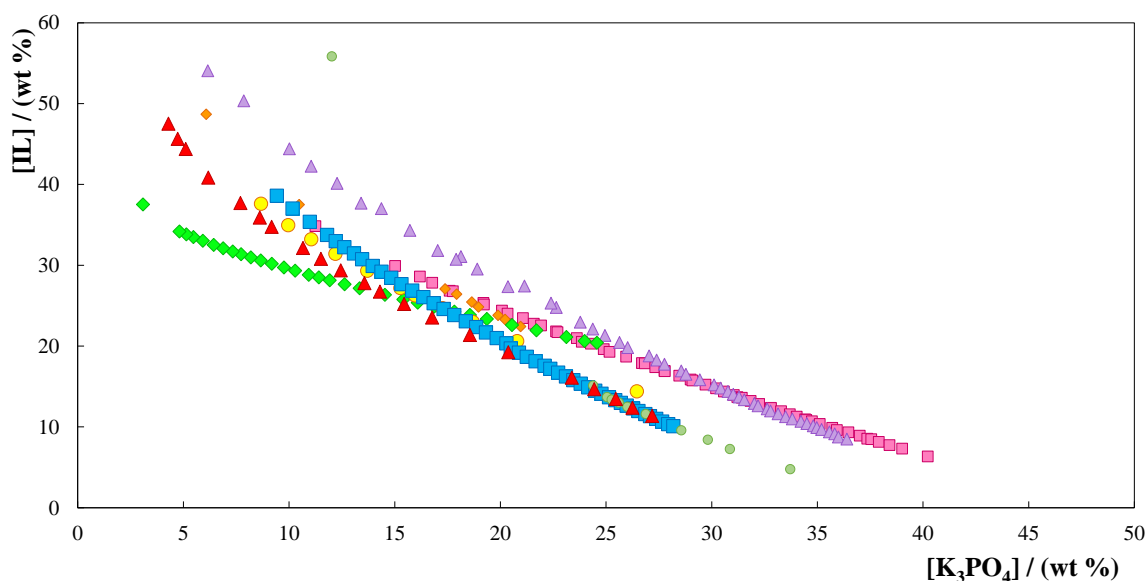


Figure 2.6. Ternary phase diagrams for systems composed of IL + K_3PO_4 + water, at 298 K and atmospheric pressure: (◆) [Ch][Adi_{1:2}], (▲) [Ch]Cl [91], (■) [Ch][Ac], (●) [Ch][Pro], (▲) [Ch][But], (●) [Ch][Pent], (■) [Ch][Hex] and (◆) [Ch][Non].

According to the binodal curves shown in Figure 2.6, with 20 wt% of K_3PO_4 , the ability of ILs to form ABS with K_3PO_4 follows the order: [Ch][But] > [Ch][Hex] > [Ch][Pro] > [Ch][Pent] \approx [Ch][Non] \approx [Ch][Adi_{1:2}] > [Ch][Ac] > [Ch]Cl. This order shows that there is a very small difference between the phase equilibria data of [Ch][Pro] \approx [Ch][But] \approx [Ch][Pent] \approx [Ch][Hex] indicating, as shown by Patinha *et al.* [98], that the influence of the alkyl chain length at the anion is less pronounced than that of the cation.

The experimental data were correlated using the relationship proposed by Merchuk *et al.* [93] described in the previous section (eq 2.1. to eq 2.5.). Regression parameters and corresponding standard deviations (σ) as well as the respective correlation coefficients are shown in Table A.3.1., in Appendix A. In general, good correlations were obtained. The values of the composition of the phases in equilibrium together with their respective lengths (TLL) are shown in Table C.1.1., in Appendix C, as well as the initial composition of each system. Examples of TLs obtained are shown in Appendix B, in Figures B.2.1 to B.2.3.

Regarding the evaluation of the investigated systems for the extraction of theobromine, the same initial mixture composition (30 wt% of IL and 30 wt% of salting-out species) was used for all systems in the following section, with the exception of the ABS formed by [Ch][Bic] + PPG 400 (24 wt% of IL and 30 wt% of salting-out species), [Ch]Cl + K_3PO_4

(20 wt % of IL and 30 wt % of salt) and [Ch][DHph]⁺ PEG 400 (33 wt % of IL and 33 wt % of polymer).

3. Extraction of Theobromine using IL- based ABS

3.1. Introduction

ABS were first proposed by Albertsson [44] as systems composed of water and two solutes, such as polyethylene glycol (PEG) and potassium phosphate [99]. More recently, ABS formed by ionic liquids (ILs) and salts were proposed [100,101]. These systems present significant advantages, such as simplicity, low cost, and the ability to provide high yields and purification factors. Through their constituent's choice, it is possible to obtain the biomolecule of interest in one phase and the contaminants in the opposite one, thus allowing the purification of target species [1]. In this Chapter, IL-based ABS were investigated in order to extract commercial theobromine for one of the phases aiming at inferring on their capacity as purification strategies without losses of the alkaloid for the opposite phase. In fact, several works already exist in the literature supporting the high performance of IL-based ABS to extract and purify small molecules derived from natural sources [49,51].

Table 3.1. depicts some thermophysical properties of theobromine at 298.15 K [102,103], while Figure 3.1 shows its chemical structure.

Table 3.1. Thermophysical properties of theobromine [102,103].

Molar mass (g.mol⁻¹)	Density (g.cm⁻³)	Melting point (K)	Solubility in water (g.dm⁻³)	pKa	Log K_{ow}
180.16	1.50	630.15	<1	9.90	-0.78

The theobromine content in food products (mg/g product) is quite variable as it can be seen from the following examples: a dark chocolate has 4.42-7.56, milk chocolate has 1.88-1.90, cocoa powder has 18.90-26.00, tea has 3.00-9.00, coffee (filter/percolated) has 0.04, and instant coffee has 0.06-0.31 [17,104].

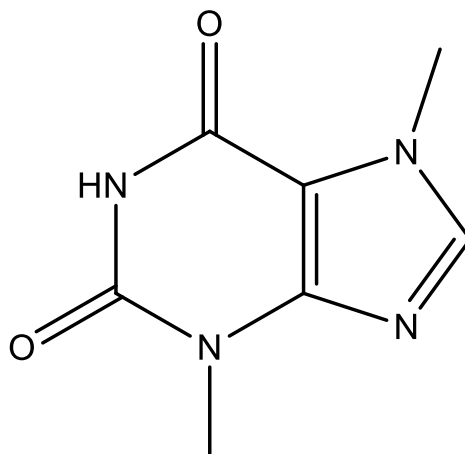


Figure 3.1. Chemical structure of theobromine.

The theobromine absorption in the human digestive tract is slower compared with caffeine, taking about 2.5 hours, while caffeine takes only 0.5 h [105]. Their metabolism occurs by demethylation of the cytochrome P450 enzyme (CP₄₅₀), being divided into 3-methylxanthine and 7-methylxanthine. Subsequently, 7-methylxanthine is metabolized to 7-methyluric acid by xanthine oxidase [106]. The main mechanism of action of theobromine is the inhibition of phosphodiesterases and the adenosine receptors blockade [23,107]. Accordingly, theobromine can be considered as a safe and natural alternative for the treatment of certain human diseases and it is used as a lead compound for the development of new drugs [23,107].

3.2. Experimental Section

3.2.1 Materials

The ILs and salting-out species used in the extraction of commercial theobromine employing ABS were described in Chapter 2, in the Experimental Section. The chemical structures of the investigated ILs and salting-out species are depicted in Chapter 2, in Figures 2.1. and Figure 2.2., respectively. Commercial theobromine was acquired from Sigma-Aldrich, with purity ≥ 99 wt %. Ultra-pure water, double distilled, passed by a reverse osmosis system and further treated with a Milli-Q plus 185 water purification equipment was used.

3.2.2. Experimental Procedure

After the determination of the phase diagrams and respective TLs, in almost all systems a ternary mixture with a common composition (30 wt % of salting-out species, 30 wt % of IL and 40 wt % of an aqueous solution containing theobromine) within the biphasic region was prepared, with a total weight of 1 g. Only in three systems, different compositions of the initial mixture were used, namely for the ABS formed by [Ch][Bic] and PPG 400 (24 wt % of IL and 30 wt % of salt), [Ch]Cl and K₃PO₄ (20 wt % of IL and 30 wt % of salt) and [Ch][DHph] and PEG 400 (33 wt % of IL and 33 wt % of polymer). A theobromine solution with a concentration of *circa* 0.2 g.L⁻¹ was used for the evaluation of the ABS extraction efficiencies. All mixtures were prepared using an analytical balance, Mettler Toledo Excellence XS205 DualRange ($\pm 10^{-4}$ g).

The initial mixture was vigorously stirred, and then centrifuged for 30 min at 12000 rpm and at 298 K to assure the complete separation of the two aqueous phases. After a careful separation of both phases, the quantification of theobromine in the two phases was carried by UV-spectroscopy, using a Sinergy|HTmicroplate reader, BioTek, at 273 nm, being the maximum observed in this work and in close agreement with literature [2]. At least two individual experiments were performed for each ABS in order to determine the average of the percentage extraction efficiency of theobromine (% EE_{TB}), as well as the respective standard deviations. The interference of the salting-out species and ILs with the quantification method was also ascertained and blank control samples were always used.

The % EE_{TB} is defined as the percentage ratio between the amount of theobromine in the IL-rich aqueous phase to that in the total mixture, and is defined according to equation 3.1.

$$\% EE_{TB} = \frac{\text{Conc}_{TB}^{IL} \times w_{IL}}{(\text{Conc}_{TB}^{IL} \times w_{IL}) + (\text{Conc}_{TB}^{SO} \times w_{SO})} \times 100 \quad (\text{eq 3.1.})$$

where w_{IL} and w_{SO} are the weight of the IL-rich phase and of the salting-out-rich-phase, respectively, and Conc_{TB}^{IL} and Conc_{TB}^{SO} are the concentration of theobromine (TB) in the IL-rich and in the salting-out-rich aqueous phases, respectively [93].

3.3. Results and Discussion

In the investigated cholinium-based ABS, when PPG 400 and PEG 400 are used, the polymer-rich aqueous phase corresponds to the top phase, while the bottom phase is the IL rich-phase. On the other hand, when K_3PO_4 is used, the salt-rich aqueous phase corresponds to the bottom phase while the top phase is the IL-rich phase.

The detailed results obtained for the extraction efficiencies of theobromine (% EE_{TB}) are depicted in Figure 3.2. and are presented in Table D.1., in Appendix D.

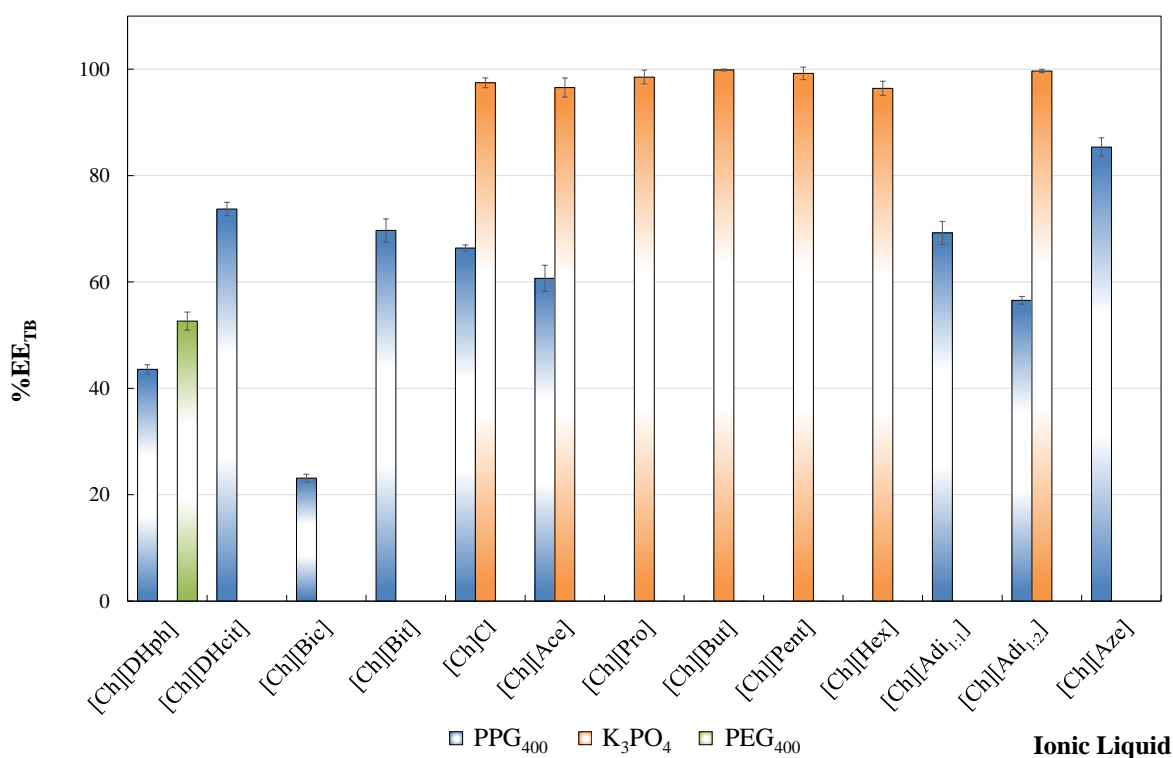


Figure 3.2. Extraction efficiencies for theobromine of the ABS composed of cholinium-based ILs + PPG 400/PEG 400/ K_3PO_4 + H_2O at 298 K.

It should be noted that some ABS are not suitable to be used as extraction systems because they have a large monophasic region, and therefore, high amounts of IL and PEG are necessary while making these systems very viscous. These ABS are [Ch][TFAc] + PPG 400, [Ch][DHcit] + PEG 400, [Ch]Cl + PEG 400, [Ch][Bit] + PEG 400, [Ch][Bic] + PEG 400, and [Ch][Ac] + PEG 400. In the case of [Ch][Non] + K_3PO_4 precipitation occurred at the common mixture composition preventing thus its use as extraction system. To

overcome this problem, other mixture compositions with lower amounts of salt and IL should be investigated in the near future.

From Figure 3.2, it can be observed that when PPG is used, theobromine extraction efficiencies range between 23.12 and 85.36%. Only one ABS containing PEG 400 was used for the extraction of theobromine, namely the ABS composed [Ch][DHph] + PEG 400, which leads to an extraction efficiency of 52.65 %, indicating that theobromine partites almost equally between the two phases. This migration pattern could be a consequence of the salting-out effect of the cholinium-based IL over theobromine which forces its migration partly toward the PEG 400-rich phase [87]. On the other hand, when K_3PO_4 is used, a strong salting-out agent, theobromine preferentially migrates to the IL-rich phase with extraction efficiencies ranging between 96.56 and 99.67 %.

When PPG 400 is used as the salting-out species, the theobromine extraction efficiencies for the IL-rich phase increase in the order: [Ch][Bic] < [Ch][DHph] < [Ch][Adi_{1:2}] < [Ch][Ac] < [Ch]Cl < [Ch][Adi_{1:1}] < [Ch][Bit] < [Ch][DHcit] < [Ch][Aze]. When K_3PO_4 is used as the salting-out species, a different order for the theobromine extraction efficiencies was observed: [Ch][Hex] < [Ch][Ac] < [Ch]Cl < [Ch][Pro] < [Ch][Pent] < [Ch][Adi_{1:2}] < [Ch][But]. This difference in the extraction efficiencies is a reflexion not only of the salting-out capacity of each one of the salting-out compounds used, but also a result of the complex and diverse interactions occurring between the solute molecule and the other compounds present in solution [90].

During the partitioning of theobromine in ABS, several interactions between IL, K_3PO_4 , polymers, theobromine and water occur. Hydrogen bonds, π - π interactions, electrostatic interactions are examples of these interactions [108]. The use of K_3PO_4 for theobromine extraction causes it's almost complete migration to the IL-rich phase, which can probably be attributed to the great salting-out capacity of the PO_4^{3-} anion. The pH of the aqueous phases is another parameter that should be considered. The K_3PO_4 inorganic salt affords aqueous phases with an alkaline pH. For IL- K_3PO_4 -based ABS the pH values of the phases are around 13 [109]. The effect of the pH in the partitioning of a biomolecule in IL- K_3PO_4 -based ABS was studied by Cláudio et al. [109] and the authors concluded that non-charged molecules have preferential affinity for the IL-rich phase (more hydrophobic phase). Although, in this work, and according to the theobromine pKa (9.90) [102], this molecule is charged in the K_3PO_4 -containing systems and it still migrates to the IL-rich

phase instead of going to the salt-rich phase. This fact was already observed in previous studies and is a result of the strong salting-out ability of the inorganic salt [110].

After the extraction of commercial theobromine through ABS consisting of ILs and polymer/salt, and which allowed to infer on the best ILs to be used as extraction solvents aiming at developing an extraction-purification integrated strategy, in the next chapter, cocoa beans were used as the source of theobromine. For this purpose, solid-liquid extractions from cocoa were carried out with aqueous solutions of different ILs, namely [Ch][Adi_{1:1}], [Ch][Adi_{1:2}], [Ch][DHcit], [Ch][DHph], [Ch]Cl, [Ch][Bit], [Ch][Bic], [Ch][Ac], [Ch][Pro], [Ch][But], [Ch][Pent] and [Ch][Hex]. Further, these aqueous solutions were recovered and used to create ABS to infer on the theobromine migration pattern.

4. Extraction and Purification of Theobromine from Biomass

4.1. Introduction

The first step in the extraction of compounds from plant matrices or biomass consists on solid-liquid extractions, so that a plant extract can be obtained. The plant extract is then purified in order to obtain other extracts enriched in one or more components or even on the pure compounds [111]. ABS can be used in the purification step through migration of a given compound between two aqueous phases [45,112]. The use of ILs in ABS allows the purification of a wide range of (bio)molecules [45] since the choice of ILs makes possible to adapt the polarity of the two phases [91].

ILs were already used to extract natural compounds from biomass through solid-liquid extractions [43]. For instance, Cláudio *et al.* [113] extracted caffeine, an alkaloid, from *Paullinia cupana*, Chowdhury *et al.* [114] extracted catechin, a flavonoid, and ellagic acid, a phenolic acid, from *Acacia catechu* and *Terminalia chebula*, Bica *et al.* [115] extracted limonene, a terpenoid, from orange peels and Usuki *et al.* [116] extracted shikimic acid, an aromatic compound, from *Ginkgo biloba*. Nevertheless, no studies on the extraction of theobromine from natural sources using ILs were found in the open literature. More conventional solvents have however been reported. Li *et al.* [2] and González-Nuñez *et al.* [4] used chloroform, while Esmelindro *et al.* [117] demonstrated the use of supercritical carbon dioxide for the extraction of theobromine from cocoa.

4.2. Experimental Section

4.2.1 Materials

The ILs used in the solid-liquid extraction of theobromine from cocoa beans were [Ch][Ac], [Ch][Pro], [Ch][But], [Ch][Pent], [Ch][Hex], [Ch][Adi_{1:1}], [Ch][Adi_{1:2}], [Ch][Bit], [Ch][Bic], [Ch][DHph] and [Ch][DHcit]. All ILs investigated were previously described in Chapter 2, in the Experimental Section. The salting-out species used was K₃PO₄, also described in Chapter 2, as well as the commercial theobromine.

Cocoa beans were purchased at a local market in Brazil. It is a 100% organic product from Nutrigold. Ethanol absolute anhydrous was obtained from Carlo Erba Reagents, and dichloromethane was from VWR Chemicals. Ultra-pure water, double distilled, passed by a reverse osmosis system and further treated with a Milli-Q plus 185 water purification equipment was used.

4.2.2. Experimental Procedure

As a first step, cocoa beans were peeled and the bean and the peel fractions were both grinded, separately, with a commercial coffee grinder. The biomass samples were further dried at 333 K for ~2 days. The average water content of these samples is 3.04 wt%.

Specific amounts of cocoa grounded beans (1 % w/w) were added to three different types of solvents, namely pure water, pure ethanol and mixtures of water + ILs (at 1.5 M). With [Ch][Bic] an IL solution at 1.2 M was used. The extractions were carried out in a commercial Carousel Radleys TECH equipment, maintaining the temperature around 343 K, and a constant stirring speed of 250 rpm, during 1h. These conditions were chosen based on a previous work concerning the extraction of caffeine from guaraná beans [113]. After the extraction period, the mixtures were filtered using a 0.45 µm cellulose membrane, and then, the obtained liquid solution was diluted in pure water in order to be quantified through UV-spectroscopy, using a Shimadzu UV-1800, Pharma-Spec Spectrometer, at a wavelength of 273 nm, using a calibration curve previously established for theobromine, presented in Figure B.2.2 in Appendix B. Two replicates were prepared for each ionic liquid.

The extracted weight percentage of theobromine or extraction yield of theobromine from the dried beans was calculated according to equation 4.1.:

$$\% \text{ TB} = \frac{[\text{TB}] \times V_{\text{solvent}}}{w_{\text{cocoa}}} \times 100 \quad (\text{eq 4.1.})$$

where [TB] is the theobromine concentration ($\text{g}\cdot\text{L}^{-1}$), determined through the calibration curve, V_{solvent} is the solvent volume (L) and w_{cocoa} is the mass of the cocoa ground beans used (g).

In order to assess the effect of other compounds present in cocoa, especially lipids, a biomass pre-treatment may be required. Therefore, 2 g of grounded cocoa was treated with 25 mL of petroleum ether according to literature [3]. The mixture was vigorously stirred in a vortex and centrifuged at 2000 rpm for 10 minutes. Afterwards, petroleum ether was decanted and a second washing step was performed with fresh solvent. Then, the residue was dried at 298 K overnight. Subsequently, the sample was used in the same way, as the untreated sample, in order to determine the theobromine extraction yield. In Figure 4.1. the aspect of untreated and treated grinded cocoa beans is depicted.

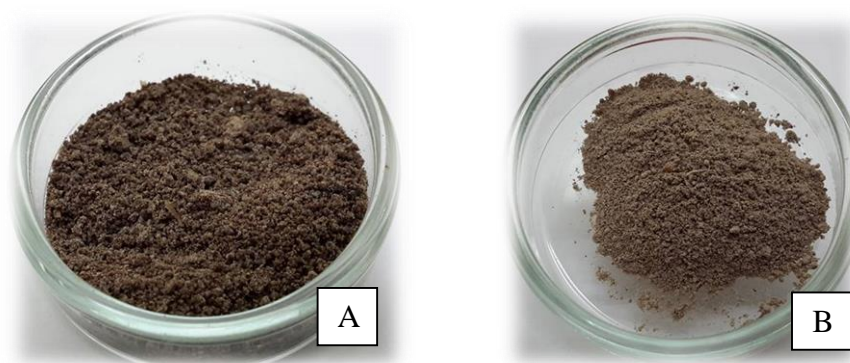


Figure 4.1. A – untreated grinded cocoa beans and B – treated grinded cocoa beans.

Aiming at comparing the performance of the IL aqueous solutions with more traditional solvents and techniques, Soxhlet extractions were also carried out using the same biomass sample. Two Soxhlet extractions were performed for 7 h, using approximately 10 g of untreated cocoa and the solvents dichloromethane and ethanol (250 mL of each). During the extraction, samples of 1 mL were taken after 15, 30, 45, 60, 120, 180, 240, 300, 360 and 420 minutes and theobromine was quantified through UV-spectroscopy at a wavelength of 273 nm, using calibration curves previously established for theobromine in solutions with dichloromethane and ethanol, and that are presented in Figures B.2.3 and B.2.4 in Appendix B. Subsequently, the dichloromethane solvent was evaporated on a rotary evaporator under vacuum at a temperature of 303 K. At the end, the resulting extract was injected and analysed by gas chromatography–mass spectrometry (GC-MS) to identify the main constituents of the samples of cocoa.

For the GC-MS analysis, nearly 10 mg of the extract was treated with 250 μL of internal standard (24.22 mg of tetracosane in 10 mL of pyridine), 250 μL of N,O-bis(trimethylsilyl)-trifluoroacetamide and 50 μL of chlorotrimethylsilane. GC-MS analyses were performed on a Trace Gas Chromatograph 2000 Series equipped with a Thermo Scientific DSQ II mass spectrometer, using helium as carrier gas (35 cm s^{-1}), equipped with a DB-1 J&W capillary column ($30 \text{ m} \times 0.32 \text{ mm i.d.}, 0.25 \mu\text{m}$ film thickness). The chromatographic conditions were as follows: initial temperature 353 K for 5 min; temperature rate 277 K min^{-1} up to 533 K and 275 K min^{-1} till the final temperature of 558 K, which was maintained for 20 minutes; injector temperature 523 K; transfer-line temperature 563 K; split ratio 1:50. The MS was operated in electron impact mode with an

electron impact energy of 70 eV, and data were collected at a 1 scan s⁻¹ rate, over a range of m/z 33-700. The ion source was maintained at 523 K.

For the theobromine purification approach using ABS, and after the extraction procedure, K₃PO₄ was added in specific amounts to the filtered IL aqueous solutions containing the soluble components. Previous calculations were made to ensure that the mixture point fits within the biphasic region according to the phase diagrams described in Chapter 2. The detailed mixture points and compositions are described in Appendix D, Table D.7. The mixture was vigorously stirred, and then centrifuged for 1h at 3500 rpm and at 298 K, to assure complete separation of the two aqueous phases. Figure 4.2. depicts an example of the ABS formed with the IL aqueous solutions containing the extract. After a careful separation of both phases, these were diluted in ultra-pure water in order to quantify theobromine by UV-spectroscopy, using a Shimadzu UV-1800, Pharma-Spec Spectrometer, at a wavelength of 273 nm, using a calibration curve previously established for theobromine. Two replicates were prepared for each ionic liquid.

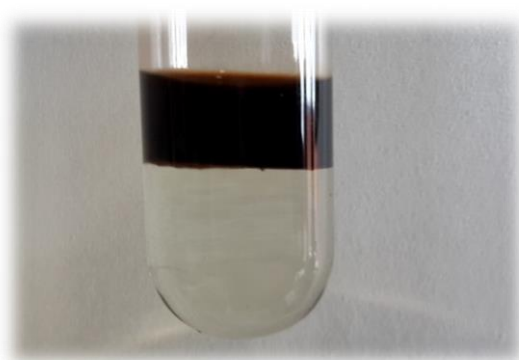


Figure 4.2. ABS formed with the IL aqueous solution containing the cocoa extract and K₃PO₄.

Scanning electron microscopy (SEM) was applied to the untreated and treated with petroleum ether cocoa samples and also to the cocoa samples after the solid-liquid extraction carried out with [Ch][Ac]. SEM pictures were used to evaluate the morphology of the cocoa particles before and after extraction, and were acquired using a Hitachi SU-70 microscope with a 15 kV acceleration voltage.

4.3. Results and Discussion

Initially, the theobromine extraction yield from the peel and core of cocoa beans was quantified. For this purpose, extractions with [Ch]Cl and [Ch][Ac] (1.5 M) aqueous solutions were performed. The results obtained are shown in Figure 4.3., and in Table D.2., in Appendix D.

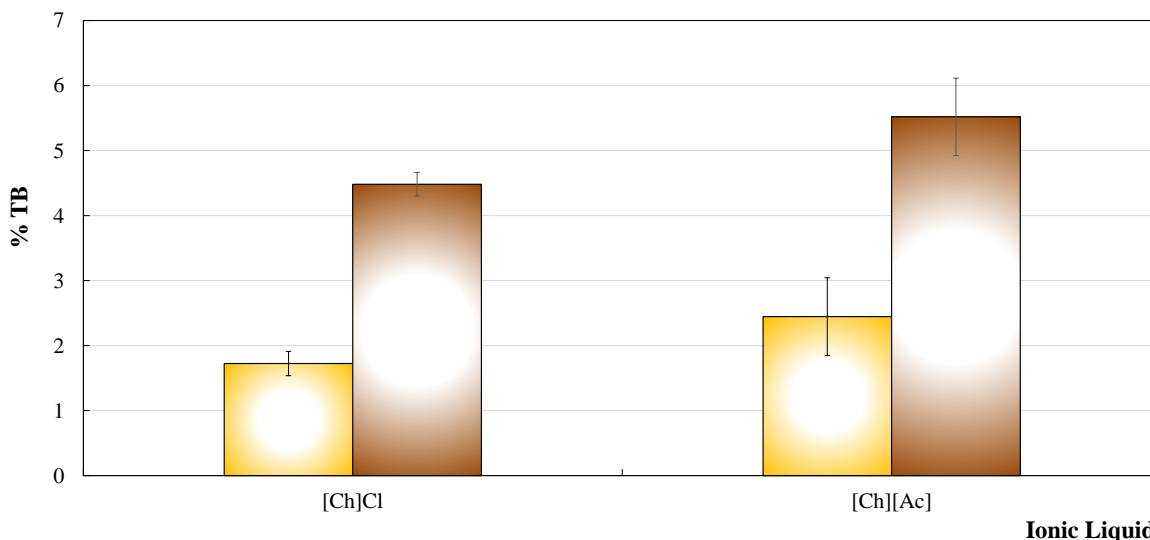


Figure 4.3. Weight percentage of theobromine extracted from cocoa peel ■ and cocoa core ■ using IL aqueous solutions (1.5 M) at 343 K.

From the data shown in Figure 4.3., it can be concluded that the extraction yield of theobromine is higher when using the cocoa beans core. Due to its higher content in the target alkaloid, as well as on the higher amount of available biomass, only the cocoa beans core was used in the following experiments.

The ability of several ILs aqueous solutions to extract theobromine from cocoa was also compared with soxhlet extractions with dichloromethane and ethanol. Moreover, and also for comparison purposes, water and ethanol were used as main solvents at the same conditions used for the extractions carried out with IL aqueous solutions.

In Figures 4.4. and 4.5. are presented the results obtained for the weight percentage of theobromine extracted (%TB) from cocoa beans, over time (minutes), using Soxhlet extraction, with the solvents ethanol and dichloromethane, respectively. The values are listed in Table D.3. and D.4., respectively, in Appendix D.

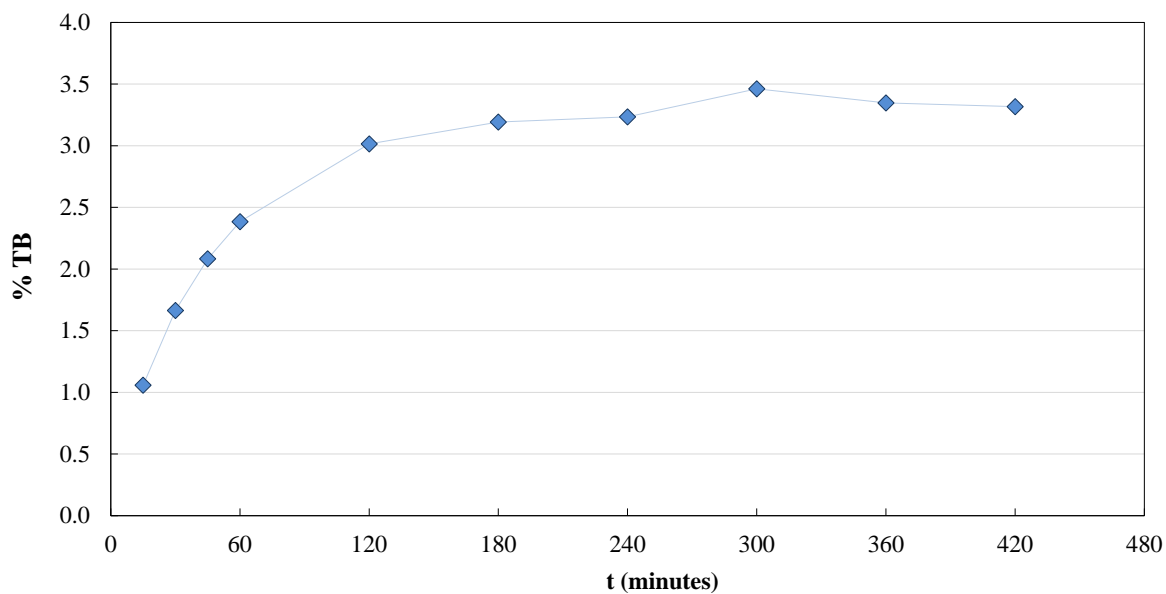


Figure 4.4. Weight percentage of theobromine extracted from cocoa beans, over time, using ethanol as solvent in a Soxhlet extraction.

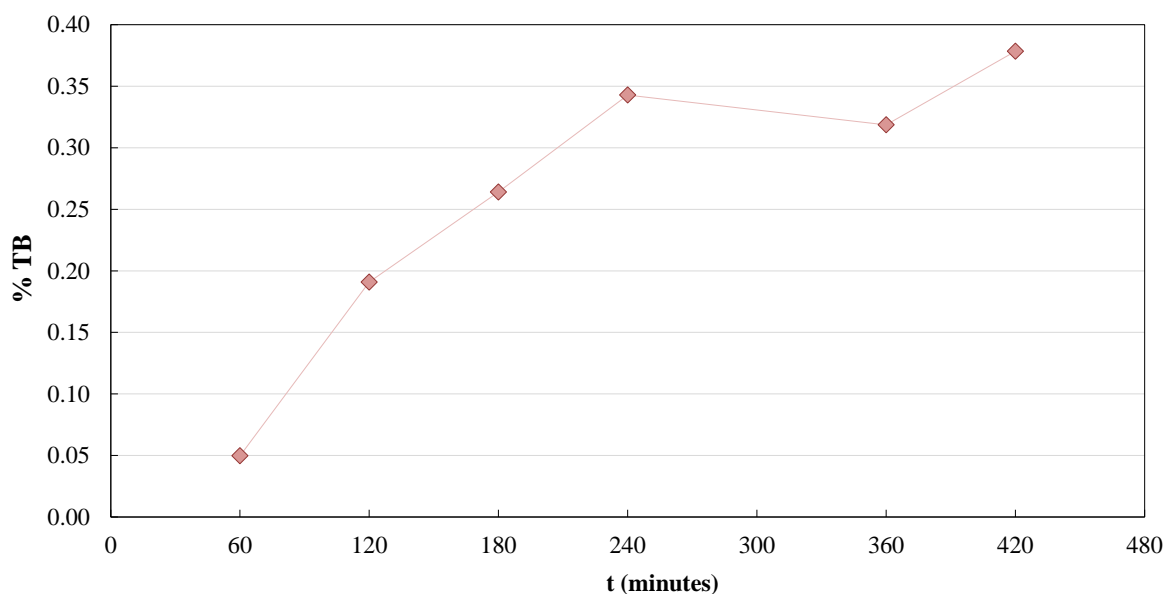


Figure 4.5. Weight percentage of theobromine extracted from cocoa beans, over time, using dichloromethane as solvent in a Soxhlet extraction.

Nowadays, there are various techniques for theobromine extraction from cocoa. The most common are extraction with supercritical carbon dioxide [117,118], conventional methods that use water and ethanol as solvents [119] and organic solvents such as

chloroform [2] and dichloromethane [120]. However, extractions performed with these solvents require many hours, and result in low extraction yields. Furthermore, VOCs are highly flammable and toxic, and hazardous for humans and the environment. In fact, the maximum extraction yield of theobromine obtained in this work with conventional solvents was 3.46 wt% (with ethanol).

The results obtained using ILs aqueous solutions (1.2 M for [Ch][Bic] and 1.5 M for the remaining ILs) are depicted in Figure 4.6, and presented in Table D.5., in Appendix D.

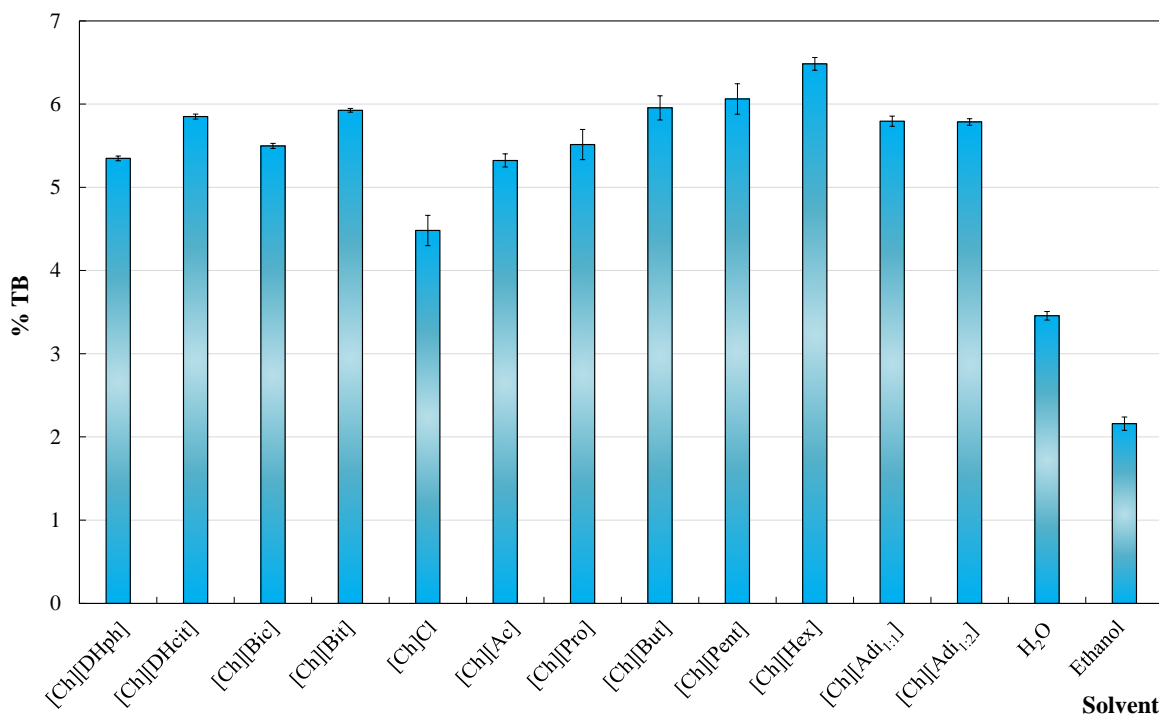


Figure 4.6. Weight percentage of theobromine extracted from cocoa core beans using different solvents: H₂O, ethanol and ILs aqueous solutions (1.2 M for [Ch][Bic] and 1.5 M for the remaining ILs) at 343 K.

For the solid-liquid extractions carried out at 343 K, it can be observed that the aqueous solutions of ILs are better extraction solvents than pure water and pure ethanol since the extraction yields are much higher than those obtained with the two molecular solvents. Extraction yields of theobromine from cocoa core beans obtained with IL aqueous solutions range between 4.48 and 6.48 % and increase in the order: Ethanol < H₂O

< [Ch]Cl < [Ch][Ac] < [Ch][DHph] < [Ch][Bic] < [Ch][Pro] < [Ch][Adi_{1:1}] < [Ch][Adi_{1:2}] < [Ch][DHcit] < [Ch][Bit] < [Ch][But] < [Ch][Pent] < [Ch][Hex].

Analysing the results obtained, aqueous solutions of [Ch]Cl have the lowest performance for extracting theobromine from cocoa core beans. Moreover, an increase on the extraction yield was observed with ILs with longer alkyl side chains at the anion ([Ch][Ac] < [Ch][Pro] < [Ch][But] < [Ch][Pent] < [Ch][Hex]). In this sense, more hydrophobic ILs, *i.e.*, with longer alkyl side chains, are more able to extract theobromine from biomass. In the same line, [Ch][DHph], one of the strongest ABS promoter and thus a highly hydrophilic IL, is amongst the worst candidates to extract theobromine from biomass.

In order to evaluate the influence of other compounds present in cocoa core beans though the IL aqueous solutions extraction ability, biomass was also previously treated with petroleum ether, and then new extractions were performed with some ILs, namely [Ch]Cl, [Ch][Ac], [Ch][But] and [Ch][Hex]. Figure 4.7. shows the comparison of the results obtained for the weight percentage of theobromine extracted (% TB) from treated and untreated cocoa core beans, using the procedures described before. Detailed data are presented in Table D.6., in Appendix D.

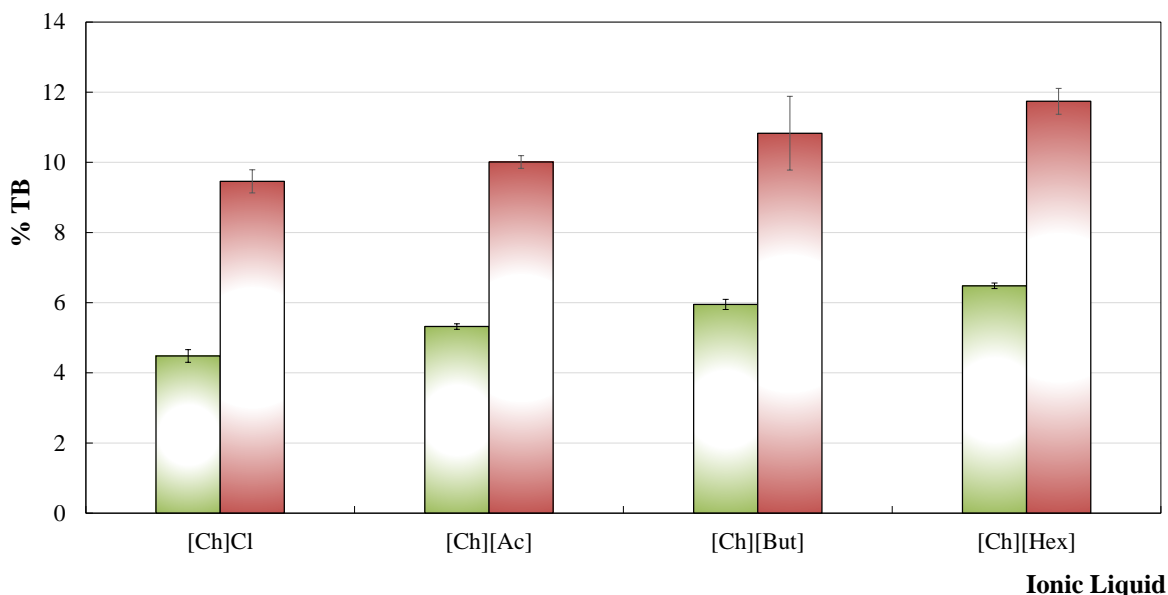


Figure 4.7. Mass percentage of theobromine extracted from treated ■ and untreated ■ cocoa core beans, using different solutions of ILs (1.5 M) at 343 K.

Evaluating the obtained results, it seems clear that after the biomass treatment the extraction yields of theobromine more than duplicates with some of the ILs used, obtaining values between 9.46 and 11.44 %, from [Ch]Cl to [Ch][Hex], respectively. In this sense, the previous removal with petroleum ether of other compounds such as oils, sterols and phospholipids is favourable for the subsequent extraction of theobromine from cocoa core beans. Nevertheless, it should be pointed out that one additional step is required and which makes use of an organic molecular solvent.

According to the literature, values of extracted theobromine from cocoa varied between 0.1 and 3.7 % [2–4,121], and for which our values fit within when considering the extractions carried out with ethanol and water. However, according to our results, IL aqueous solutions are highly promising solvents for the extraction of alkaloids from biomass, and being in accordance with the high extraction yields of caffeine from guaraná beans previously reported by Cláudio *et al.* [113].

After the extraction of theobromine from cocoa core beans through solid-liquid extraction using IL aqueous solutions, these were then used to create ABS with K_3PO_4 envisaging the theobromine purification. In Figure 4.8. are presented the extraction efficiencies for the IL-rich phase using the aqueous solutions of ILs containing the extract and those obtained with commercial theobromine. The values are presented in Table D.8., in Appendix D.

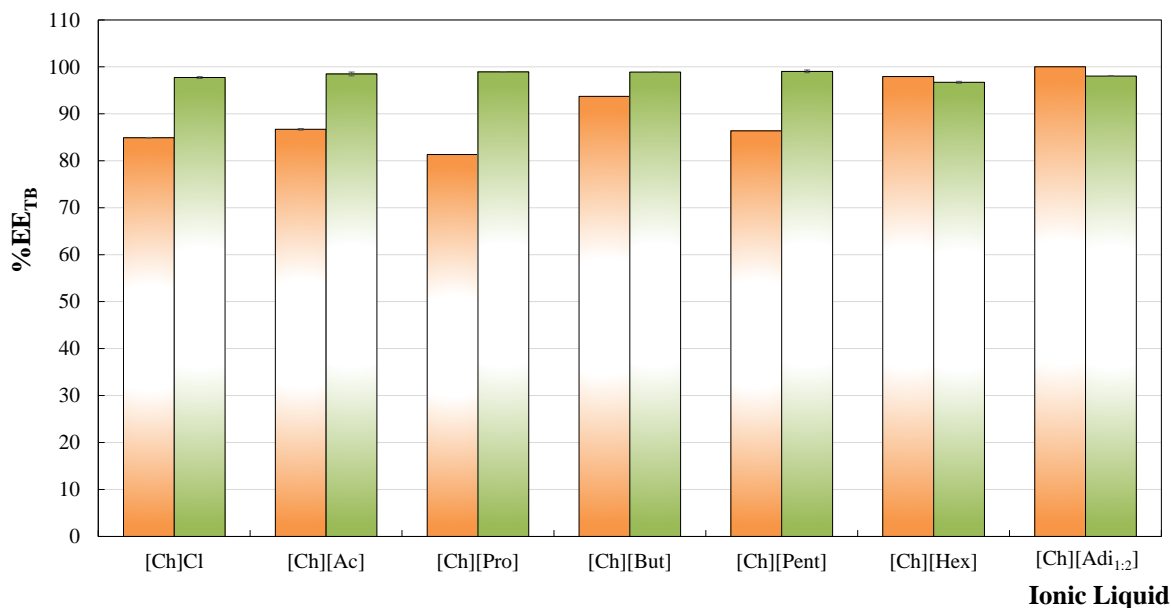


Figure 4.8. Extraction efficiencies for theobromine of the ABS composed of cholinium-based ILs + K_3PO_4 + H_2O at 298 K using commercial ■ and the aqueous solution containing the cocoa core extract ■.

Analysing Figure 4.8., it can be concluded that, in most situations, the extraction of theobromine for the IL-rich phase is more favourable with the aqueous solution containing the cocoa core extract, with the exception of [Ch][Hex] and [Ch][Adi_{1,2}]. Therefore, the presence of other contaminants at the aqueous phase seems to be favourable to induce the migration of the alkaloid for the IL-rich phase. This trend was previously observed with the extraction of alkaloids and endocrine disruptors for the IL-rich phase that suffered an enhancement in presence of more complex media [110,122].

In Figure 4.10 are presented the UV spectra of theobromine in different solutions: aqueous solution of commercial theobromine, aqueous solution of [Ch][Ac] with commercial theobromine, aqueous solution of [Ch][Ac] with theobromine extracted from treated cocoa core beans and aqueous solutions of the IL-phase and K_3PO_4 -rich phases after the extraction with [Ch][Ac].

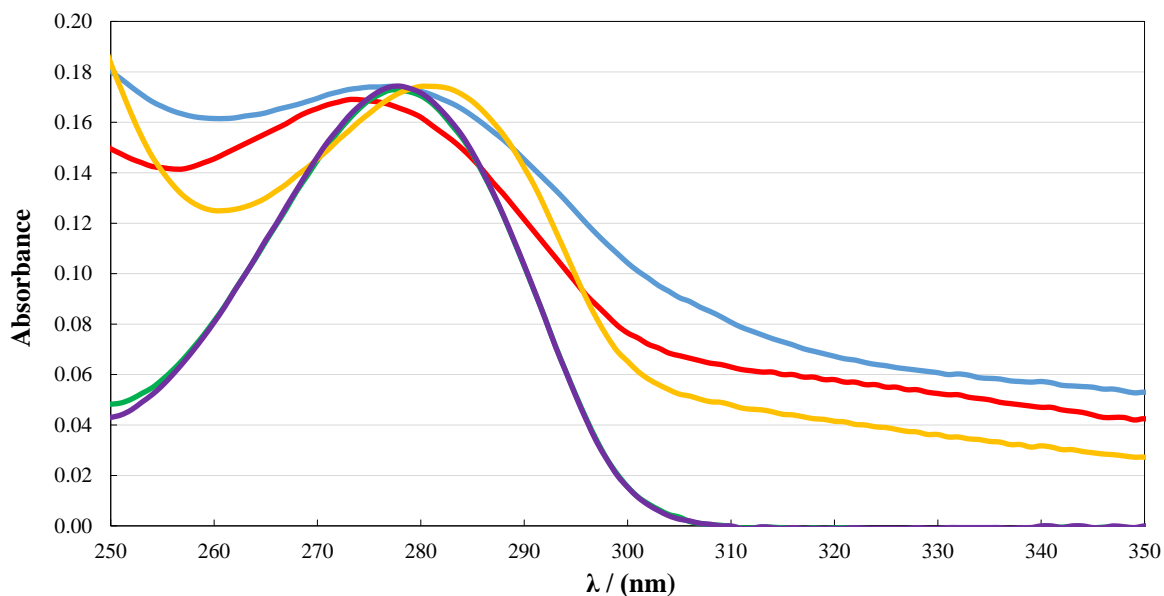


Figure 4.9. Spectra of the diluted aqueous solutions of commercial theobromine (—), [Ch][Ac] with commercial theobromine (—), [Ch][Ac] with treated cocoa core beans after extraction (—) and IL (—) and K_3PO_4 phases (—) after an extraction with [Ch][Ac].

From Figure 4.9. it is safe to admit that theobromine is present in all solutions, *i.e.*, theobromine presents a maximum of absorbance at a wavelength of 273 nm, and all spectra have a peak around 273 nm. Deviations may be caused by other molecules in solution that are being extracted together with theobromine from cocoa.

To evaluate the effect of cocoa core beans washing with petroleum ether, as well as the use of IL aqueous solutions to extract theobromine, SEM was used to obtain images of cocoa samples. In Figure 4.10. SEM pictures of fresh cocoa and after washing with petroleum ether are presented. In Figure 4.11. are presented the SEM pictures of cocoa core and washed cocoa core beans after extraction with [Ch][Ac] aqueous solutions.

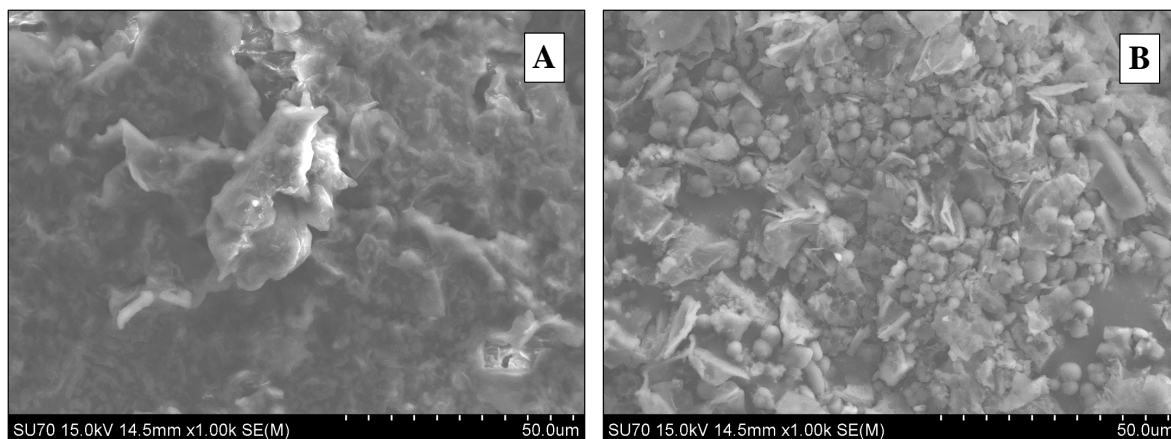


Figure 4.10. SEM images of the cocoa core samples: untreated (A) and treated (B) with petroleum ether.

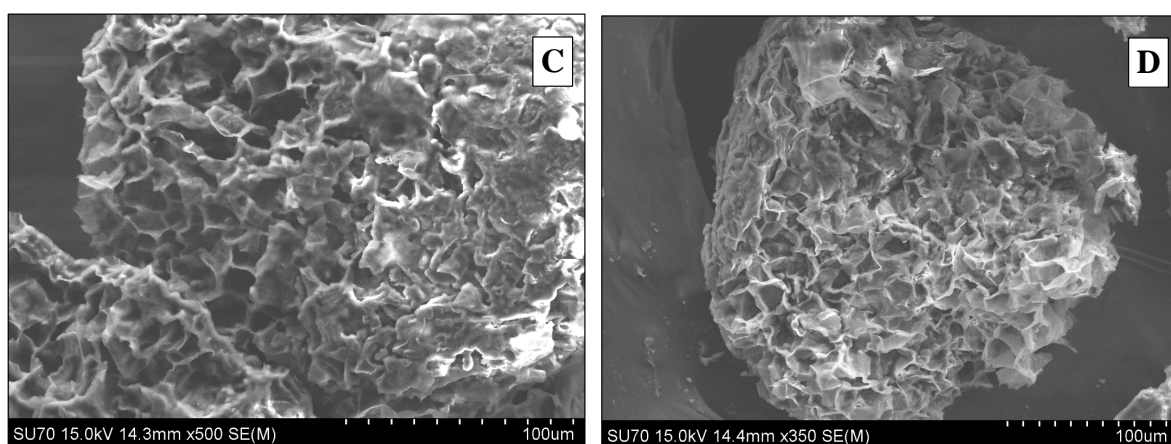


Figure 4.11. SEM images of the cocoa core samples, untreated (C) and treated with petroleum ether (D) after extraction with an aqueous solution of [Ch][Ac].

The cocoa core washing with petroleum shows that the cell walls suffer some morphological effects and the surface appears as less homogenous which can be a result of the lipids removal. However, in both samples, after the extraction step carried out with aqueous solutions of ILs, it is found that the cell structures are much more affected and appear as more disrupted, which can explain the high extraction of theobromine obtained using IL aqueous solutions. This rupture seems to allow the access of the IL aqueous solutions to the target alkaloid favouring thus its extraction and is in agreement with previous discussions found in the literature [113].

In order to evaluate the purification factor achievable with ABS, back-extractions from each aqueous phase with dichloromethane were performed and submitted to GC-MS

aiming at identifying all compounds present in each phase. However, some difficulties were found since major contaminants have been found even with the injection of standards. An example of a GC-MS spectrum is shown in Appendix B in Figure B.4.1. , and where cyclosiloxanes appear in high quantity. Due to a limited timeframe, no further discussions can be made regarding the purification factors achievable with ABS. In this context, it is of high importance to carry out in the near future new GC-MS and MS-HPLC experiments to infer on the composition of each phase. However, it is safe to admit that no significant losses of the alkaloid occur when using an aqueous solution containing the cocoa core extract.

5. Final Remarks

5.1. Conclusions and Future Work

This work demonstrates that aqueous solutions of ILs are outstanding solvents for the extraction of alkaloids from biomass and that it is possible to use an integrated process using these aqueous solutions in the formation of ABS for further purification of the target compounds.

As an initial study, and in order to infer on the best ILs to be used in the extraction of theobromine from cocoa, the ability of some ILs with PPG 400, PEG 400 and K_3PO_4 to form aqueous biphasic systems and to extract cocoa from an aqueous solution was evaluated. Extraction efficiency values ranging between 96.41 – 99.86% were obtained in a single-step using ABS formed with K_3PO_4 (the strongest salting-out agent evaluated). The extractions in which PPG 400 and PEG 400 were used in the formulation of ABS led to lower extraction efficiencies, ranging between 23.12 and 85.36%.

After the selection of the best ILs and the best salting-out agent to create ABS, solid-liquid extractions of theobromine from cocoa were carried out using aqueous solutions of ILs. Extraction yields ranging between 4.48 – 6.48 wt% were obtained with non-treated samples of cocoa core beans. However, if a previous washing step with ether petroleum is performed extraction yields up to 11.74 % can be obtained.

As a final step, the aqueous solutions containing the extract were used to create ABS with K_3PO_4 to infer on their capability to act as purification strategies. Values between 96.7% – 99.0% of theobromine extraction efficiencies were obtained. As with commercial theobromine, theobromine extracted from cocoa also preferentially migrates for the IL-rich phase with no significant losses of the alkaloid for the opposite phase. However, due to some problems found in the GC-MS it is not possible to infer on the purification level of theobromine at this stage. As future work, it is essential to continue these studies and to characterize each aqueous phase, *i.e.*, to identify the major components extracted from cocoa and how they partition between the coexisting phases. Since high extraction yields have been obtained with aqueous solutions of ILs, the next step, and aiming at reducing the process overall cost, should consist on applying a factorial planning in order to decrease the amount of IL, time of extraction and temperature required. Furthermore, new SEM images, in particular after the extractions carried out with water and ethanol, should be acquired to confirm the effect of ILs on the disruption of biomass the cell walls.

6. References

1. Martínez-Aragón, M.; Burghoff, S.; Goetheer, E.L.V.; de Haan, A.B. *Guidelines for solvent selection for carrier mediated extraction of proteins*. Separation and Purification Technology. 2009; **65** p. 65–72.
2. Li, S.; Berger, J.; Hartland, S. *UV spectrophotometric determination of theobromine and caffeine in cocoa beans*. Analytica Chimica Acta. 1990; **232** p. 409–412.
3. Caudle, A.G.; Gu, Y.; Bell, L.N. *Improved analysis of theobromine and caffeine in chocolate food products formulated with cocoa powder*. Food Research International. 2001; **34** p. 599–603.
4. González-Nuñez, L.N.; Cañizares-Macías, M.P. *Focused microwaves-assisted extraction of theobromine and caffeine from cacao*. Food Chemistry. 2011; **129** p. 1819–1824.
5. Wang, Y.; Cai, S.; Chen, Y.; Deng, L.; Zhou, X.; Liu, J.; Xu, X.; Xia, Q.; Lin, M.; Zhang, J.; Huang, W.; Wang, W.; Xiang, C.; Cui, G.; Du, L.; He, H.; Qi, B. *Separation and purification of five alkaloids from Aconitum duclouxii by counter-current chromatography*. Journal of separation science. 2015; **38** p. 2320–2326.
6. Dewick, P.M. *Alkaloids. Medicinal Natural Products - A Biosynthetic Approach*. 3rd ed. Wiley; 2009. p. 311–417.
7. Ashihara, H.; Sano, H.; Crozier, A. *Caffeine and related purine alkaloids: biosynthesis, catabolism, function and genetic engineering*. Phytochemistry. 2008; **69** p. 841–856.
8. De Sena, A.R.; de Assis, S.A.; Branco, A. *Analysis of theobromine and related compounds by reversed phase high-performance liquid chromatography with ultraviolet detection: An update (1992-2011)*. Food Technology and Biotechnology. 2011. p. 413–423.
9. Daly, J.W. *Caffeine analogs: biomedical impact*. Cellular and molecular life sciences. 2007; **64** p. 2153–2169.
10. Porkka-Heiskanen, T.; Zitting, K.-M.; Wigren, H.-K. *Sleep, its regulation and possible mechanisms of sleep disturbances*. Acta physiologica. 2013; **208** p. 311–328.
11. Wu, S.; Han, J.; Song, F.; Cho, E.; Gao, X.; Hunter, D.J.; Qureshi, A.A. *Caffeine Intake, Coffee Consumption, and Risk of Cutaneous Malignant Melanoma*. Epidemiology. 2015; **26** p. 898–908.
12. Schmidt, B.; Roberts, R.S.; Davis, P.; Doyle, L.W.; Barrington, K.J.; Ohlsson, A.; Solimano, A.; Tin, W. *Caffeine Therapy for Apnea of Prematurity*. The New England Journal of Medicine. 2006; **354** p. 2112–2121.

13. Stavric, B. *Methylxanthines: Toxicity to humans. 1. Theophylline*. Food and Chemical Toxicology. 1988; **26** p. 541–565.
14. Mitchell, E.S.; Slettenaar, M.; vd Meer, N.; Transler, C.; Jans, L.; Quadt, F.; Berry, M. *Differential contributions of theobromine and caffeine on mood, psychomotor performance and blood pressure*. Physiology & behavior. 2011; **104** p. 816–822.
15. Li, Y.; Feng, Y.; Zhu, S.; Luo, C.; Ma, J.; Zhong, F. *The effect of alkalization on the bioactive and flavor related components in commercial cocoa powder*. Journal of Food Composition and Analysis. 2012; **25** p. 17–23.
16. Harkins, J.; Rees, W.; Mundy, G.; Stanley, S.; Tobin, T. *An overview of the methylxanthines and their regulation in the horse*. Equine Practice. 1998; **20** p. 10–16.
17. Smit, H.J. *Theobromine and the pharmacology of cocoa*. Handbook of experimental pharmacology. 2011; p. 201–234.
18. Mogollon, J.A.; Boivin, C.; Philippe, K.; Turcotte, S.; Lemieux, S.; Blanchet, C.; Bujold, E.; Dodin, S. *Consumption of chocolate in pregnant women and risk of preeclampsia: a systematic review*. Systematic reviews. 2013; **2** p. 114.
19. Klebanoff, M.A.; Zhang, J.; Zhang, C.; Levine, R.J. *Maternal serum theobromine and the development of preeclampsia*. Epidemiology. 2009; **20** p. 727–732.
20. Baggott, M.J.; Childs, E.; Hart, A.B.; de Bruin, E.; Palmer, A.A.; Wilkinson, J.E.; de Wit, H. *Psychopharmacology of theobromine in healthy volunteers*. Psychopharmacology. 2013; **228** p. 109–118.
21. Pendleton, M.; Brown, S.; Thomas, C.; Odle, B. *Potential Toxicity of Caffeine When Used as a Dietary Supplement for Weight Loss*. Journal Of Dietary Supplements. 2012; **10** p. 10-15.
22. Berends, L.M.; van der Velpen, V.; Cassidy, A. *Flavan-3-ols, theobromine, and the effects of cocoa and chocolate on cardiometabolic risk factors*. Current opinion in lipidology. 2015; **26** p. 10–19.
23. Martínez-Pinilla, E.; Oñatibia-Astibia, A.; Franco, R. *The relevance of theobromine for the beneficial effects of cocoa consumption*. Frontiers in pharmacology. 2015; **6** p. 30.
24. Araujo, Q.R.; Fernandes, C.A.F.; Ribeiro, D.O.; Efraim, P.; Steinmacher, D.; Lieberei, R.; Bastide, P.; Araujo, T.G. *Cocoa Quality Index – A proposal*. Food Control. 2014; **46** p. 49–54.
25. Dillinger, T.L.; Barriga, P.; Escárcega, S.; Jimenez, M.; Salazar Lowe, D.; Grivetti, L.E. *Food of the gods: cure for humanity? A cultural history of the medicinal and ritual use of chocolate*. The Journal of nutrition. 2000; **130** p. 2057S – 2072S.

26. Todorovic, V.; Redovnikovic, I.R.; Todorovic, Z.; Jankovic, G.; Dodevska, M.; Sobajic, S. *Polyphenols, methylxanthines, and antioxidant capacity of chocolates produced in Serbia*. Journal of Food Composition and Analysis. 2015; **41** p. 137–143.
27. Jalil, A.M.M.; Ismail, A. *Polyphenols in Cocoa and Cocoa Products: Is There a Link between Antioxidant Properties and Health?* Molecules. 2008; **13** p. 2190–2219.
28. Smit, H.J.; Gaffan, E.A.; Rogers, P.J. *Methylxanthines are the psychopharmacologically active constituents of chocolate*. Psychopharmacology. 2004; **176** p. 412–419.
29. Scapagnini, G.; Davinelli, S.; Di Renzo, L.; De Lorenzo, A.; Olarte, H.H.; Micali, G.; Cicero, A.F.; Gonzalez, S. *Cocoa bioactive compounds: significance and potential for the maintenance of skin health*. Nutrients. 2014; **6** p. 3202–3213.
30. Corti, R.; Flammer, A.J.; Hollenberg, N.K.; Lüscher, T.F. *Cocoa and cardiovascular health*. Circulation. 2009; **119** p. 1433–1441.
31. Ellam, S.; Williamson, G. *Cocoa and human health*. Annual review of nutrition. 2013; **33** p. 105–128.
32. Solà, R.; Valls, R.M.; Godàs, G.; Perez-Busquets, G.; Ribalta, J.; Girona, J.; Heras, M.; Cabré, A.; Castro, A.; Domenech, G.; Torres, F.; Masana, L.; Anglés, N.; Reguant, J.; Ramírez, B.; Barriach, J.M. *Cocoa, hazelnuts, sterols and soluble fiber cream reduces lipids and inflammation biomarkers in hypertensive patients: a randomized controlled trial*. Public Library of Science. 2012; **7** p. e31103.
33. Lee, K.W.; Kim, Y.J.; Lee, H.J.; Lee, C.Y. *Cocoa has more phenolic phytochemicals and a higher antioxidant capacity than teas and red wine*. Journal of agricultural and food chemistry. 2003; **51** p. 7292–7295.
34. Zomer, E.; Owen, A.; Magliano, D.J.; Liew, D.; Reid, C.M. *The effectiveness and cost effectiveness of dark chocolate consumption as prevention therapy in people at high risk of cardiovascular disease: best case scenario analysis using a Markov model*. BMJ. 2012; **344** p. e3657.
35. Suzuki, K.; Nakagawa, K.; Miyazawa, T.; Kato, S.; Kimura, F.; Kamei, M.; Miyazawa, T. *Oxidative stress during development of alcoholic fatty liver: therapeutic potential of cacao polyphenol*. Bioscience, biotechnology, and biochemistry. 2013; **77** p. 1792–1794.
36. Katz, D.L.; Doughty, K.; Ali, A. *Cocoa and chocolate in human health and disease*. Antioxidants & redox signaling. 2011; **15** p. 2779–2811.
37. Yamashita, Y.; Okabe, M.; Natsume, M.; Ashida, H. *Prevention mechanisms of glucose intolerance and obesity by cacao liquor procyanidin extract in high-fat*

- diet-fed C57BL/6 mice*. Archives of biochemistry and biophysics. 2012; **527** p. 95–104.
38. Matsui, N.; Ito, R.; Nishimura, E.; Yoshikawa, M.; Kato, M.; Kamei, M.; Shibata, H.; Matsumoto, I.; Abe, K.; Hashizume, S. *Ingested cocoa can prevent high-fat diet-induced obesity by regulating the expression of genes for fatty acid metabolism*. Nutrition. 2005; **21** p. 594–601.
 39. Bi, W.; Tian, M.; Row, K.H. *Selective extraction and separation of oxymatrine from Sophora flavescens Ait. extract by silica-confined ionic liquid*. Journal of chromatography. B, Analytical technologies in the biomedical and life sciences. 2012; **880** p. 108–113.
 40. Bogdanov, M.G.; Keremedchieva, R.; Svinyarov, I. *Ionic liquid-supported solid–liquid extraction of bioactive alkaloids. III. Ionic liquid regeneration and glaucine recovery from ionic liquid-aqueous crude extract of Glaucium flavum Cr. (Papaveraceae)*. Separation and Purification Technology. 2015; **155** p. 13–19.
 41. Zhang, W.; Zhu, D.; Fan, H.; Liu, X.; Wan, Q.; Wu, X.; Liu, P.; Tang, J.Z. *Simultaneous extraction and purification of alkaloids from Sophora flavescens Ait. by microwave-assisted aqueous two-phase extraction with ethanol/ammonia sulfate system*. Separation and Purification Technology. 2015; **141** p. 113–123.
 42. Chemat, F.; Vian, M.A.; Cravotto, G. *Green extraction of natural products: concept and principles*. International journal of molecular sciences. 2012; **13** p. 8615–8627.
 43. Passos, H.; Freire, M.G.; Coutinho, J.A.P. *Ionic liquid solutions as extractive solvents for value-added compounds from biomass*. Green chemistry. 2014; **16** p. 4786–4815.
 44. Albertsson, P.Å. *Partition of Proteins in Liquid Polymer–Polymer Two-Phase Systems*. Nature. 1958; **182** p. 709–711.
 45. Freire, M.G.; Cláudio, A.F.M.; Araújo, J.M.M.; Coutinho, J.A.P.; Marrucho, I.M.; Canongia Lopes, J.N.; Rebelo, L.P.N. *Aqueous biphasic systems: a boost brought about by using ionic liquids*. Chemical Society reviews. 2012; **41** p. 4966–4995.
 46. Daugulis, A.J.; Axford, D.B.; Ciszek, B.; Malinowski, J.J. *Continuous fermentation of high-strength glucose feeds to ethanol*. Biotechnology Letters. 1994; **16** p. 637–642.
 47. Ding, X.; Wang, Y.; Zeng, Q.; Chen, J.; Huang, Y.; Xu, K. *Design of functional guanidinium ionic liquid aqueous two-phase systems for the efficient purification of protein*. Analytica chimica acta. 2014; **815** p. 22–32.

48. Pérez, R.L.; Loureiro, D.B.; Nerli, B.B.; Tubio, G. *Optimization of pancreatic trypsin extraction in PEG/citrate aqueous two-phase systems*. Protein expression and purification. 2015; **106** p. 66–71.
49. Ribeiro, B.D.; Coelho, M.A.Z.; Rebelo, L.P.N.; Marrucho, I.M. *Ionic Liquids as Additives for Extraction of Saponins and Polyphenols from Mate (Ilex paraguariensis) and Tea (Camellia sinensis)*. Industrial & Engineering Chemistry Research. 2013; **52** p. 12146–12153.
50. Freire, M.G.; Pereira, J.F.B.; Francisco, M.; Rodríguez, H.; Rebelo, L.P.N.; Rogers, R.D.; Coutinho, J.A.P. *Insight into the interactions that control the phase behaviour of new aqueous biphasic systems composed of polyethylene glycol polymers and ionic liquids*. Chemistry. 2012; **18** p. 1831–1839.
51. Cláudio, A.F.M.; Ferreira, A.M.; Shahriari, S.; Freire, M.G.; Coutinho, J.A.P. *Critical assessment of the formation of ionic-liquid-based aqueous two-phase systems in acidic media*. The journal of physical chemistry B. 2011; **115** p. 11145–11153.
52. Walden, P. *Bulletin de l'Académie Impériale des Sciences de St.-Pétersbourg*. 1914; **8** p. 405–422.
53. Letcher, T.M. *Ionic Liquids in Separation Process*. Chemical Thermodynamics for Industry. 2004. p. 76–82.
54. Hurley, F.H. *Electrodeposition of Aluminum*. United States; US2446331 A, 1948.
55. ScienceDirect. *Science Direct* [Internet]. [cited 2015 Oct 13]. Available from: <http://www.sciencedirect.com/>
56. Earle, M.J.; Esperança, J.M.S.S.; Gilea, M.A.; Lopes, J.N.C.; Rebelo, L.P.N.; Magee, J.W.; Seddon, K.R.; Widegren, J.A. *The distillation and volatility of ionic liquids*. Nature. 2006; **439** p. 831–834.
57. Rogers, R.D.; Seddon, K.R. *Chemistry. Ionic liquids--solvents of the future?* Science. 2003; **302** p. 792–793.
58. Ventura, S.P.M.; Marques, C.S.; Rosatella, A.A.; Afonso, C.A.M.; Gonçalves, F.; Coutinho, J.A.P. *Toxicity assessment of various ionic liquid families towards Vibrio fischeri marine bacteria*. Ecotoxicology and environmental safety. 2012; **76** p. 162–168.
59. Berthod, A.; Ruiz-Angel, M.J.; Carda-Broch, S. *Ionic liquids in separation techniques*. Journal of chromatography A. 2008; **1184** p. 6–18.
60. Li, Z.; Jia, Z.; Luan, Y.; Mu, T. *Ionic liquids for synthesis of inorganic nanomaterials*. Current Opinion in Solid State and Materials Science. 2008; **12** p. 1–8.

61. Sedev, R. *Surface tension, interfacial tension and contact angles of ionic liquids*. *Current Opinion in Colloid & Interface Science*. 2011; **16** p. 310–316.
62. Hong, K.; Zhang, H.; Mays, J.W.; Visser, A.E.; Brazel, C.S.; Holbrey, J.D.; Reichert, W.M.; Rogers, R.D. *Conventional free radical polymerization in room temperature ionic liquids: a green approach to commodity polymers with practical advantages*. *Chemical Communications*. 2002; p. 1368–1369.
63. Hao, J.; Zemb, T. *Self-assembled structures and chemical reactions in room-temperature ionic liquids*. *Current Opinion in Colloid & Interface Science*. 2007; **12** p. 129–137.
64. Moniruzzaman, M.; Nakashima, K.; Kamiya, N.; Goto, M. *Recent advances of enzymatic reactions in ionic liquids*. *Biochemical Engineering Journal*. 2010; **48** p. 295–314.
65. Liu, C.-Z.; Wang, F.; Stiles, A.R.; Guo, C. *Ionic liquids for biofuel production: Opportunities and challenges*. *Applied Energy*. 2012; **92** p. 406–414.
66. Visser, A.E.; Swatloski, R.P.; Reichert, W.M.; Davis Jr., J.H.; Rogers, R.D.; Mayton, R.; Sheff, S.; Wierzbicki, A. *Task-specific ionic liquids for the extraction of metal ions from aqueous solutions*. *Chemical Communications*. 2001; p. 135–136.
67. Ferreira, A.M.; Coutinho, J.A.P.; Fernandes, A.M.; Freire, M.G. *Complete removal of textile dyes from aqueous media using ionic-liquid-based aqueous two-phase systems*. *Separation and Purification Technology*. 2014; **128** p. 58–66.
68. Taungbodhitham, A.K.; Jones, G.P.; Wahlqvist, M.L.; Briggs, D.R. *Evaluation of extraction method for the analysis of carotenoids in fruits and vegetables*. *Food Chemistry*. 1998; **63** p. 577–584.
69. Ding, J.; Welton, T.; Armstrong, D.W. *Chiral ionic liquids as stationary phases in gas chromatography*. *Analytical chemistry*. American Chemical Society; 2004; **76** p. 6819–6822.
70. Gutowski, K.E.; Broker, G.A.; Willauer, H.D.; Huddleston, J.G.; Swatloski, R.P.; Holbrey, J.D.; Rogers, R.D. *Controlling the aqueous miscibility of ionic liquids: aqueous biphasic systems of water-miscible ionic liquids and water-structuring salts for recycle, metathesis, and separations*. *Journal of the American Chemical Society*. 2003; **125** p. 6632–6633.
71. Yu, C.; Han, J.; Wang, Y.; Yan, Y.; Hu, S.; Li, Y.; Zhao, X. *Liquid–liquid equilibrium composed of imidazolium tetrafluoroborate ionic liquids+sodium carbonate aqueous two-phase systems and correlation at (288.15, 298.15, and 308.15)K*. *Thermochimica Acta*. 2011; **523** p. 221–226.
72. Kresheck, G.C.; Wang, Z. *A new micellar aqueous two-phase partitioning system (ATPS) for the separation of proteins*. *Journal of chromatography B*. 2007; **858** p. 247–253.

73. Vázquez-Villegas, P.; Aguilar, O.; Rito-Palomares, M. *Study of biomolecules partition coefficients on a novel continuous separator using polymer-salt aqueous two-phase systems*. Separation and Purification Technology. 2011; **78** p. 69–75.
74. Yixin, G.; Lehe, M.; Ziqiang, Z. *Recovery of antibiotics by aqueous two-phase partition? Partitioning behavior of pure acetylspiramycin solution in polyethylene glycol/potassium phosphate aqueous two-phase systems*. Biotechnology Techniques. 1994; **8** p. 491–496
75. Almeida, M.R.; Passos, H.; Pereira, M.M.; Lima, Á.S.; Coutinho, J.A.P.; Freire, M.G. *Ionic liquids as additives to enhance the extraction of antioxidants in aqueous two-phase systems*. Separation and Purification Technology. 2014; **128** p. 1–10.
76. Freire, M.G.; Louros, C.L.S.; Rebelo, L.P.N.; Coutinho, J.A.P. *Aqueous biphasic systems composed of a water-stable ionic liquid + carbohydrates and their applications*. Green Chemistry. 2011; **13** p. 1536–1545.
77. Cláudio, A.F.M.; Freire, M.G.; Freire, C.S.R.; Silvestre, A.J.D.; Coutinho, J.A.P. *Extraction of vanillin using ionic-liquid-based aqueous two-phase systems*. Separation and Purification Technology. 2010; **75** p. 39–47.
78. Passos, H.; Trindade, M.P.; Vaz, T.S.M.; da Costa, L.P.; Freire, M.G.; Coutinho, J.A.P. *The impact of self-aggregation on the extraction of biomolecules in ionic-liquid-based aqueous two-phase systems*. Separation and Purification Technology. 2013; **108** p. 174–180.
79. Keremedchieva, R.; Svinyarov, I.; Bogdanov, M. *Ionic Liquid-Based Aqueous Biphasic Systems—A Facile Approach for Ionic Liquid Regeneration from Crude Plant Extracts*. Processes. 2015; **3** p. 769–778.
80. Muhammad, N.; Hossain, M.I.; Man, Z.; El-Harbawi, M.; Bustam, M.A.; Noaman, Y.A.; Mohamed Alitheen, N.B.; Ng, M.K.; Hefter, G.; Yin, C.-Y. *Synthesis and Physical Properties of Choline Carboxylate Ionic Liquids*. Journal of Chemical & Engineering Data. 2012; **57** p. 2191–2196.
81. Fukaya, Y.; Iizuka, Y.; Sekikawa, K.; Ohno, H. *Bio ionic liquids: room temperature ionic liquids composed wholly of biomaterials*. Green Chemistry. 2007; **9** p. 1155–1157.
82. Zhang, Y.; Zhang, S.; Chen, Y.; Zhang, J. *Aqueous biphasic systems composed of ionic liquid and fructose*. Fluid Phase Equilibria. 2007; **257** p. 173–176.
83. Ferreira, A.M.; Esteves, P.D.O.; Boal-Palheiros, I.; Pereiro, A.B.; Rebelo, L.P.N.; Freire, M.G. *Enhanced tunability afforded by aqueous biphasic systems formed by fluorinated ionic liquids and carbohydrates*. Green Chemistry. 2015; DOI: 10.1039/C5GC01610J.

84. Pereira, J.F.B.; Kurnia, K.A.; Cojocar, O.A.; Gurau, G.; Rebelo, L.P.N.; Rogers, R.D.; Freire, M.G.; Coutinho, J.A.P. *Molecular interactions in aqueous biphasic systems composed of polyethylene glycol and crystalline vs. liquid cholinium-based salts*. *Physical chemistry chemical physics*. 2014; **16** p. 5723–5731.
85. Pereira, J.F.B.; Kurnia, K.A.; Freire, M.G.; Coutinho, J.A.P.; Rogers, R.D. *Controlling the Formation of Ionic-Liquid-based Aqueous Biphasic Systems by Changing the Hydrogen-Bonding Ability of Polyethylene Glycol End Groups*. *Chemphyschem*. 2015; **16** p. 2219–2225.
86. Pereira, J.F.B.; Ventura, S.P.M.; e Silva, F.A.; Shahriari, S.; Freire, M.G.; Coutinho, J.A.P. *Aqueous biphasic systems composed of ionic liquids and polymers: A platform for the purification of biomolecules*. *Separation and Purification Technology*. 2013; **113** p. 83–89.
87. Pereira, J.F.B.; Vicente, F.; Santos-Ebinuma, V.C.; Araújo, J.M.; Pessoa, A.; Freire, M.G.; Coutinho, J.A.P. *Extraction of tetracycline from fermentation broth using aqueous two-phase systems composed of polyethylene glycol and cholinium-based salts*. *Process Biochemistry*. 2013; **48** p. 716–722.
88. Wu, C.; Wang, J.; Pei, Y.; Wang, H.; Li, Z. *Salting-Out Effect of Ionic Liquids on Poly(propylene glycol) (PPG): Formation of PPG + Ionic Liquid Aqueous Two-Phase Systems*. *Journal of Chemical & Engineering Data*. 2010; **55** p. 5004–5008.
89. Mourão, T.; Tomé, L.C.; Florindo, C.; Rebelo, L.P.N.; Marrucho, I.M. *Understanding the Role of Cholinium Carboxylate Ionic Liquids in PEG-Based Aqueous Biphasic Systems*. *ACS Sustainable Chemistry & Engineering*. 2014; **2** p. 2426–2434.
90. Quental, M. V; Caban, M.; Pereira, M.M.; Stepnowski, P.; Coutinho, J.A.P.; Freire, M.G. *Enhanced extraction of proteins using cholinium-based ionic liquids as phase-forming components of aqueous biphasic systems*. *Biotechnology journal*. 2015; **10** p. 1457–1466.
91. Shahriari, S.; Tomé, L.C.; Araújo, J.M.M.; Rebelo, L.P.N.; Coutinho, J.A.P.; Marrucho, I.M.; Freire, M.G. *Aqueous biphasic systems: a benign route using cholinium-based ionic liquids*. *Royal Society of Chemistry Advances*; 2013; **3** p. 1835–1843.
92. Willauer, H.D.; Huddleston, J.G.; Rogers, R.D. *Solute Partitioning in Aqueous Biphasic Systems Composed of Polyethylene Glycol and Salt: The Partitioning of Small Neutral Organic Species*. *Industrial & Engineering Chemistry Research*. 2002; **41** p. 1892–1904.
93. Merchuk, J.C.; Andrews, B.A.; Asenjo, J.A. *Aqueous two-phase systems for protein separation*. *Journal of Chromatography B: Biomedical Sciences and Applications*. 1998; **711** p. 285–293.

94. Glusker, J.P. *Citrate conformation and chelation: enzymic implications*. Accounts of Chemical Research. 1980; **13** p. 345–352.
95. Pei, Y.; Wang, J.; Liu, L.; Wu, K.; Zhao, Y. *Liquid–Liquid Equilibria of Aqueous Biphasic Systems Containing Selected Imidazolium Ionic Liquids and Salts*. Journal of Chemical & Engineering Data. 2007; **52** p. 2026–2031.
96. Neves, C.M.S.S.; Ventura, S.P.M.; Freire, M.G.; Marrucho, I.M.; Coutinho, J.A.P. *Evaluation of cation influence on the formation and extraction capability of ionic-liquid-based aqueous biphasic systems*. The journal of physical chemistry B. 2009; **113** p. 5194–5199.
97. Shahriari, S.; Neves, C.M.S.S.; Freire, M.G.; Coutinho, J.A.P. *Role of the Hofmeister Series in the Formation of Ionic-Liquid-Based Aqueous Biphasic Systems*. The Journal of Physical Chemistry B. 2012; **116** p. 7252–7258.
98. Patinha, D.J.S.; Alves, F.; Rebelo, L.P.N.; Marrucho, I.M. *Ionic liquids based aqueous biphasic systems: Effect of the alkyl chains in the cation versus in the anion*. The Journal of Chemical Thermodynamics. 2013; **65** p. 106–112.
99. Santos, J.H.; E Silva, F.A.; Ventura, S.P.M.; Coutinho, J.A.P.; de Souza, R.L.; Soares, C.M.F.; Lima, A.S. *Ionic liquid-based aqueous biphasic systems as a versatile tool for the recovery of antioxidant compounds*. Biotechnology progress. 2015; **31** p. 70–77.
100. Freire, M.G.; Neves, C.M.S.S.; Canongia Lopes, J.N.; Marrucho, I.M.; Coutinho, J.A.P.; Rebelo, L.P.N. *Impact of self-aggregation on the formation of ionic-liquid-based aqueous biphasic systems*. The journal of physical chemistry B. 2012; **116** p. 7660–7668.
101. Passos, H.; Ferreira, A.R.; Cláudio, A.F.M.; Coutinho, J.A.P.; Freire, M.G. *Characterization of aqueous biphasic systems composed of ionic liquids and a citrate-based biodegradable salt*. Biochemical Engineering Journal. 2012; **67** p. 68–76.
102. Santa Cruz Biotechnology. *Theobromine* [Internet]. [cited 2015 Aug 18]. Available from: <http://www.scbt.com/datasheet-203296-theobromine.html>.
103. PubChem. *Theobromine* [Internet]. [cited 2015 Aug 18]. Available from: <http://pubchem.ncbi.nlm.nih.gov/compound/theobromine#section=Computed-Properties>.
104. Heck, C.I.; de Mejia, E.G. *Yerba Mate Tea (Ilex paraguariensis): a comprehensive review on chemistry, health implications, and technological considerations*. Journal of food science. 2007; **72** p. R138–R151.
105. Mumford, G.K.; Benowitz, N.L.; Evans, S.M.; Kaminski, B.J.; Preston, K.L.; Sannerud, C.A.; Silverman, K.; Griffiths, R.R. *Absorption rate of methylxanthines following capsules, cola and chocolate*. European Journal of Clinical Pharmacology. 1996; **51** p. 319–325.

106. Gates, S.; Miners, J.O. *Cytochrome P450 isoform selectivity in human hepatic theobromine metabolism*. *British Journal of Clinical Pharmacology*. 2001; **47** p. 299–305.
107. Snyder, S.H.; Katims, J.J.; Annau, Z.; Bruns, R.F.; Daly, J.W. *Adenosine receptors and behavioral actions of methylxanthines*. *Proceedings of the National Academy of Sciences of the United States of America*. 1981; **78** p. 3260–3264.
108. Cláudio, A.F.M.; Swift, L.; Hallett, J.P.; Welton, T.; Coutinho, J.A.P.; Freire, M.G. *Extended scale for the hydrogen-bond basicity of ionic liquids*. *Physical Chemistry Chemical Physics*. 2014; **16** p. 6593–6601.
109. Cláudio, A.F.M.; Ferreira, A.M.; Freire, C.S.R.; Silvestre, A.J.D.; Freire, M.G.; Coutinho, J.A.P. *Optimization of the gallic acid extraction using ionic-liquid-based aqueous two-phase systems*. *Separation and Purification Technology*. 2012; **97** p. 142–149.
110. Freire, M.G.; Neves, C.M.S.S.; Marrucho, I.M.; Canongia Lopes, J.N.; Rebelo, L.P.N.; Coutinho, J.A.P. *High-performance extraction of alkaloids using aqueous two-phase systems with ionic liquids*. *Green Chemistry*. 2010; **12** p. 1715–1718.
111. Raaman, N. *Chapter 4 - Methods of extraction*. *Phytochemical Techniques*. New India Publishing; 2006. p. 9–18.
112. Albertsson, P.A. *Partitioning of Cell Particles and Macromolecules*. 3rd editio. New York: Wiley; 1986.
113. Cláudio, A.F.M.; Ferreira, A.M.; Freire, M.G.; Coutinho, J.A.P. *Enhanced extraction of caffeine from guaraná seeds using aqueous solutions of ionic liquids*. *Green Chemistry*. 2013; **15** p. 2002–2010.
114. Chowdhury, S.A.; Vijayaraghavan, R.; MacFarlane, D.R. *Distillable ionic liquid extraction of tannins from plant materials*. *Green Chemistry*. 2010; **12** p. 1023–1028.
115. Bica, K.; Gaertner, P.; Rogers, R.D. *Ionic liquids and fragrances – direct isolation of orange essential oil*. *Green Chemistry*. 2011; **13** p. 1997–1999.
116. Usuki, T.; Yasuda, N.; Yoshizawa-Fujita, M.; Rikukawa, M. *Extraction and isolation of shikimic acid from Ginkgo biloba leaves utilizing an ionic liquid that dissolves cellulose*. *Chemical communications*. 2011; **47** p. 10560–10562.
117. Esmelindro, M.C.; Toniazzo, G.; Lopes, D.; Oliveira, D.; Dariva, C. *Effects of processing conditions on the chemical distribution of mate tea leaves extracts obtained from CO₂ extraction at high pressures*. *Journal of Food Engineering*. 2005; **70** p. 588–592.
118. Li, S.; Hartland, S. *A new industrial process for extracting cocoa butter and xanthines with supercritical carbon dioxide*. *Journal of the American Oil Chemists' Society*. 1996; **73** p. 423–429.

119. Xie, D.-T.; Wang, Y.-Q.; Kang, Y.; Hu, Q.-F.; Su, N.-Y.; Huang, J.-M.; Che, C.-T.; Guo, J.-X. *Microwave-assisted extraction of bioactive alkaloids from *Stephania sinica**. *Separation and Purification Technology*. 2014; **130** p. 173–181.
120. De Melo, M.M.R.; Oliveira, E.L.G.; Silvestre, A.J.D.; Silva, C.M. *Supercritical fluid extraction of triterpenic acids from *Eucalyptus globulus* bark*. *The Journal of Supercritical Fluids*. 2012; **70** p. 137–145.
121. Pura Naik, J. *Improved High-Performance Liquid Chromatography Method to Determine Theobromine and Caffeine in Cocoa and Cocoa Products*. *Journal of Agricultural and Food Chemistry*. 2001; **49** p. 3579–3583.
122. Passos, H.; Sousa, A.C.A.; Pastorinho, M.R.; Nogueira, A.J.A.; Rebelo, L.P.N.; Coutinho, J.A.P.; Freire, M.G. *Ionic-liquid-based aqueous biphasic systems for improved detection of bisphenol A in human fluids*. *Analytical Methods*. 2012; **4** p. 2664–2667.

Appendix A - Experimental binodal data

A.1. Experimental binodal data for systems composed of IL + PPG 400 + H₂O

Table A.1.1. Experimental weight fraction data for the system composed of [Ch][Adi_{1:1}] (1) + PPG 400 (2) + H₂O (3) at 298 K and at atmospheric pressure.

[Ch][Adi _{1:1}] <i>M_w</i> = 249.304 g.mol ⁻¹					
100 <i>w</i> ₁	100 <i>w</i> ₂	100 <i>w</i> ₁	100 <i>w</i> ₂	100 <i>w</i> ₁	100 <i>w</i> ₂
4.5300	61.0913	13.9080	33.7912	24.6290	18.9032
5.0044	58.0734	14.8916	31.3119	25.3257	18.3518
5.6903	56.4836	15.2081	30.2515	25.8906	17.8053
6.3201	54.9785	15.4243	29.7704	26.5790	17.1522
6.9640	53.3988	16.5309	27.9365	27.5083	16.4784
7.4319	51.5448	16.7245	27.6449	28.3398	15.8409
7.9609	49.9506	17.8404	25.5742	28.7632	15.2227
8.7841	47.4915	18.4961	25.1030	30.0955	14.2621
9.0908	45.9086	18.9001	24.4044	31.0926	13.1541
9.3073	44.9453	20.0684	23.3612	32.4743	12.4090
11.1121	40.2196	20.6488	22.9065	33.3056	11.6408
11.4560	39.3753	21.3085	22.2751	34.6014	10.9259
11.9840	38.5202	22.0769	21.5345	35.6496	10.2936
12.2585	37.6705	22.6517	20.9118	37.1268	9.3714
12.8629	36.1342	23.3654	20.1402		
13.2479	35.0798	24.0675	19.4846		

Table A.1.2. Experimental weight fraction data for the system composed of [Ch][Adi_{1,2}] (1) + PPG 400 (2) + H₂O (3) at 298 K and at atmospheric pressure.

[Ch][Adi _{1,2}]					
$M_w = 352.467 \text{ g.mol}^{-1}$					
100 w_1	100 w_2	100 w_1	100 w_2	100 w_1	100 w_2
5.5367	59.0483	15.7669	30.0868	24.1585	18.7605
5.5954	57.1420	15.8001	29.2477	24.7103	18.2507
6.0384	55.5837	16.1834	29.2022	25.3525	17.7324
6.0953	54.0617	16.3215	28.4045	25.9378	17.1736
6.8078	52.4758	16.7163	28.4003	26.5980	16.6601
7.3937	50.7674	17.2402	27.4688	27.3677	15.9623
8.0363	48.9924	17.2469	26.8382	28.1722	15.3051
8.5661	47.1405	17.5521	26.7520	28.7162	14.8652
8.8843	46.0328	17.8892	25.9217	29.4508	14.4190
9.7296	44.3122	18.2380	25.9204	30.2175	13.8406
10.0953	42.9045	18.8079	25.1320	31.2852	13.2830
10.5993	41.8683	18.9360	24.3719	31.8930	12.7317
11.0757	40.6274	19.2634	24.1639	32.6489	12.2627
11.3851	39.4966	19.8831	23.4721	33.6474	11.6415
11.6797	38.3773	20.2166	22.8629	34.7566	11.0578
12.3996	37.1424	21.3165	21.4013	35.7193	10.5022
13.0195	35.2466	21.7981	20.7103	36.8187	9.9957
13.2257	34.1456	22.5880	20.1349	38.5280	9.3121
15.1365	31.1947	23.2669	19.5493		
15.2788	30.1860	23.7256	19.3675		

Table A.1.3. Experimental weight fraction data for the system composed of [Ch][Ac] (1) + PPG 400 (2) + H₂O (3) at 298 K and at atmospheric pressure.

		[Ch][Ac]			
		$M_w = 163.215 \text{ g.mol}^{-1}$			
100 w_1	100 w_2	100 w_1	100 w_2	100 w_1	100 w_2
3.4066	55.7831	6.6189	34.5467	13.4190	16.9031
3.4596	52.9536	6.8769	33.1032	13.9096	16.2305
3.7154	51.5615	7.2401	31.6511	14.3114	15.6218
3.9604	49.7641	7.6720	30.2367	14.6948	14.8571
4.3015	48.2616	8.1037	28.0878	15.1559	14.3010
4.3917	47.8903	8.4800	27.1783	15.5514	13.7077
4.5606	46.3810	8.8768	26.0765	15.9412	13.2304
5.1050	42.5526	9.1659	25.4088	16.5243	12.4389
5.2416	41.8762	9.4569	24.5812	17.0446	11.9445
5.4245	41.0603	10.1734	22.6225	17.4993	11.4266
5.5687	39.6487	10.5665	21.6978	17.8906	10.9146
5.7459	39.3178	11.0677	20.8927	18.5834	10.3381
5.8224	38.2841	12.0095	19.6433	18.9699	9.8704
6.0761	37.5968	12.4874	18.6047	19.6289	9.2923
6.1428	37.1213	13.0343	17.6524	20.1999	8.7906

Table A.1.4. Experimental weight fraction data for the system composed of IL (1) + PPG 400 (2) + H₂O (3) at 298 K and at atmospheric pressure.

[Ch][TFAc] $M_w = 217.186 \text{ g.mol}^{-1}$		[Ch][Aze] $M_w = 291.384 \text{ g.mol}^{-1}$		[Ch][Bic] $M_w = 165.188 \text{ g.mol}^{-1}$	
100 w_1	100 w_2	100 w_1	100 w_2	100 w_1	100 w_2
35.6245	51.4103	4.2279	68.0676	4.2456	52.7430
36.4494	50.0223	4.4496	66.1979	4.4920	48.3261
37.4572	48.4390	5.1927	64.3500	4.9431	45.7506
38.5763	46.8659	6.0444	62.4086	5.2750	43.3155
39.3427	45.7386	6.6839	60.5809	5.5025	41.6341
40.2709	44.3276	7.2253	58.7817	5.9179	39.6721
41.1668	43.0212	8.5470	56.5891	6.2863	37.8280
42.0435	41.7310	9.6566	54.1438	6.8245	35.5047
42.5005	40.9223	10.6983	51.8157	7.2905	33.0420
43.2088	39.1138	11.4752	49.9430	8.1088	30.2211
44.1843	38.0301	12.5038	48.2356	9.1835	27.5780
44.7196	37.2720	13.3324	46.4133	9.8643	24.8044
45.4031	36.4514	13.5929	45.4829	10.8807	22.6975
45.8342	35.7216	14.4180	44.2036	12.4376	19.7879
46.3209	34.9950	15.1461	42.8043	16.2930	13.4993
46.8561	33.7425	15.8474	41.8808	17.8945	11.9966
47.2024	33.1043	16.1912	41.1117	18.6121	10.8153
47.6980	32.4179	17.6681	38.9243	19.4359	10.0134
48.3563	31.6016	18.3956	38.0151	19.9013	9.2066
49.0745	30.7552	19.3834	36.9295		
49.6085	30.0169	21.3659	33.7126		
49.9677	29.4772	22.1096	32.8607		
50.0460	29.2100	22.9113	31.8652		
50.4758	28.2846	23.5738	31.2213		
50.8180	27.8264	24.0643	30.6335		
51.2006	27.3022	24.7373	29.9475		
51.5025	26.8607	25.6548	29.1197		
51.7971	26.4741	28.6229	27.0479		
52.0173	26.1822	31.5048	25.2513		
52.3423	25.7490	33.8974	23.5149		
52.5108	25.4056	36.9457	21.3654		
52.7876	24.9796	40.3280	19.4490		
53.2449	24.3331	43.8732	17.3343		
53.7579	23.6107	47.8638	14.9606		
54.0936	23.0801	52.5298	12.6613		
54.6713	22.3890	87.2632	1.9223		
55.2905	21.6649				
56.2373	20.6133				
63.6031	11.8325				
67.2611	9.2733				
86.1111	2.7778				

A.2. Experimental binodal data for systems composed of IL + K₃PO₄ + H₂O

Table A.2.1. Experimental weight fraction data for the system composed of [Ch][Ac] (1) + K₃PO₄ (2) + H₂O (3) at 298 K and at atmospheric pressure.

[Ch][Ac] $M_w = 163.215 \text{ g}\cdot\text{mol}^{-1}$					
100 w_1	100 w_2	100 w_1	100 w_2	100 w_1	100 w_2
34.8638	11.2389	19.2994	25.1594	12.3549	32.7929
29.9277	15.0144	18.7136	25.9442	11.9587	33.2749
28.6205	16.1817	17.9298	26.6952	11.5901	33.6929
27.8545	16.7698	17.8823	26.8271	11.2952	34.0124
26.8703	17.5930	17.4101	27.3202	10.9471	34.4191
26.8035	17.7428	16.9460	27.7644	10.8758	34.4666
25.3648	19.1889	16.9112	27.7713	10.7093	34.7320
25.1743	19.2138	16.3653	28.4568	10.3818	35.1024
24.4068	20.0696	15.8806	28.9928	9.9109	35.6930
24.0303	20.3362	15.7724	29.0789	9.6349	35.9192
23.4845	21.0584	15.2522	29.7007	9.3599	36.4594
22.7842	21.5758	14.7972	30.2012	8.9301	36.9963
22.5625	21.9151	14.3964	30.5737	8.5632	37.3544
21.8486	22.6282	13.9686	31.0381	8.4972	37.5434
21.7411	22.6995	13.7107	31.2068	8.1656	37.8980
21.0001	23.6093	13.6198	31.4159	7.7593	38.4095
20.5575	23.8454	13.2314	31.8320	7.3313	39.0029
20.3186	24.2817	12.8507	32.2326	6.3610	40.2156
19.6493	24.8879	12.3829	32.7842		

Table A.2.2. Experimental weight fraction data for the system composed of [Ch][Adi_{1:2}] (1) + K₃PO₄ (2) + H₂O (3) at 298 K and at atmospheric pressure.

[Ch][Adi _{1:2}] $M_w = 163.215 \text{ g}\cdot\text{mol}^{-1}$					
100 w_1	100 w_2	100 w_1	100 w_2	100 w_1	100 w_2
85.7981	0.7329	26.4269	17.9247	23.2967	20.2212
48.7033	6.0768	25.4606	18.6462	22.4288	20.9514
37.5085	10.4723	24.8430	18.9624		
27.0813	17.3823	23.8258	19.8856		

Table A.2.3. Experimental weight fraction data for the system composed of IL (1) + K₃PO₄ (2) + H₂O (3) at 298 K and at atmospheric pressure.

[Ch][Pro] $M_w = 177.242 \text{ g.mol}^{-1}$		[Ch][Pent] $M_w = 205.295 \text{ g.mol}^{-1}$		[Ch][Non] $M_w = 261.401 \text{ g.mol}^{-1}$	
100 w_1	100 w_2	100 w_1	100 w_2	100 w_1	100 w_2
37.6192	8.6740	55.8515	12.0194	20.4237	24.5629
34.9589	9.9581	15.1284	24.3866	20.6416	23.9797
33.2239	11.0544	13.6967	25.0411	21.1248	23.1210
31.4257	12.1977	13.3909	25.2599	21.9595	21.7080
29.3268	13.7001	13.0255	25.5972	22.6189	20.5477
27.1845	15.2684	12.4937	26.0020	23.3697	19.3537
26.2754	15.9686	11.6112	26.8730	23.8539	18.5516
24.6923	17.2628	9.5982	28.5589	24.2679	17.8187
22.9893	18.6934	8.4155	29.8138	24.8819	16.8630
20.6084	20.7979	7.2804	30.8600	25.3728	16.0860
14.4079	26.4577	4.7857	33.7142	25.7778	15.4084
				26.3541	14.5361
				27.1589	13.3391
				27.6514	12.6279
				28.1551	11.9219
				28.5165	11.4070
				28.8291	10.9313
				29.3322	10.2829
				29.7303	9.7540
				30.1885	9.1803
				30.6100	8.6597
				30.9893	8.1888
				31.3834	7.7308
				31.7130	7.3374
				32.1191	6.8803
				32.5340	6.4344
				33.0467	5.9197
				33.5052	5.4706
				33.8426	5.1371
				34.1983	4.8095
				37.5352	3.0857

A.3. Correlation parameters

Table A.3.1. Correlation parameters for the fitting using equation 2.1.[93].

Salting-out	Ionic Liquid	$A \pm \sigma$	$B \pm \sigma$	$10^{-5} (C \pm \sigma)$	R^2
PPG 400	[Ch][Adi _{1:1}]	141.84 ± 3.39	-0.380 ± 0.008	0.86 ± 0.12	0.9961
PPG 400	[Ch][Adi _{1:2}]	152.44 ± 2.53	-0.405 ± 0.005	0.65 ± 0.07	0.9979
PPG 400	[Ch][TFAc]	112.02 ± 11.64	-0.085 ± 0.019	0.60 ± 0.02	0.9991
PPG 400	[Ch][Aze]	117.97 ± 1.76	-0.260 ± 0.005	0.27 ± 0.03	0.9971
PPG 400	[Ch][Ac]	178.18 ± 3.13	-0.635 ± 0.008	1.67 ± 0.42	0.9989
PPG 400	[Ch][DHcit]	342.60 ± 13.21	-0.616 ± 0.010	0.25 ± 0.88	0.9991
PPG 400	[Ch][DHph]	215.03 ± 5.16	-0.816 ± 0.011	1.00 ± 0.85	0.9989
PPG 400	[Ch][Bit]	205.79 ± 12.83	-0.566 ± 0.022	1.00 ± 0.45	0.9962
PPG 400	[Ch]Cl	201.60 ± 31.85	-0.615 ± 0.057	0.01 ± 1.81	0.9902
PPG 400	[Ch][Bic]	195.96 ± 7.96	-0.653 ± 0.017	1.12 ± 0.75	0.9983
PEG 400	[Ch][Ac]	48.18 ± 17.35	0.049 ± 0.065	0.76 ± 0.07	0.9993
PEG 400	[Ch][DHcit]	125.32 ± 1.86	-0.138 ± 0.003	0.21 ± 0.01	0.9998
PEG 400	[Ch][DHpho]	94.94 ± 1.29	-0.162 ± 0.004	1.24 ± 0.02	0.9996
PEG 400	[Ch][Bit]	107.80 ± 1.85	-0.145 ± 0.004	0.29 ± 0.01	0.9996
PEG 400	[Ch]Cl	133.20 ± 2.05	-0.134 ± 0.003	0.38 ± 0.01	0.9999
PEG 400	[Ch][Bic]	130.69 ± 2.33	-0.164 ± 0.004	0.54 ± 0.02	0.9995
K ₃ PO ₄	[Ch][Adi _{1:2}]	115.24 ± 0.70	-0.346 ± 0.004	0.40 ± 0.18	0.9998
K ₃ PO ₄	[Ch]Cl	66.07 ± 0.46	-0.191 ± 0.002	1.67 ± 0.03	0.9995
K ₃ PO ₄	[Ch][Ac]	101.76 ± 1.35	-0.254 ± 0.004	1.92 ± 0.04	0.9993
K ₃ PO ₄	[Ch][Pro]	48.45 ± 0.31	-0.155 ± 0.002	0.67 ± 0.06	0.9989
K ₃ PO ₄	[Ch][But]	84.60 ± 1.47	-0.273 ± 0.006	1.95 ± 0.09	0.9998
K ₃ PO ₄	[Ch][Pent]	86.21 ± 1.09	-0.292 ± 0.005	2.29 ± 0.11	0.9994
K ₃ PO ₄	[Ch][Hex]	745.41 ± 55.44	-0.738 ± 0.022	1.82 ± 0.21	0.9998
K ₃ PO ₄	[Ch][Non]	93.55 ± 0.83	-0.281 ± 0.003	3.26 ± 0.03	0.9999

Appendix B – Additional experimental data

B.1. Ternary phase diagrams in molality

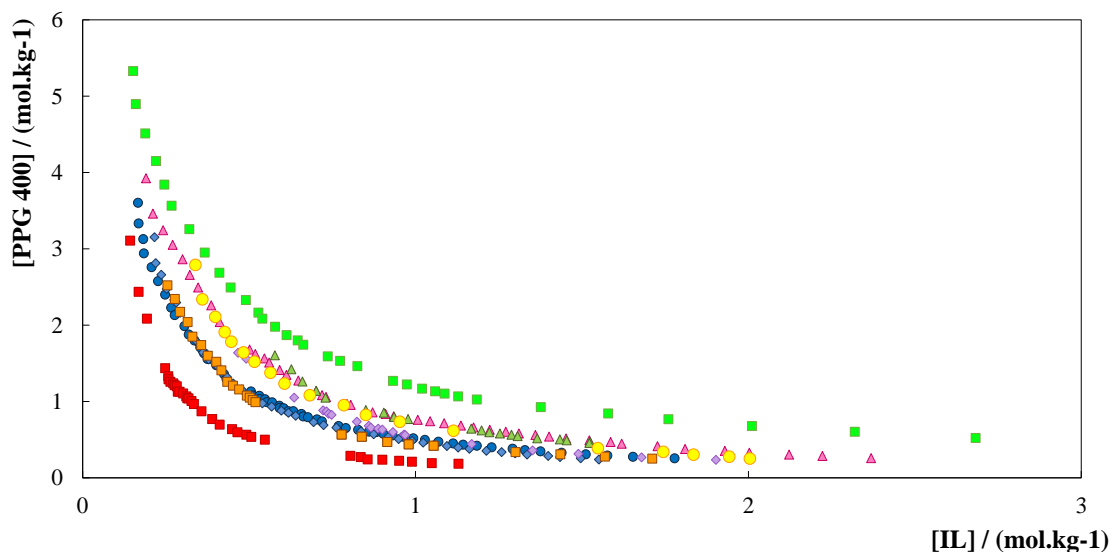


Figure B.1.1. Ternary phase diagrams for systems composed of IL + PPG 400 + water, at 298 K and atmospheric pressure: (■) [Ch][DHph], (◆) [Ch][Ac], (▲) [Ch]Cl, (■) [Ch][Bit], (●) [Ch][Bic], (◆) [Ch][DHcit], (▲) [Ch][Adi](1:1), (●) [Ch][Adi](1:1), (■) [Ch][Aze], (◆) [Ch][TFAc].

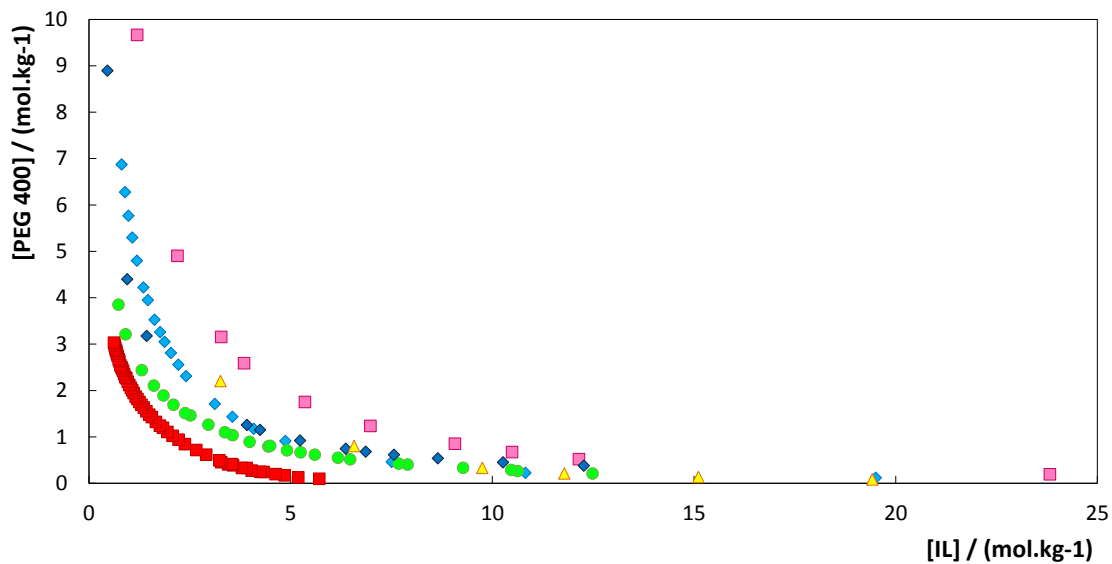


Figure B.1.2. Ternary phase diagrams for systems composed of IL + PEG 400 + water, at 298 K and atmospheric pressure: (■) [Ch][DHph], (◆) [Ch][Bic], (▲) [Ch][Ac], (●) [Ch][Bit], (■) [Ch]Cl, (◆) [Ch][DHcit].

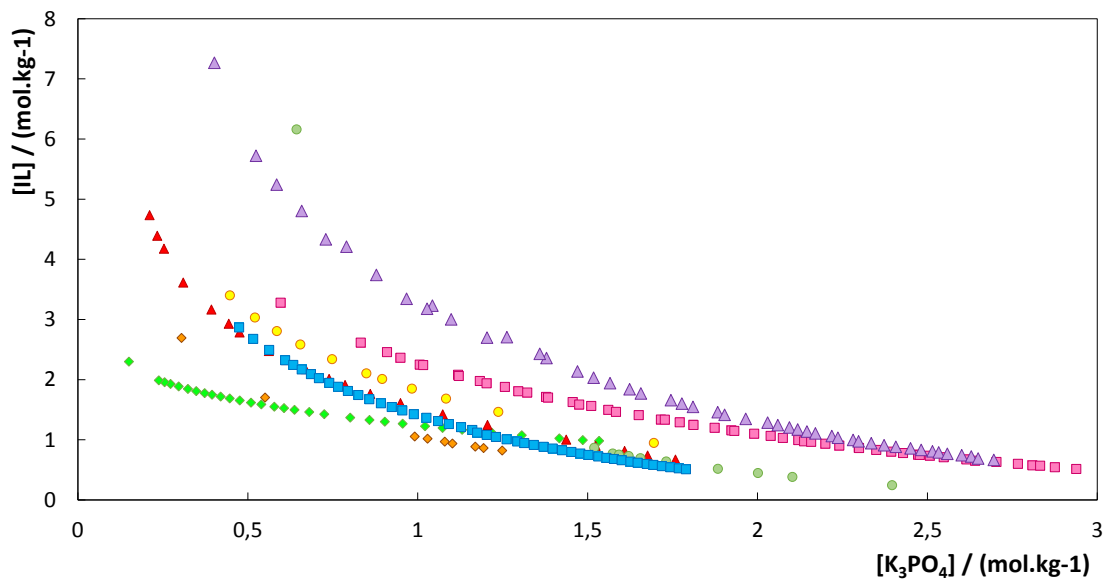


Figure B.1.3. Ternary phase diagrams for systems composed of IL + K_3PO_4 + water, at 298 K and atmospheric pressure: (◆) [Ch][Adi_{1:2}], (▲) [Ch]Cl, (■) [Ch][Ac], (●) [Ch][Pro], (▲) [Ch][But], (●) [Ch][Pent], (■) [Ch][Hex] and (◆) [Ch][Non].

B.2. Examples of TLs obtained

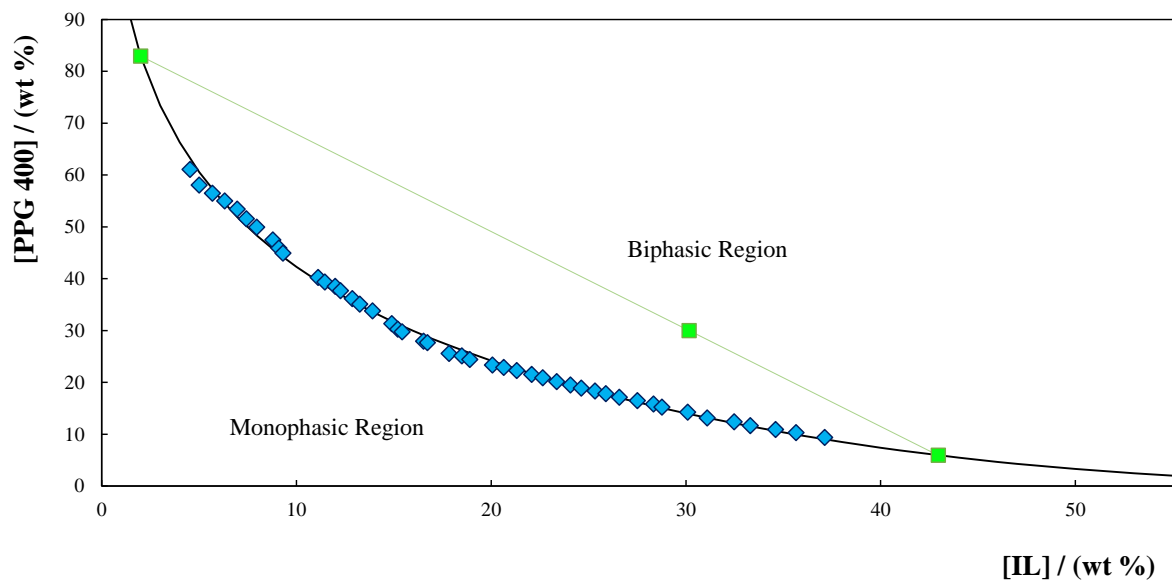


Figure B.2.1. Phase diagram for [Ch][Adi_{1:1}] + PPG 400 + H_2O . Binodal equilibrium data (◆); TL data (■); correlation using equation 2.1. (—).

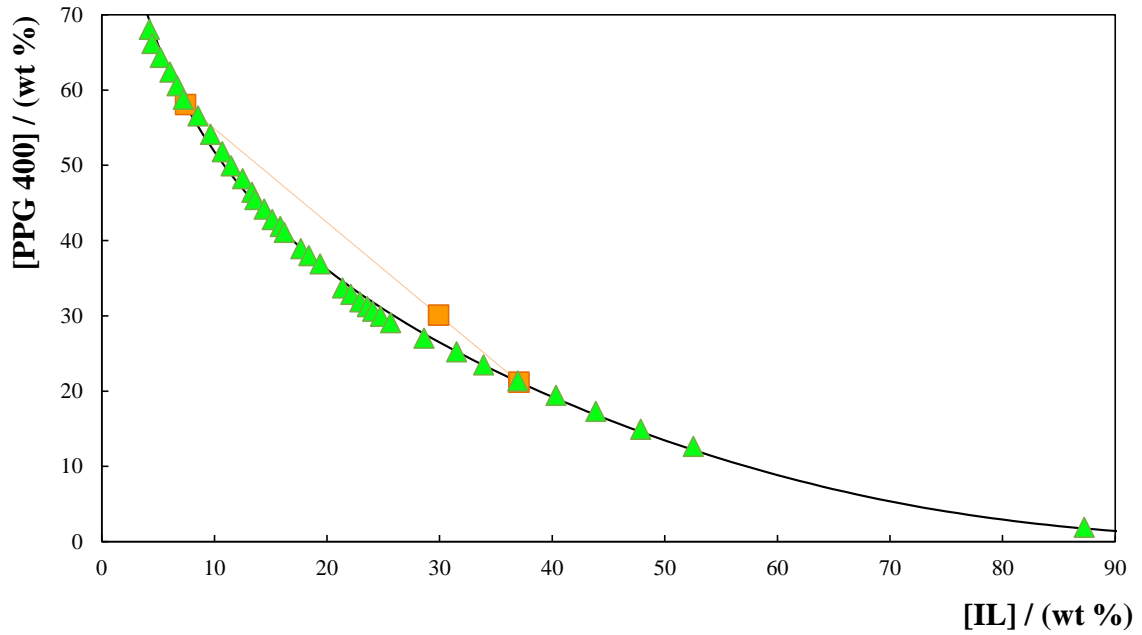


Figure B.2.2. Phase diagram for [Ch][Aze] + PPG 400 + H₂O. Binodal equilibrium data (\blacktriangle); TL data (\blacksquare); correlation using equation 2.1. (—).

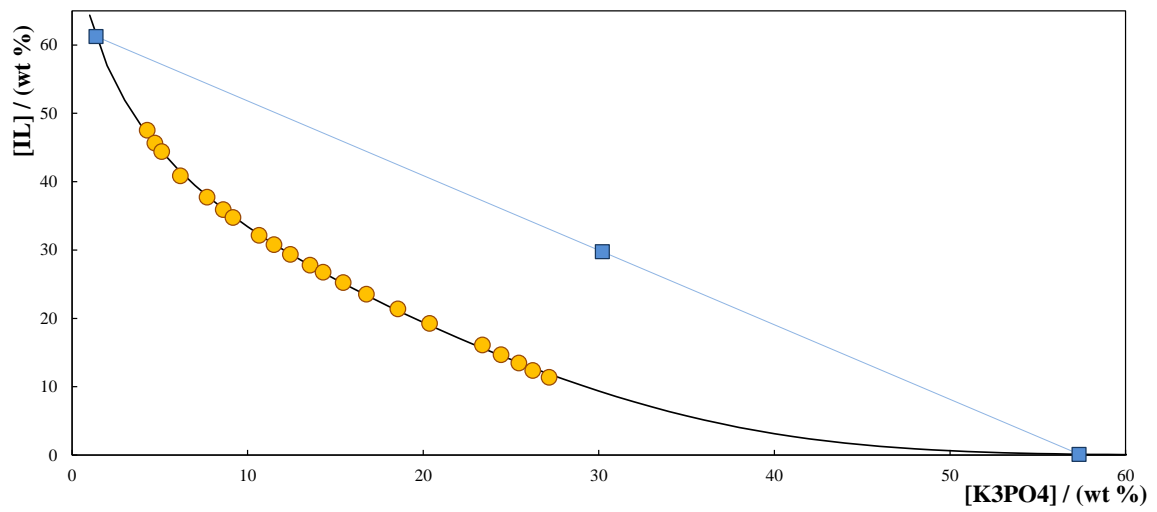


Figure B.2.3. Phase diagram for [Ch][But] + K₃PO₄ + H₂O. Binodal equilibrium data (\bullet); TL data (\blacksquare); correlation using equation 2.1. (—).

B.3. Calibration curves

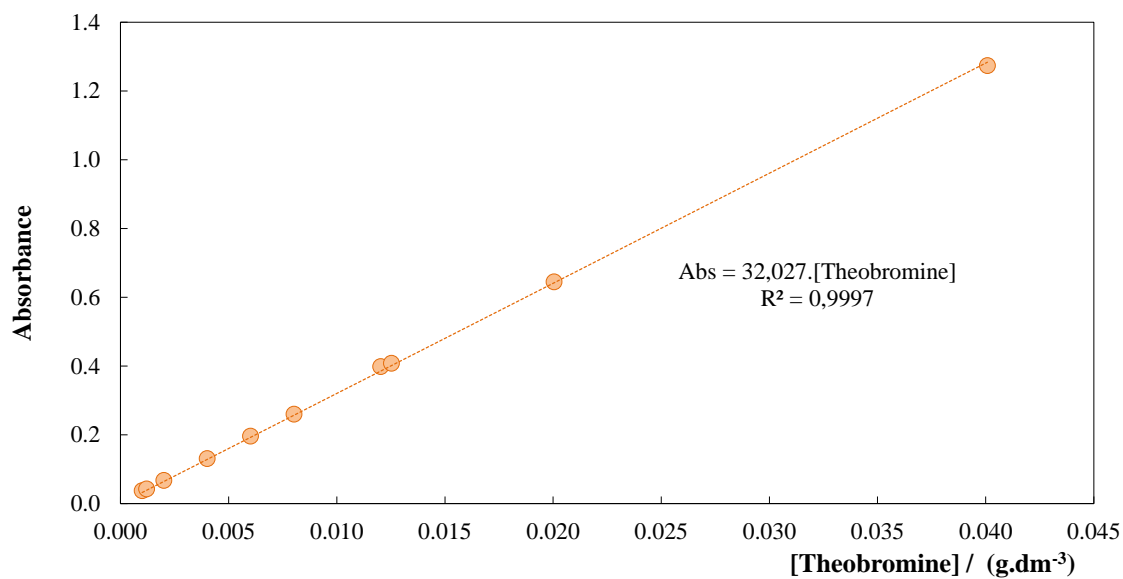


Figure B.3.1. Theobromine calibration curve with water as solvent using the UV-microplate reader, with maximum of absorbance at a wavelength of 273 nm.

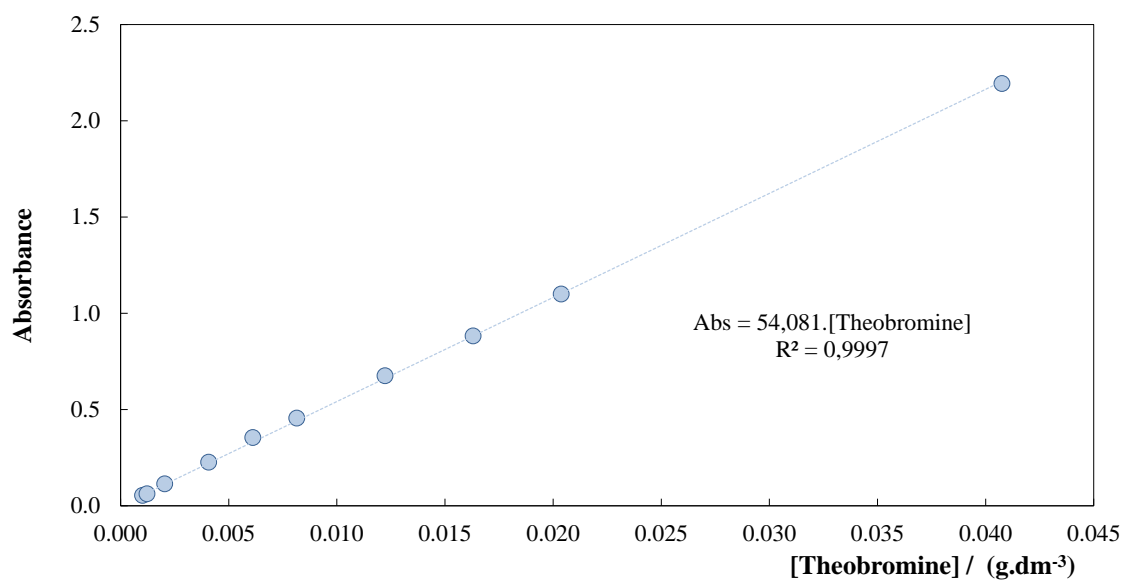


Figure B.3.2. Theobromine calibration curve with water as solvent using the UV-Spectrometer, with maximum of absorbance at a wavelength of 273 nm.

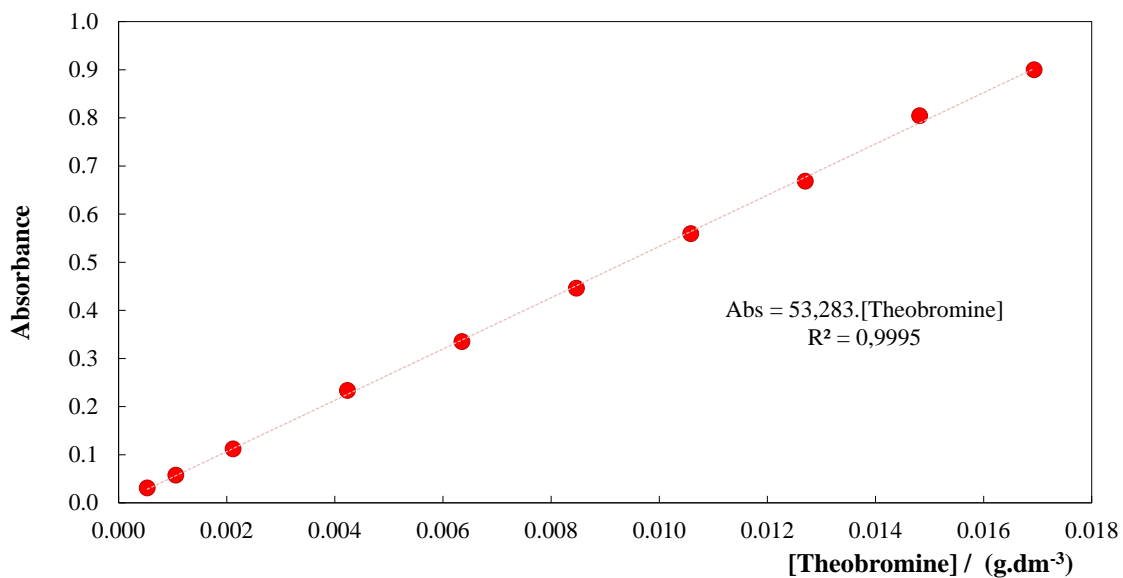


Figure B.3.3. Theobromine calibration curve with ethanol as solvent using the UV-Spectrometer, with maximum of absorbance at a wavelength of 273 nm.

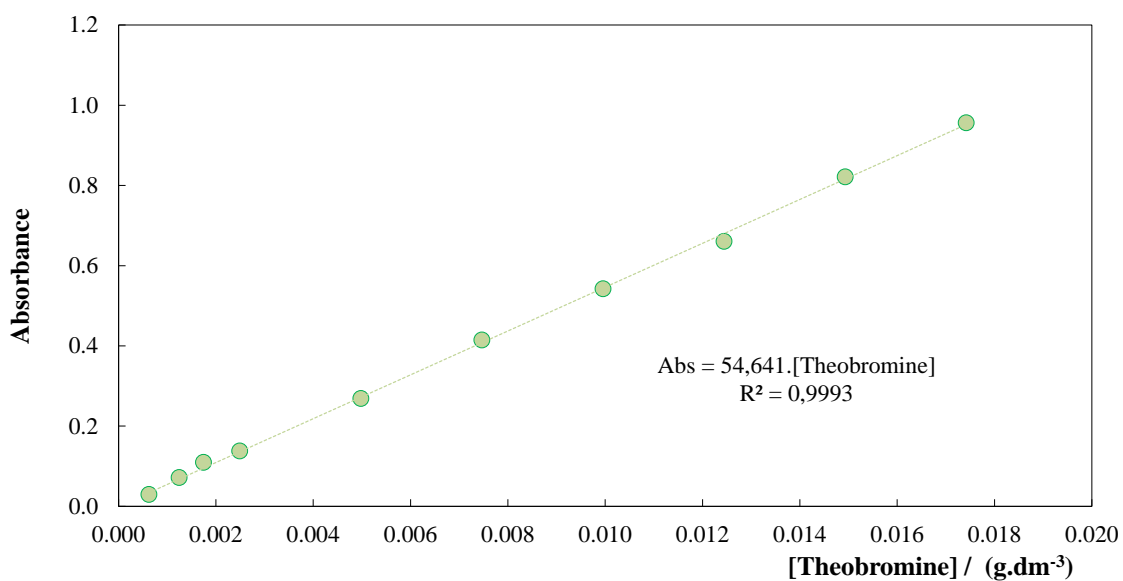


Figure B.3.4. Theobromine calibration curve with dichloromethane as solvent using the UV-Spectrometer, with maximum of absorbance at a wavelength of 273 nm.

B.4. GC-MS spectrum

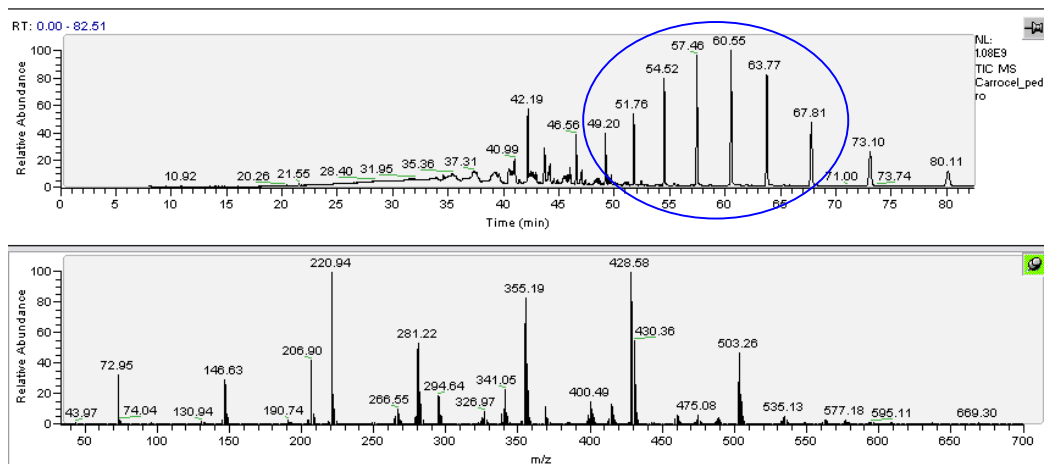


Figure B.4.1. GC-MS spectrum of treated cocoa after extraction with [Ch][Ac].

**Appendix C – Weight
fraction percentage (wt %) of
ABS**

C.1. Weight fraction percentage (wt %) of ABS composed of IL + salting-out species + H₂O

Table C.1.1 Weight fraction percentage (wt %) of each compound at the coexisting phases of the ABS investigated and respective TLL.

Salting-out	Ionic Liquid	[IL] _{IL}	[IL] _{so}	[IL] _M	[SO] _M	[SO] _{IL}	[SO] _{so}	TLL
PPG 400	[Ch][Adi _{1:1}]	5.94	82.92	29.98	30.16	42.96	2.00	87.19
		6.51	86.21	29.95	29.98	41.76	1.72	89.20
PPG 400	[Ch][Adi _{1:2}]	6.58	81.83	29.82	30.04	42.45	2.26	85.30
		6.44	80.37	29.92	29.96	42.79	2.40	84.25
PPG 400	[Ch][Aze]	21.19	58.06	30.09	29.91	37.06	7.44	47.29
		21.31	56.44	29.79	29.93	36.89	8.03	45.47
PPG 400	[Ch][Ac]	0.85	100.51	30.02	29.92	41.97	0.81	107.83
		0.84	99.98	29.86	29.95	42.01	0.83	107.36
PPG 400	[Ch][DHcit]	6.96	90.24	29.93	30.00	39.64	4.68	90.32
		6.43	82.73	30.09	30.09	41.23	5.31	84.33
PPG 400	[Ch][DHph]	0.42	93.65	29.81	30.36	43.86	1.04	102.59
		0.44	91.46	29.67	29.81	43.40	1.10	100.37
PPG 400	[Ch][Bit]	2.09	85.52	29.72	30.11	43.83	2.40	93.15
		2.68	100.42	29.90	30.22	41.27	1.60	105.48
PPG 400	[Ch]Cl	3.57	89.17	30.20	30.07	42.85	1.76	94.94
		3.62	88.57	30.10	29.89	42.61	1.79	94.25
PPG 400	[Ch][Bic]	1.15	75.65	23.98	30.26	42.68	2.13	84.82
		1.19	75.78	24.15	30.00	42.41	2.12	84.78
PEG 400	[Ch][DHph]	2.37	68.38	33.16	32.94	58.18	4.07	85.36
		2.45	68.80	32.94	33.12	57.95	3.92	85.56
K ₃ PO ₄	[Ch][Adi _{1:2}]	56.05	4.45	29.79	30.38	4.34	55.52	72.68
		55.45	4.49	29.92	29.97	4.47	55.36	72.02
K ₃ PO ₄	[Ch]Cl	46.77	4.57	20.47	29.79	9.05	42.33	53.75
		45.97	4.50	20.31	29.86	9.42	42.45	53.02
K ₃ PO ₄	[Ch][Ac]	0.58	60.72	29.85	29.95	58.18	0.20	83.54
		0.52	60.52	29.74	30.22	58.70	0.21	83.79
K ₃ PO ₄	[Ch][Pro]	59.11	0.18	30.17	29.96	1.73	59.22	82.32
		60.19	0.16	31.03	29.86	1.56	59.83	83.66
K ₃ PO ₄	[Ch][But]	0.13	61.26	29.78	30.19	57.35	1.36	82.90
		0.09	60.19	29.85	30.42	58.78	1.51	83.02
K ₃ PO ₄	[Ch][Pent]	62.96	0.73	30.04	29.99	10.99	46.90	71.85
		62.17	0.69	30.18	29.90	11.10	47.24	71.32
K ₃ PO ₄	[Ch][Hex]	66.13	0.08	30.08	29.99	1.53	53.69	84.16
		66.79	0.09	29.98	30.02	1.44	53.22	84.44

Appendix D – Theobromine extraction

Table D.1. % EE_{TB} for the IL-rich phase, and respective standard deviation (σ), for commercial theobromine, using the ABS composed of IL + PPG 400/PEG 400/K₃PO₄ + H₂O at 298 K.

Salting-out	IL	% EE _{TB} \pm σ	TLL
PPG 400	[Ch][DHph]	43.57 \pm 0.86	102.59
PPG 400	[Ch][DHcit]	73.72 \pm 1.26	90.32
PPG 400	[Ch][Bic]	23.12 \pm 0.75	98.00
PPG 400	[Ch][Bit]	69.71 \pm 2.17	93.15
PPG 400	[Ch]Cl	66.38 \pm 0.58	94.94
PPG 400	[Ch][Ac]	60.70 \pm 2.46	107.83
PPG 400	[Ch][Adi 1:1]	69.23 \pm 2.17	87.19
PPG 400	[Ch][Adi 1:2]	56.55 \pm 0.75	85.30
PPG 400	[Ch][Aze]	85.36 \pm 1.73	47.29
PEG 400	[Ch][DHph]	52.65 \pm 1.71	85.36
K ₃ PO ₄	[Ch]Cl	97.45 \pm 0.92	53.75
K ₃ PO ₄	[Ch][Ac]	96.56 \pm 1.79	83.54
K ₃ PO ₄	[Ch][Pro]	98.52 \pm 1.31	82.32
K ₃ PO ₄	[Ch][But]	99.86 \pm 0.18	82.90
K ₃ PO ₄	[Ch][Pent]	99.23 \pm 1.17	71.85
K ₃ PO ₄	[Ch][Hex]	96.41 \pm 1.33	84.16
K ₃ PO ₄	[Ch][Adi 1:2]	99.67 \pm 0.31	72.68

Table D.2. % TB, and respective standard deviation (σ), from cocoa peels and cocoa core, using different solutions of ILs (1.5 M), in a solid-liquid extraction, at 343 K.

Solvent	% TB (peel)	% TB (core)
[Ch]Cl	1.72 \pm 0.19	4.48 \pm 0.18
[Ch][Ac]	2.45 \pm 0.60	5.52 \pm 0.60

Table D.3. % TB from cocoa beans, over time, using ethanol as solvent in a Soxhlet extraction.

Time (minutes)	% TB	Time (minutes)	% TB
15	1.06	180	3.19
30	1.66	240	3.23
45	2.08	300	3.46
60	2.38	360	3.35
120	3.02	420	3.32

Table D.4. % TB from cocoa beans, over time, using dichloromethane as solvent in a Soxhlet extraction.

Time (minutes)	% TB
15	.000
30	0.00.
45	0.00.
60	0.05
120	0.19
180	0.26
240	0.34
360	0.32
420	0.38

Table D.5. % TB, and respective standard deviation (σ), from cocoa beans using different solvents at 343 K: ILs + H₂O (1.2 M to [Ch][Bic] and 1.5 M for the remaining ILs), H₂O and ethanol.

Solvent	% TB \pm σ
[Ch][DHph]	5.35 \pm 0.03
[Ch][DHcit]	5.85 \pm 0.03
[Ch][Bic]	5.50 \pm 0.03
[Ch][Bit]	5.93 \pm 0.02
[Ch]Cl	4.48 \pm 0.18
[Ch][Ac]	5.32 \pm 0.08
[Ch][Pro]	5.51 \pm 0.18
[Ch][But]	5.95 \pm 0.15
[Ch][Pent]	6.06 \pm 0.18
[Ch][Hex]	6.48 \pm 0.08
[Ch][Adi _{1:1}]	5.79 \pm 0.06
[Ch][Adi _{1:2}]	5.79 \pm 0.04
H ₂ O	3.46 \pm 0.05
Ethanol	2.16 \pm 0.08

Table D.6. % TB, and respective standard deviation (σ), from treated and untreated biomass, using different solutions of ILs (1.5 M) at 343 K.

Solvent	% TB (treated)	% TB (untreated)
[Ch]Cl	9.46 \pm 0.33	4.48 \pm 0.18
[Ch][Ac]	10.01 \pm 0.18	5.32 \pm 0.08
[Ch][But]	10.83 \pm 1.05	5.95 \pm 0.15
[Ch][Hex]	11.74 \pm 0.37	6.48 \pm 0.08

Table D.7. Mixture points

IL	IL (wt %)	K₃PO₄ (wt %)
[Ch]Cl	14	33
[Ch][Ac]	17	31
[Ch][Pro]	13	31
[Ch][But]	22	27
[Ch][Pent]	16	26
[Ch][Hex]	24	27
[Ch][Adi _{1:2}]	26	27

Table D.8. Theobromine extraction efficiencies and respective standard deviation (σ) with commercial theobromine and with theobromine extracted from biomass.

Ionic Liquid	%EE_{TB}	
	Commercial Theobromine	Biomass
[Ch]Cl	84.90 \pm 0.77	97.72 \pm 0.19
[Ch][Ac]	86.70 \pm 0.00	98.48 \pm 0.39
[Ch][Pro]	81.34 \pm 0.80	98.93 \pm 0.06
[Ch][But]	93.73 \pm 0.61	98.89 \pm 0.02
[Ch][Pent]	86.37 \pm 0.53	99.04 \pm 0.27
[Ch][Hex]	97.94 \pm 0.39	96.71 \pm 0.20
[Ch][Adi _{1:2}]	100.00 \pm 0.00	98.04 \pm 0.07